VAAL UNIVERSITY OF TECHNOLOGY

SYNTHESIS OF CROSS-LINKED PINE CONE BIOSORBENT AND ITS APPLICATIONS IN INDUSTRIAL WASTEWATER TREATMENT.

ALBERT JERRY KAFUSHE KUPETA

Student number: 209134550

BSc, BTech (Chemistry)

Dissertation submitted in fulfilment of the requirement for the degree of

MAGISTER TECHNOLOGIAE: CHEMISTRY

FACULTY OF APPLIED AND COMPUTER SCIENCES

DEPARTMENT OF CHEMISTRY

SUPERVISOR: Dr A.E. OFOMAJA (BSc Hons, MSc, DTech Chemistry)

CO-SUPERVISOR: Prof E.B. NAIDOO (BSc Hons, MSc, PhD Chemistry)

November 2014

DECLARATION

I declare that unless indicated, this dissertation is my own, unaided work. It is being submitted for the Degree Magister Technologiae to the Department of Chemistry, Vaal University of Technology, Vanderbijlpark and has not been submitted before for any degree or examination to any other University.

_____on this _____day of _____2014

CANDIDATE

_____on this _____day of _____2014

SUPERVISOR

_____on this _____day of _____2014

CO-SUPERVISOR

DEDICATION

In memory of my late father, Maxwell.

ACKNOWLEDGEMENTS

I sincerely wish to express my profound appreciation and gratitude to the following for their various contributions:

- My supervisors, Dr A.E Ofomaja and Prof. E.B Naidoo for their educative and constructive comments, guidance, inputs and support throughout this research.
- The Vaal University of Technology through the Research Directorate for providing the research funding. The Department of Chemistry for providing the structures necessary for the research.
- My fellow postgraduate students in the research laboratory for creating a supportive and friendly working environment.
- My loving mother, Enisia and my siblings, Abigail, Ethel and Gerald for their undying support and encouragement. Thank you for being my pillar of strength.
- God the Almighty for giving me the strength and opportunity to tackle this mammoth task.

PRESENTATIONS

The work presented in this dissertation has been presented at the launch and conference of the Centre for Renewable Energy and Water (CREW) Vanderbijlpark October 2013, Oral presentation, *Polysaccharide membrane: A suitable material for selective removal of phenol-derivatives from wastewater*. The 41st South African Chemical Institute (SACI) national convention East London December 2013, Oral presentation, *Hydrophobic biomaterial composite for removal of 2-nitrophenol from aqueous solution*. ANALITIKA 2014 conference Parys September 2014, Poster presentation, *Effect of hexamethylene diisocyanate cross-linking on the adsorption of 2-nitrophenol onto Fenton's treated pine cone*.

ABSTRACT

The widespread use of phenols and phenolic derivatives in industrial applications has resulted in their discharge as part of industrial wastewater. These chemicals are toxic and need to be removed from the aqueous environment. Amongst the available pollutant removal technologies, adsorption has been widely used due to its simplicity, ease of operation, cost-effectiveness and ability to sequester pollutants at very low concentrations. Different adsorbents have been applied for removal of phenols and their derivatives. Use of agricultural waste as adsorbents seems to offer a much cheaper alternative in pollutant removal. This study examines the synthesis of a hydrophobic biomaterial composite by cross-linking of Fenton treated pine cone and applying the prepared adsorbent for 2-nitrophenol removal from aqueous solution.

Pine cone biomass, in its raw and modified forms was tested for its ability to remove 2-nitrophenol from simulated industrial wastewater. The experimental procedure is divided into two main parts: (1) pine cone modification using Fenton's reagent and 1.6-hexamethylene diisocyanate and (2) application of the prepared hydrophobic adsorbent for 2-nitrophenol removal from wastewater. Fenton's reagent was used to remove pigments, extractives and other soluble organic compounds from the raw pine. FTIR spectroscopy showed an increase in magnitude of oxygenated surface groups which resulted in a decrease in pH_{pzc}. The effect of Fenton treatment on further modification of the pine biomass via cross-linking using 1.6-hexamethylene diisocyanate was investigated. Optimum reaction variables for the cross-linking using dibutyltin dilaurate as catalyst under an inert nitrogen gas atmosphere in anhydrous hexane solvent were determined using FTIR spectroscopy. Success of the cross-linking procedure was confirmed by use of analytical techniques (XRD, TGA, SEM, EDX and BET surface area) and weight percent gain calculations.

Pine and modified pine biomass were tested for their ability to sequester 2-nitrophenol via batch adsorption technique. The effect of pine modification on affinity for the biosorbate was investigated. The mechanism of the adsorption process was determined via use of kinetic, diffusion and equilibrium isotherm models. Two error functions (coefficient of determination and percent variable error) were employed to substantiate the model showing a good fit to the experimental adsorption data.

The experimental adsorption kinetic data was fit to the pseudo-first-order and pseudo-second-order kinetic models. Due to the large size of the pollutant molecules diffusion process analysis was also conducted. The effect of pine modification on kinetic and diffusion parameters was determined.

The experimental equilibrium adsorption data was fit to the Freundlich, Redlich-Peterson and Hill isotherm models. The initial shapes of the adsorption isotherms for 2-nitrophenol adsorption onto pine and modified pine biomass determined the type of equilibrium isotherm models to fit the experimental data to. Thermodynamic parameters were calculated to determine the spontaneity, feasibility and energy changes associated with the adsorption process. The degree of disorder at the solid/liquid interface after the adsorption was determined. The effect of temperature on the adsorption process was used to show whether the adsorption is physical or chemical. The effect of pine modification on equilibrium isotherm parameters was determined.

The study is divided into seven chapters:

Chapter 1:
The chapter covers the introduction, problem statement, aim and objectives of the research. It gives an insight into the research project.

Chapter 2:
The literature review of pollutants in industrial wastewater and methods of their removal is dealt with in this chapter. Adsorption is introduced as an alternative technique for pollutant removal from aqueous systems. An in-depth review of various adsorbents (including pine cone), their merits and limitations are also discussed together with methods of modifying and use of modified adsorbents. Equilibrium, kinetic and thermodynamic models used to treat adsorption experimental data are presented.

Chapter 3:
The experimental procedures on the synthesis, characterization and application of the hydrophobic biosorbent in the removal of 2-nitrophenol from aqueous solution are presented. Kinetic and equilibrium experiments are described in detail.

Chapter 4:

It describes the first part of the results and discussions. The chapter focuses on optimization of reaction variables and characterization (using various analytical techniques) of the hydrophobic biomaterial composite.

Chapter 5

The chapter discusses the second part of the results. It focuses on magnitude of surface charge, pH_{pzc} and kinetic studies. Fitting of the adsorption experimental data to kinetic and diffusion models is presented together with the error functions.

Chapter 6

The chapter discusses part three of the results on equilibrium studies. The adsorption experimental data is fitted to equilibrium isotherm equations and error determination is presented. Thermodynamic parameters are calculated and interpreted.

Chapter 7:

Conclusion and recommendations are presented.

The optimum reaction variables for cross-linking of Raw and Fenton treated pine cone were determined using FTIR analysis and found to be: 0.2 g pine biomass, 3.5 cm^3 1.6-hexamethylene diisocyanate cross-linker, 50 cm^3 anhydrous hexane solvent, 1.5 cm^3 dibutyltin dilaurate catalyst, temperature of 50 °C and a reaction time of 4 hours. The pine surface showed an increase in phenolic, lactonic and carboxylic acid groups due to the modification. The pH_{pzc} showed a decrease due to modification of the pine cone biomass. The pH_{pzc} values for the pine and modified pine cone biomass were found to be: Raw = 7.49, Raw-HMDI modified = 6.68, Fenton treated pine = 5.40 and Fenton-HMDI modified = 6.12. The optimum pH for the adsorption of 2-nitrophenol onto raw pine and modified pine cone biomass was determined to be 6. The optimum adsorbent dosage was determined as 1.5 g/dm^3. The adsorption kinetics show a good fit with the pseudo-second-order model. This suggests that surface adsorption is the controlling step in the adsorption of 2-nitrophenol onto pine cone biomass. The analysis of diffusion processes showed that the initial rapid stage during the adsorption is due to external mass transfer processes. The adsorption experimental data also showed that pore diffusion was rate-limiting amongst the diffusion processes. Pine

modification using Fenton's reagent and 1.6-hexamethylene diisocyanate increased magnitude of kinetic and diffusion parameters. Experimental data for 2-nitrophenol adsorption onto pine and modified pine cone biomass showed better correlation with the Redlich-Peterson and Hill isotherm models and poor correlation with the Freundlich isotherm model. This suggests that the mechanism does not show complete multilayer coverage with cooperative phenomena between adsorbate molecules. Thermodynamic parameters showed that the adsorption is feasible, spontaneous, and exothermic and results in a decrease in degree of disorder at the solid/liquid interface. An increase in temperature resulted in a decrease in adsorption capacity showing that the adsorption is physical. Pine modification using Fenton's reagent and 1.6-hexamethylene diisocyanate increased magnitude of kinetic, diffusion and isotherm parameters. The kinetic and equilibrium results show that the adsorption of 2-nitrophenol onto pine cone biomass follows the order: Fenton treated-HMDI > Fenton treated > Raw-HMDI > Raw. Hence, it can be concluded that Fenton treatment and HMDI cross-linking modification did increase the adsorptive capabilities of the pine cone biomass.

TABLE OF CONTENTS

LISTS OF ABBREVIATIONS AND SYMBOLS

q_e	Equilibrium capacity
q_t	Equilibrium capacity at time t
k_1	Pseudo-first order rate constant
k_2	Pseudo-second order rate constant
$t^{0.5}$	The time in min raised to the power of 0.5
r^2	Coefficient of determination
C_o	Initial Concentration
C_e	Equilibrium concentration
m	Mass of the adsorbent
V	Solution volume
% R	Percentage removal
h	The initial sorption rate
S_{xx}	Sum of square of x
S_{yy}	Sum of square of y
S_{xy}	Sum of square of x and y
$q_{e,m}$	Equilibrium capacity obtained by calculating from model
BET	Brunauer-Emmett-Teller
EDX	Electron dispersive spectroscopy
FTIR	Fourier-transform infrared spectroscopy
HMDI	Hexamethylene diisocyanate
SEM	Scanning electron microscopy
TGA	Thermogravimetric analysis
UV-vis	Ultra-violet-visible spectroscopy
WPG	Weight percent gain
XRD	X-ray diffraction

LISTS OF FIGURES

Chapter 2

Chapter 3

Chapter 4

Chapter 5

Chapter 6

LISTS OF TABLES

Chapter 2

Chapter 4

Chapter 5

Chapter 6

1 INTRODUCTION

1.1 INTRODUCTION

The use of phenol and its derivatives in chemical, petroleum, dye and pesticide industries has resulted in the discharge of toxic effluent in potable waters (Lua and Jia, 2009). Phenols are toxic to life even when they are present in very low concentrations. These pollutants have been found to have carcinogenic and mutagenic effects on living organisms. Strict legislation on discharge of toxic pollutants in industrial wastewaters makes it paramount to develop efficient technologies for their removal. A number of methods have been used for the removal of phenols from industrial wastewaters. These techniques include advanced oxidation, electrochemical oxidation, biological degradation, photo-catalytic degradation, membrane filtration, and adsorption (Annachhatre and Gheewala, 1996; Rzeszutek and Chow, 1998; Nevskaia et al., 1999; Rodgers et al., 1999; Esplugas et al., 2002; Dabrowski et al., 2005; Guo et al., 2006). Among these removal technologies, adsorption has been widely used. The design and operation of adsorption systems is not complicated as is the case with some of the separation technologies earlier mentioned.

Adsorbents of biological origin have been found to be efficient in the removal of pollutants at very low concentrations but are limited by their low extraction capacities, poor mechanical strength and selectivity for targeted pollutants. Organic-based adsorbents produced by cross-linking biological materials with carbon nanotubes have been used for water treatment (Salipira et al., 2008). Although these adsorbents are extremely efficient, the large scale production of these co-polymers does not provide a viable economic alternative due to the exorbitant cost of producing the carbon nanotubes (Li et al., 2003). This research seeks to synthesize a low cost polysaccharide-based biosorbent with improved extraction capacities and selectivity using Fenton treated cross-linked pine cone as a replacement for current conventional methods of removing phenols from aqueous media.

1.2 PROBLEM STATEMENT

Different biosorbents from agricultural waste products have been prepared and applied for wastewater treatment. These materials though effective, show some major drawbacks which

include: (1) low biosorption capacities for pollutants, (2) poor selectivity for target pollutants, (3) biologically unstable (degrade rapidly), (4) possess poor mechanical properties in a packed column and (5) leaching of pigments and extractives resulting in discolouration of treated water and an increase in total organic carbon, biological and chemical oxygen demand (Gaballah et al., 1997). This research seeks to improve on the above weaknesses by use of Fenton's reagent to remove soluble organics from the pine cone biomass and incorporating a bi-functional cross-linker (1.6-hexamethylene diisocyanate) onto the biomass and apply the synthesized hydrophobic biosorbent for removal of 2-nitrophenol from simulated industrial wastewater. The research seeks to compare the effect of Fenton treatment of pine cone on cross-linking with 1.6-hexamethylene diisocyanate. Cross-linkers have the advantage of increasing the number of sorption sites for pollutant removal, thus improving, the capacities and selectivity's for the target pollutant from aqueous solution, the biological stability and mechanical strength of the matrix. The use of chemical modification to improve the adsorption potentials of pine cone biomass for industrial wastewater treatment is scanty in literature and much research has not been carried out in this area.

1.3 AIM

This research aims to synthesize a cost-effective hydrophobic biosorbent from cross-linked Fenton treated pine cone biomass and apply it in the removal of 2-nitrophenol from aqueous solution by achieving the following research objectives:

1. To prepare the pine cone powder material.
2. Synthesis of the hydrophobic cross-linked pine cone biosorbent using 1.6-hexamethylene diisocyanate.
3. Optimizing the preparation conditions for these modification methods.
4. Application of the produced biosorbent for removal of 2-nitrophenol from aqueous solution in a batch adsorption system.
5. Perform equilibrium, kinetic and thermodynamic analysis on the experimental adsorption data.

1.4 RESEARCH OUTLINE

The research focuses on Fenton treatment of pine cone and its modification via cross-linking using 1.6-hexamethylene diisocyanate. The dissertation is divided into three parts, with the first part describing the adsorption process, types of adsorbents and their applications,

composition of agricultural wastes and treatment of adsorption experimental data. The second part describes the synthesis of the hydrophobic biomaterial composite via Fenton treatment and cross-linking of the pine biomass. The third part involves application of the prepared biosorbent for the removal of 2-nitrophenol from aqueous solution. It describes kinetic and equilibrium adsorption experiments whose results are used to determine the adsorption mechanism and calculate thermodynamic parameters.

1.5 REFERENCE

1. ANNACHHATRE, A.P. and GHEEWALA, S.H. (1996) Biodegradation of chlorinated phenolic compounds, *Biotechnology Advances*. 14(1), pp. 35-36.

2. DABROWSKI, A., PODKOSCIELNY, P., HUBICKI, Z. and BARCZAK, M. (2005) Adsorption of phenolic compounds by activated carbon-a critical review, *Chemosphere*. 58(8), pp. 1049-1070.

3. ESPLUGAS, S., GIMENEZ, J., CONTRERAS, S., PASCUAL, E. and RODRIGUEZ, M. (2002) Comparison of different advanced oxidation processes for phenol degradation, *Water Research*. 36(4), pp. 1034-1042.

4. GABALLAH, I., GOY, D., ALLAIN, E., KILBERTUS, G. and THAURONT, J. (1997) Recovery of copper through decontamination of synthetic solutions using modified barks, *Metallurgical and Materials Transactions*. B 28(1), pp. 13–23.

5. GUO, Z.F., MA, R.X. and LI, G.J. (2006) Degradation of phenol by nanomaterial TiO_2 in wastewater, *Chemical Engineering Journal*. 119(1), pp. 55-59.

6. LI, W.Z., WEN, J.G., SENNETT, M. and REN, Z.F. (2003) Clean double-walled carbon nanotubes synthesized by chemical vapour deposition, *Chemical Physics Letters*. 368(3-4), pp. 299-306.

7. LUA, A.C. and JIA, Q.P. (2009) Adsorption of phenol by oil-palm-shell activated carbons in a fixed bed, *Chemical Engineering Journal*. 150(2-3), pp. 455-461.

8. NEVSKAIA, D.M., SANTIANES, A., MUNOZ, V. and GUERRERO-RUIZ, A. (1999) Interaction of aqueous solutions of phenol with commercial activated carbons: an adsorption and kinetic study, *Carbon*. 37(7), pp. 1065-1074.

9. RODGERS, J.D., JEDRAL, W. and BUNCE, N.J. (1999) Electrochemical oxidation of chlorinated phenols, *Environmental Science & Technology*. 33(9), pp. 1453-1457.

10. RZESZUTEK, K. and CHOW, A. (1998) Extraction of phenols using polyurethane membrane, *Talanta*. 46(4), pp. 507-519.

11. SALIPIRA K.L., MAMBA B.B., KRAUSE R.W., MALEFETSE T.J. and DURBACH S.H. (2008) Cyclodextrin polyurethanes polymerized with carbon

nanotubes for the removal of organic pollutants in water, *Water SA*. 34(1), pp. 113-118.

2 LITERATURE REVIEW

2.1 POLLUTANTS IN INDUSTRIAL WASTEWATER

Anthropogenic activities and advances in technology have immensely contributed to contamination of water resources around the world. Freshwater pollution is mainly caused by release of municipal and industrial effluent together with run-off from agricultural activity (Bhatnagar and Sillanpää, 2010). Industrial effluents have been found to be major contributors of heavy metals and dyes (Banat et al., 1996; Reddy et al., 2011). Heavy metals, being non-biodegradable tend to bioaccumulate at each trophic level in the ecological food chain damaging the ecosystem (Crini, 2005). Aromatic compounds are recalcitrant, toxic and mutagenic to various organisms (Lee et al., 2003). Synthetic dyes strongly colour industrial wastewater and colour greatly reduces the aesthetics of water (Banat et al., 1996).

2.1.1 Heavy metals

'Heavy metals' are a group of metals and metalloids whose atomic density is greater than 6 g/cm^3. Unlike most organic pollutants, there is always a normal background concentration of heavy metals in the environment as they occur naturally in mineral ores. Industrial uses of metals and other domestic processes (e.g. burning of fossils, incineration of wastes, automobile exhausts, smelting processes and the use of sewage sludge as landfill material and fertiliser) do introduce substantial amounts of toxic heavy metals into the hydrosphere (O'Connell et al., 2008). Several industrial disasters have also led to heavy metal contamination of water bodies such as the Minamata tragedy in Japan due to methyl mercury contamination and 'Itai-Itai' (Japanese for agony) due to contamination of cadmium in Jintsu river of Japan (Nordberg, 1974; Kjellstrom et al., 1977). Natural processes like weathering of rocks and volcanic eruptions also release heavy metals into the environment. Table 2.1 outlines major anthropogenic sources of heavy metals in the ecosystem.

Table 2.1 Significant anthropogenic sources of metals in the environment (O'Connell et al., 2008).

Industry	**Metals**	**Pollution arising**
Metalliferous mining		
Mineral ores	Cd, Cu, Ni, Cr, Co, Zn.	Acid mine drainage, tailings (mine dumps) and slag heaps.
Agricultural materials		
Fertilisers	Cd, Cr, Mo, Pb, U, V, Zn.	Run-off, surface and groundwater contamination, plant bioaccumulation.
Manure sewage sludge	Zn, Cu, Ni, Pb, Cd, Cr, As, Hg.	Landspreading threat to ground and surface water.
Metallurgical industries		
Specialist alloys and steels	Pb, Mo, Ni, Cu, Cd, As, Te, U, Zn.	Manufacture, disposal and recycling of metals. Tailings and slag heaps.
Waste disposal		
Landfill leachate	Zn, Cu, Cd, Pb, Ni, Cr, Hg.	Landfill leachate, contamination of ground and surface water.
Engineering		
Electronics	Pb, Cd, Hg, Pt, Au, Cr, As, Ni, Mn.	Aqueous and solid metallic waste from manufacturing and recycling process.
Metal finishing industry		
Electroplating	Cr, Ni, Zn, Cu.	Liquid effluents from plating processes.
Miscellaneous sources		
Batteries	Pb, Sb, Zn, Cd, Ni, Hg.	Waste battery fluid, contamination of soil and groundwater.
Paints and pigments	Pb, Cr, As, Ti, Ba, Zn.	Aqueous waste from manufacture, old paint deterioration and soil pollution.

While many of the heavy metals are needed by organisms in very minute quantities, higher concentrations are known to produce a range of physiological, gastro-intestinal, immunological and neurological effects. The most dangerous heavy metals include the 'toxic trio': lead, cadmium and mercury, for which no biological function has yet been found (Chojnacka, 2010). Other heavy metals of concern to environmental scientists and engineers are chromium, iron, selenium, vanadium, copper, nickel, arsenic, zinc, etc. These heavy metals are of specific concern due to their toxicity, bioaccumulation tendency, long persistence and biomagnification in food chains causing ecological disequilibrium (Garg et al., 2007; Vaughan et al., 2001; Zhou et al., 2004; Celik and Demirbas, 2005).

At high exposure levels, lead causes encephalopathy, cognitive impairment, behavioural disturbances, kidney damage, disruption to biosynthesis of haemoglobin causing anaemia and toxicity to the reproductive system (Pagliuca and Mufti, 1990). Cadmium is associated with nephrotoxic effects and long-term exposure may cause bone damage (Friberg, 1985). High concentrations of mercury can lead to neurobehavioral disorders like rheumatoid arthritis (autoimmune disease) and developmental disabilities including dyslexia, attention deficit hyperactivity disorder (ADHD) and intellectual retardation (Weiss and Landrigan, 2000). Chromium is widely recognised to exert toxic effects in its hexavalent form. Potable waters containing more than 0.05 mg/dm^3 Cr^{6+} are considered toxic (Baral and Engelken, 2002). Human exposure to Cr^{6+} compounds is associated with a higher incidence of respiratory cancers (Rowbotham et al., 2000). Excessive copper concentration can lead to lethargy, insomnia, Wilson's disease, anorexia and damage to gastro-intestinal tract (Theophanides and Anastassopoulou, 2002).

As a result of development of advanced analytical techniques and better health monitoring technologies, the acceptable maximum concentration (fraction of mg/dm^3 or µg/dm^3) of these metal ions in industrial wastewaters is progressively decreasing (Sud et al., 2008; Chojnacka, 2010). This and stringent regulations ensure industries treat metal-contaminated effluent before discharging it into natural water-bodies. Wastewater regulations were established to minimise human and environmental exposure to hazardous chemicals (Barakat, 2011).

2.1.2 Aromatic compounds

Most common aromatic pollutants found in industrial wastewater are phenolic derivatives (such as nitrophenols, chlorophenols, etc) and polycyclic aromatic compounds (especially pesticides) (Crini, 2005). They have been classified as priority pollutants since they are persistent, toxic, mutagenic, tumorogenic and carcinogenic to organisms even at low concentrations. For example, compounds such as 2.4.6-trinitrotoluene (TNT) which has been widely used in the weapons industry for bomb and grenade production have been found to be very lethal to organisms (Lee et al., 2003). Contamination of potable water by phenolics at low concentrations like 0.005 mg/dm^3 brings about significant taste and odour problems making it unfit for human use. The most important and common pesticide pollutants are organochlorine compounds like dichlorodiphenyltrichloroethane and its metabolites (DDTs), polychlorinated biphenyls (PCBs), hexachlorocyclohexane isomers (HCHs), hexachlorobenzene (HCB), cyclodienes, dieldrin, etc which are mostly used in households and in agriculture. The lipophilic nature, hydrophobicity, low chemical and biological degradation rates of these aromatic pollutants leads to their bioaccumulation, bioconcentration and biomagnification in higher organisms (Aksu, 2005).

2.1.3 Synthetic dyes

Dyes strongly colour water causing an aesthetic problem and public perception of water quality is greatly influenced by colour (Choy et al., 2004). There are more than 100 000 commercial dyes with more than 7×10^8 kg being produced annually (Pearce et al., 2003). According to Greluk and Hubicki (2010), dyes can be classified into three categories: (1) anionic – acid, direct and reactive dyes, (2) cationic – basic dyes, and (3) non-ionic – disperse dyes. They are used in textile, paper, plastic, pharmaceutical, leather, paint, food packaging and other industries to colour products. Wastewater containing dyes is very difficult to treat since they are carcinogenic, highly soluble, recalcitrant organic molecules, resistant to aerobic digestion and are stable to light, heat and oxidising agents (Sun and Yang, 2003). This is due to their complex chemical structure, xenobiotic nature and synthetic organic origin (Crini, 2006). Disposal of dye wastewater without proper treatment causes a myriad of problems to the aquatic environment, such as reducing gas solubility, light penetration and photosynthesis. Dyes may also be toxic to some aquatic life due to presence of aromatics, metals, chlorides and other elements in them (Fu and Viraraghavan, 2001). Traditional

biological wastewater treatment techniques based on aerobic and anaerobic digestion are not efficient at dye removal from wastewater since dyes are toxic to the organisms being used (Kušić et al., 2007). Dye-wastewater is usually treated by physical and chemical methods.

2.2 TECHNOLOGIES FOR INDUSTRIAL WASTEWATER TREATMENT

Water is a unique substance which is able to cleanse itself via dilution and sedimentation. This natural process is inhibited at high pollutant concentrations found in industrial wastewaters. Physical, chemical and biological techniques have been applied for treatment of industrial wastewaters. Conventional methods for removal of metal ions and organics from aqueous solutions include chemical precipitation, ion-exchange, chemical oxidation/reduction, reverse osmosis, electrodialysis, nanofiltration, electrochemical treatment, solvent extraction, aerobic and anaerobic treatment, microbial reduction, adsorption etc (Shen and Wang, 1994; Gardea-Torresdey et al., 1998; Zhang et.al, 1998; Bell et al., 2000; LaPara et al., 2000; Lin and Juang, 2002; Van der Bruggen and Vandecasteele, 2003; Lee et al., 2003; Martínez et al., 2003). These conventional techniques have their own limitations such as less efficiency, sensitive operating conditions, use of aggressive reaction conditions, high reagent or energy requirements, production of toxic sludge and other waste products which are costly to dispose (Ahluwalia and Goyal, 2005; Izanloo and Nasseri, 2005). There is also a possibility that a secondary pollution problem will arise due to excessive chemical use. Amongst the numerous techniques of pollutant removal from aqueous solutions, adsorption is the best procedure for wastewater decontamination due to convenience, ease of operation, simplicity of design and results in high-quality treated effluent (Jain et al., 2003; Zhou et al., 2004; Bhatnagar and Sillanpää, 2011). Furthermore, adsorption can remove or minimise different types of pollutants from dilute solutions to $\mu g/dm^3$ (ppb) levels broadening its application in water pollution control.

2.2.1 Chemical precipitation

Coagulants such as alum, lime, limestone and iron salts are able to precipitate metal ions from aqueous solutions. The most widely used chemical precipitation method of removing heavy metals from inorganic effluents is to increase the pH of the effluent (to about pH 9-11), thus converting the soluble metal into an insoluble hydroxide (O'Connell et al., 2008). The

conceptual mechanism of heavy metal removal by chemical precipitation is represented in Equation (2.1) below (Wang et al., 2004):

$$M^{n+} + n(OH)^{-} \leftrightarrow M(OH)n \downarrow \quad (2.1)$$

where, M^{n+} and OH^{-} represent the dissolved metal ions and the precipitant, respectively, while $M(OH)_n$ is the insoluble metal hydroxide. Chemical precipitation is not metal selective and requires a large amount of chemicals to reduce metals to an acceptable level for discharge. Main disadvantage of the technique is production of large amounts of sludge which might be toxic or expensive to dispose (Aderhold et al., 1996). Other drawbacks include slow metal precipitation, poor settling and the aggregation of metal precipitates (Aziz et al., 2008).

2.2.2 Ion-exchangers

Ion-exchange resins possess active ion groups such as sulphonic, amino and carboxylic acids. These active ion groups exchange their ions for metal ions in dilute solutions. They are highly selective depending on the active ion group that they possess. The resins can be classified as cationic, anionic or amphoteric exchange resins. Ion-exchangers are capable of reducing metal ion concentrations to parts per million levels. Limitations of ion-exchangers include: (1) their regeneration creates sludge disposal problem, (2) require high-tech operation and maintenance which is expensive, (3) sensitivity to effluent pH, (4) failure to handle concentrated metal solutions as the matrix gets easily fouled by organics and other solids in the wastewater (Barakat, 2011); and (5) presence of competing mono- and divalent ions such as Na^{+} and Ca^{2+} which inhibits their activity (Rengaraj et al., 2001; Mohan and Pittman, 2007).

2.2.3 Membrane processes

There are different techniques of membrane filtration such as reverse osmosis, ultrafiltration, nanofiltration and electrodialysis (Pedersen, 2003; Barakat, 2011). The processes involve ionic concentration by the use of selective membrane with a specific driving force. Membrane processes have been proven as an effective wastewater metal decontamination

technology. Advantages include low solid waste generation and low chemical consumption. The methods are expensive and require a high level of technical expertise to operate (Ning, 2002).

2.2.4 Electrochemical treatment

A current is passed through an aqueous metal-bearing solution containing a cathode plate and an insoluble anode. Metallic ions are electrically discharged and accumulate at the cathode. The technology does not require chemicals and can be engineered to tolerate suspended solids. It is moderately metal selective and treats effluent to >2000 mg/dm^3. Demerits include production of hydrogen gas (with some processes), electrode corrosion and high initial capital cost (Kongsricharoern and Polprasert, 1996).

2.2.5 Adsorption

Adsorption is an equilibrium separation process (Dabrowski, 2001) in which molecules/ions (adsorbate) are attached onto the surface of another material (adsorbent or substrate). It involves accumulation of adsorbate from a bulk solution onto the external and internal surfaces of the adsorbent. Adsorption based techniques are non-denaturing, highly selective, energy efficient and relatively inexpensive because of convenience, ease of operation and simplicity of design. They are used for bulk separation and purification in food, pharmaceuticals and chemical industries (Barkakati et al., 2010). Current research is focused on application of adsorption techniques to remove non-biodegradable pollutants (heavy metal ions and organics) from wastewater (Ho and McKay, 2003).

At the surface of the adsorbent, there are unbalanced forces of attraction which are responsible for the adsorption process. This process involves various interactions such as hydrophobic, electrostatic attraction, hydrogen bonding etc. Depending on type of interactions between adsorbate and adsorbent, three types of adsorption can be distinguished from each other: (1) physisorption, (2) chemisorption, and (3) exchange adsorption.

2.2.5.1 Physisorption

It is due to van der Waals' forces of attraction and is reversible due to low activation energy. Either monolayer or multilayer adsorption can occur during physical adsorption.

2.2.5.2 Chemisorption

Chemisorption results in formation of a chemical bond (usually covalent) and is irreversible. The process is highly specific since a chemical bond need to be formed between adsorbate and adsorbent. Only monolayer adsorption takes place during chemisorption.

2.2.5.3 Exchange adsorption or ion-exchange

The process involves exchange of ions from adsorbent surface with adsorbate ions having charges of the same magnitude but greater affinity. It is generally reversible and proceeds stoichiometrically (Khan, 1992).

2.3 TYPES OF ADSORBENTS

Most synthetic adsorbents are expensive, regenerative and non-biodegradable since they are petrochemically derived (Wing, 1996a; Wilpiszewska and Spychaj, 2007). Adsorbents can be of mineral, organic or biological origin (Crini, 2005). Mineral adsorbents include activated carbon (Pereira, 2003), red mud (López et al., 1998), silica beads (Krysztafkiewicz et al., 2002; Ghoul et al., 2003), clays, etc (Celis et al., 2000; Yavuz et al., 2003). Organic polymer resins (Atia et al., 2003) and cyclodextrin urethanes (Salipira et al., 2008) are some of the organic adsorbents that have been used in decontamination of wastewaters. Biological adsorbents can be micro-organisms (Aksu et al., 1992; Loukidou et al., 2003; Malkoc et al., 2003; Pearce et al., 2003) or agricultural by-products (Acar and Malkoc, 2004; Reddad et al., 2003; Ho and Ofomaja, 2006; Ghodbane et al., 2008; Awwad and Salem, 2012).

2.3.1 Commercial adsorbents

Adsorbents that are being used in water pollution control include activated carbon, zeolites, silica gel and activated alumina, etc.

2.3.1.1 Activated carbon

Activated carbon is a form of graphite with an amorphous, highly porous structure with a broad range of pore sizes (Hamerlinck, 1994). It is produced by raw material dehydration and carbonisation followed by activation. Activated carbon is a versatile adsorbent with a large surface area and is able to remove different types of pollutants such as metal ions, anions, dyes, phenols, detergents, pesticides and chlorinated hydrocarbons (Perez-Candela et al., 1995; Bele et al., 1998; Bao et al., 1999; Chern and Chien, 2002; Sotelo et al., 2002; Pereira et al., 2003). Adsorption using activated carbon is a powerful technology for treating industrial wastewater (Horikoshi et al., 1981; Hosea et al., 1986) but, its use is restricted by high cost involved during its synthesis and its loss during regeneration.

2.3.1.2 Zeolites

Zeolites are crystalline, hydrated aluminosilicates of alkali and alkaline earth metals, having infinite, three-dimensional structures (Mohan and Pittman, 2007). The three-dimensional structure of zeolite possesses large channels containing negatively charged sites resulting from Al^{3+} replacement of Si^{4+} in the tetrahedral. Zeolite-based materials are mainly used for manufacture of detergents, ion-exchange resins (water softeners), catalysts in the petroleum industry, separation process (molecular sieves) and as adsorbent for water, hydrogen sulphide and carbon dioxide. They can be natural or synthetic but both types are selective adsorbents for the removal of metal ion pollutants in wastewater (Ellis and Korth, 1993; Okolo et al., 2000; Meteš et al., 2004; Wang and Peng, 2009).

2.3.1.3 Silica gel

Silica gels are amorphous forms of silicon dioxide and are classified into three types: regular, intermediate and low density gels. Regular density silica gel shows high surface area (about 750 m^2/g). Intermediate and low density silica gels have low surface areas, that is, 300-350 and 100-200 m^2/g (Bhatnagar and Sillanpää, 2010). Silica gels are utilized in dehumidification process due to their great pore surface area and good adsorption capacity (Chang et al., 2008). Modified forms of silica have been used for the sequestration of different pollutants (Ahmed and Ram, 1992; Backhaus et al., 2001).

2.3.1.4 Activated alumina

Activated alumina consists of forms of partially hydroxylated alumina oxide, Al_2O_3. It is prepared by thermal degradation of aluminium hydroxide thus removing hydroxyl groups and forming a porous solid structure. Activated alumina is used in dehydration of organic liquids like gasoline, kerosene, oils, aromatic hydrocarbons and chlorinated hydrocarbons (Kasprzyk-Hordern, 2004).

2.3.2 Low-costs adsorbents

An adsorbent can be considered low-cost if it requires little processing, is abundant in nature or is a by-product or waste material from another industry (Bailey et al., 1999). These include: micro-organisms, industrial by-products and agricultural wastes.

2.3.2.1 Micro-organisms

Micro-organisms (fungi, algae and bacteria) are eco-friendly, low-cost and effective biosorbents in wastewater decontamination (Das et al., 2008). Substantial research has been conducted on the use of live and dead microbial cells as biosorbents for pollutant removal from wastewater. Use of dead microbes is advantageous because: (1) they do not need a constant supply of nutrients hence a decrease in the levels of chemical oxygen demand and biological oxygen demand, (2) the biosorbents can be easily regenerated and re-used for a number of cycles, and (3) dead microbes are not affected by toxic waste. Many yeast, algae and bacteria have shown capability to remove metal ions from dilute aqueous solutions (Aksu et al., 1990; Vymazal, 1990; Kapoor and Viraraghavan, 1995; Nuhoglu et al., 2002). Dead cells are able to remove heavy metal ions to the same or greater extent than living cells. The reason for this is the inhibition of microbial growth when concentration of metal ions becomes high or when significant amounts of metal ions have been sorbed by the micro-organisms (Aksu et al., 1991). Cell walls of eubacteria are made up of a polysaccharide called peptidoglycan and that of archaebacteria consists of the polysaccharide pseudomurein. The fungal cell walls are made from the polysaccharides chitin and chitosan. Algae cell walls are mainly cellulose. These polysaccharides have functional groups (amino, amido, carboxyl, hydroxyl, phosphate and sulphate) which can act as biosorption active sites for metal immobilization (Vieira and Volesky, 2000; Davis et al., 2003). Metal uptake by different parts of inactive microbial cells is a complex phenomenon. It can occur via different passive

processes including complexation, chelation, co-ordination, ion-exchange, precipitation and reduction (Tsezos and Remoudaki, 1997). The metal adsorption kinetics has been proposed to take place in two stages. The first rapid stage, thought to be physical adsorption or ion-exchange at the cell surface. The subsequent stage is slower and called chemisorption (Aksu et al., 1990; Vymazal, 1990). Chemicals isolated from the microbial biomass (e.g. chitin, chitosan and alginate) are also used as biosorbents (Chojnacka, 2010).

2.3.2.2 Industrial by-products

Industrial activities in power generation, metallurgy, fertiliser, paper, and leather industries produce huge amounts of solid waste. Use of these industrial by-products as low-cost adsorbents reduces the volume of waste materials and pollution of industrial wastewaters. Some of the industrial wastes products that have been investigated as adsorbents for sequestration of heavy metal ions include fly ash, metallurgical slag, red mud, activated sludge, etc (Dimitrova, 1996; López et al., 1998; Alinnor, 2007).

2.3.2.3 Agricultural wastes

Agricultural by-products are high volume, low value and underutilized biopolymers. Wing (1996b), reported that agricultural by-products exceed 320 billion kilograms annually in the United States alone. This poses a serious environmental disposal problem. Their use in adsorption might contribute significantly to environmental protection and additional income to farmers. Use of agricultural by-products as sorbents is a cost effective alternative for wastewater treatment. Usually, the biomass that one would not suspect to have biosorptive properties can show ability to effectively remove metal ions from solution, for example, crushed egg shells, bones, etc (Kuyukac, 1997; Aksu, 2005). Table 2.2 shows some agricultural wastes that have been used as adsorbents for the sequestration of divalent heavy metal ions, chlorinated phenols and dyes.

Table 2.2 Agricultural wastes as adsorbents for decontamination of industrial wastewater (Bhatnagar and Sillanpää, 2010).

Adsorbent	**Adsorbate**	**Adsorption capacity (mg/g)**
Rice husk	p-chlorophenol	14.36
Coffee residue	Pb^{2+}	63
Orange peel	Ni^{2+}	158
Mango peel	Pb^{2+}	99.05
Garlic peel	Methylene blue	86.64 – 142.86
Sunflower stalks	Basic red 9	317
Maize cob	2.4-dichlorophenol	17.94
Coconut	2.4.6-trichlorophenol	716.10
Sugarcane bagasse	Cd^{2+}	38.03
Cotton stalk	Remazol Black B	35.7
Banana peel	Phenolic compounds	689
Peanut husk	Neutral Red	37.5

2.4 MODIFICATION OF AGRICULTURAL WASTE BIOMASS

Agricultural waste products are used in treatment of industrial wastewater in their natural form or after modification. Biosorbent modification involves physical (usually thermal) or chemical manipulation of biomaterial surface properties such as type and amount of functional groups, surface area and porosity by extraction of chemical components. The use of untreated agricultural waste as biosorbents results in high chemical and biological oxygen demand caused by leaching of soluble organics , reducing content of oxygen in water thus threatening aquatic organisms (Gaballah et al., 1997). Hence, modification of biomass is essential to preventing colouration of treated wastewater and disintegration of biosorbent during prolonged contact with water (Bailey et al., 1999), thereby: (1) increasing the adsorption capacity of the biosorbent by swelling of the material to increase the internal and external surfaces (Wing, 1996b, Sciban et al., 2006), and (2) modifying biosorbent surface to increase cation exchange capacity (Marshall and Johns, 1996) and allow for penetration of polyfunctional organic moieties into the biosorbent matrix to increase sorption sites (Marshall et al., 1999; Wartelle and Marshall, 2000).

Agricultural waste materials show good reactivity since most are lignocellulosic (mainly contain lignin, hemicelluloses and cellulose). They possess acetamido, hydroxyl, carboxyl, carbonyl, phenolic, imine, amine, imidazole, thioether, phosphate, phosphodiester and sulphydryl functional groups (Vieira and Volesky, 2000; Robinson et al., 2002; Garg et al., 2003; Argun et al., 2008; Sud et al., 2008). These functional groups are able to undergo chemical derivatization via esterification, etherification, hydrolysis, enzymatic degradation, oxidation or grafting reactions.

A number of biomass modification techniques which include the use of mineral or organic acids (sulphuric acid, nitric acid, phosphoric acid, hydrochloric acid, citric acid, tartaric acid), strong bases (calcium hydroxide, sodium hydroxide, sodium carbonate), oxidising agents (Fenton's reagent, potassium permanganate), organic compounds (ethylenediaminetetraacetic acid, formaldehyde, epichlorohydrin), grafting and solvent extraction have been reported in literature by several authors (Wing, 1996a; Ahn et al., 1999; Wartelle and Marshall, 2000; Sciban et al., 2006; Basha and Murthy, 2007; Argun et al., 2009; Ofomaja et al., 2010a; Ofomaja et al., 2012; Reddy et al., 2012; Pholosi et al., 2013).

2.4.1 Base modification or mercerization

Pre-treatment with dilute sodium hydroxide solution has been the most widely used technique to improve surface properties and remove soluble organic compounds of plant wastes used for biosorption (Xuan et al., 2006; Li et al., 2007; Lu et al., 2008; Zhu et al., 2008). Sodium hydroxide treatment of lignocelluloses causes swelling of the biomass leading to an increase in internal surface area, separation of structural linkages between lignin and carbohydrates and disruption of lignin structure (Min et al., 2004; Ofomaja et al., 2009). This reduces extend of polymerization and crystallinity. Alkali solutions such as sodium hydroxide or calcium hydroxide are good reagents for saponification or the conversion of an ester linkage to carboxylic and alcohol functions. Swelling lignocellulosic materials in sodium hydroxide increases accessibility of cellulose hydroxyl groups (Gassan and Bledzki, 1999; Földváry et al., 2003; El Seoud et al., 2008). Ofomaja et al. (2009) applied both raw and sodium hydroxide modified pine cone powder for Cu^{2+} ions removal from aqueous solution. The authors noted that surface modification of pine cone with dilute sodium hydroxide solution affected quantities of carboxylic and phenolic functional groups, reduced pH_{pzc} from 7.49 to

2.55, increase in internal surface area of pine cone biomass and increased biosorbent capacity for Cu^{2+} ions with increase in sodium hydroxide concentration. Zhou and Banks (1993) also applied dilute sodium hydroxide as a base modifying agent to microbial (fungal) biomass. They observed that the biosorption capacity improved depending on duration of base treatment. The workers suggested that sodium hydroxide treatment could remove proteins and glucans from the cell wall thus increasing accessibility of chitin and cellulose which contain the functional groups acting as binding sites in biosorption process. Other researchers have also used dilute calcium hydroxide as a base modifying agent and shown its ability to increase agricultural waste metal ion sorption capacity (Dhakal et al., 2005; Ofomaja and Naidoo, 2011a). Biosorptive capacities of base modified agricultural wastes can be further enhanced by grafting of other organic moieties (Zhu et al., 2008).

2.4.2 Organic or mineral acid modification

Wong et al. (2003) modified rice husk with a variety of organic acids (nitriloacetic, citric, oxalic, salicylic, tartaric, malic and mandelic). The authors concluded that tartaric acid modification gave the biosorbent the highest metal sorption capacity for lead and copper ions in aqueous solution. A number of researchers have also treated lignocelluloses with carboxylic acids and applied the prepared biosorbents for divalent heavy metal decontamination of aqueous solutions with similar result (Marshall et al., 1999; Marchetti et al.; 2000a; Low et al., 2004; Altundogan et al., 2007; Li et al., 2007; Zhu et al., 2008). The researchers postulated that at elevated temperatures carboxylic acids produce carboxylic acid anhydrides, which combine with the cellulosic hydroxyl groups to form ester linkages and introduce carboxyl groups onto biosorbent surface as shown in Figure 2.1.

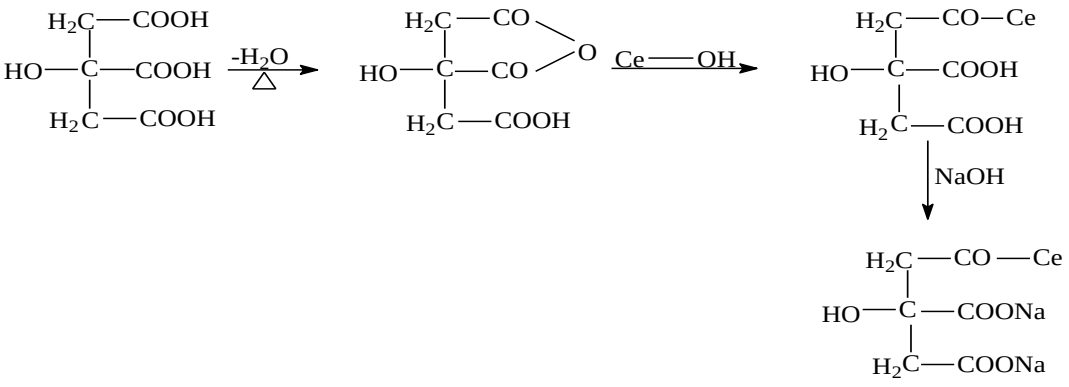

Figure 2.1 Thermochemical esterification of citric acid on cellulose (Ce – OH).

These additional carboxyl functional groups increase biomass binding capacity with positively charged metals. A decrease of 74 % and 80 % in copper and lead ion uptake by esterified tartaric acid modified rice husk supports the idea that the carboxyl functional groups play a crucial role in the sequestration of metal ions (Wong et al., 2003).

Mineral acids like hydrochloric, sulphuric, phosphoric and nitric acid have also been utilised by various researchers to investigate their effects on enhancing biosorptive capabilities of agricultural wastes (Garg et al., 2004; Leyva-Ramos et al., 2005; Argun et al., 2007; Lata et al., 2007; Sud et al., 2008; Wan Ngah and Hanafiah, 2008). Ofomaja et al. (2013) concluded that studies have shown that mineral acid treatment of biosorbents have very little or no impact on their surface properties.

2.4.3 Oxidation techniques

Carboxylic acid functionality is considered responsible for heavy metal binding through the phenomenon of ion-exchange (Kartel et al., 1999; Khotimchenko et al., 2007). Direct oxidation of polysaccharidic moieties increases their adsorption capacities by generating new carboxylate functions. Maekawa and Koshijima (1984), synthesized dialdehyde cellulose via periodate oxidation of cellulose. The dialdehyde cellulose was oxidised further by use of mildly acidified sodium chlorite to form 2.3-dicarboxy cellulose. Heavy metal adsorption capability of 2.3-dicarboxy cellulose was the explored. Uptake levels of 184 mg/g and 236 mg/g were noted for Ni^{2+} and Cu^{2+}, respectively. Harchem et al. (2012) demonstrated that adsorption capacities of crude polysaccharides (Douglas fir, argan tree bark and argan endocarp) are lower than those of carboxylic acid-functionalized biosorbents. This observation can be attributed to an increase in acidic functions and reduction in steric hindrance affecting accessibility of carboxylate groups. Figure 2.2 shows possible reaction pathways for oxidation of polysaccharides: route 1, selective oxidation of the primary alcohol by NaOBr catalysed by TEMPO [(2.2.6.6-tetramethylpiperidin-1-yl)oxidanyl]; route 2, periodic oxidation of cellulosic moiety and subsequent oxidation of aldehydic and primary alcohol functions.

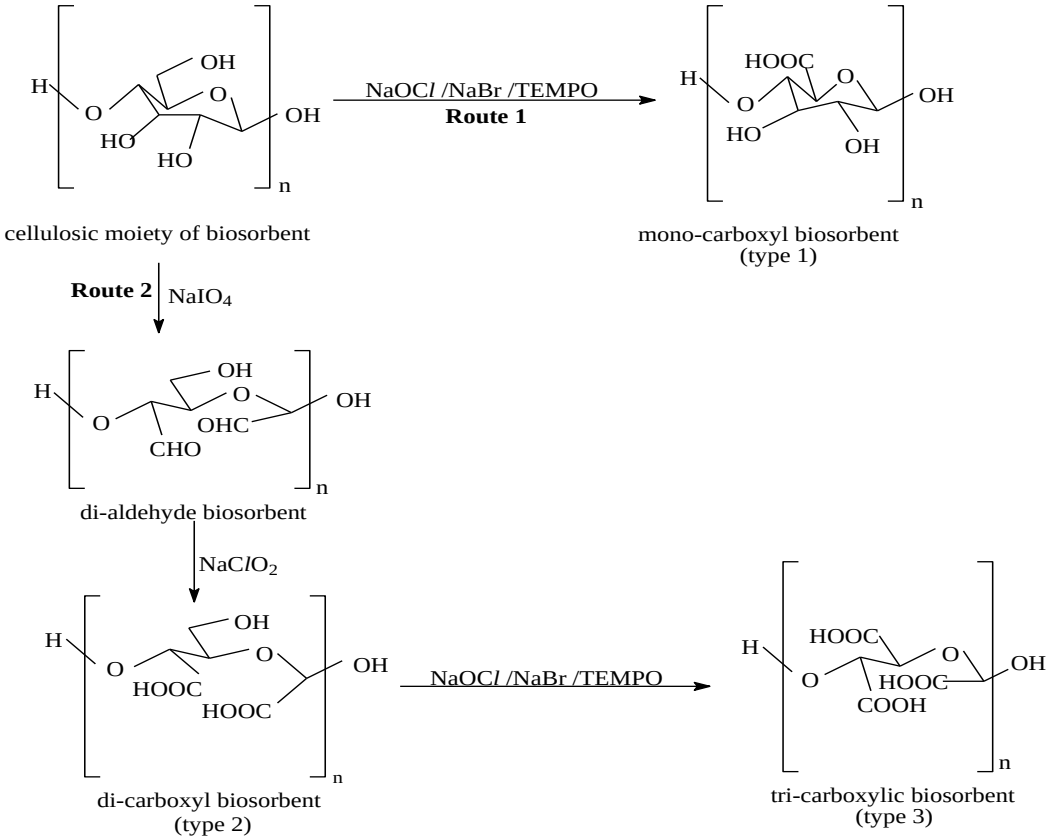

Figure 2.2 General scheme of carboxyl functionalization of polysaccharide biosorbent (Hachem et al., 2012).

Argun et al. (2008), used Fenton's oxidation reagents (Fe^{2+}/H_2O_2) to activate pine cone powder and successfully applied the prepared biosorbent for Cd^{2+} and Pb^{2+} ions removal from aqueous solution. The Fenton reaction results in rupture of oxidant (H_2O_2) forming highly reactive hydroxyl radicals which are able to degrade complex organics and phenolic structures (Walling, 1975; Ahn et al., 1999). The authors noted an increase in BET specific surface area, porosity and surface oxygenated groups which increase adsorption capacity of biosorbent. Lignin fraction increased while cellulosic, hemicellulosic materials and extractives content decreased. This change might be beneficial since earlier research by Gaballah and Kilbertus (1998) suggested that heavy metal adsorption takes place on lignin rather than on cellulose and hemicelluloses.

2.4.4 Solvent extraction

Chemical extraction has been used to remove plant extractives such as pigments, resin acids and soluble tannins in wood preservation (Papadopoulos et al., 2010). A number of

researchers have applied these methods for biosorbent modification. Sciban et al. (2006) reported formaldehyde-sodium hydroxide treatment of sawdust of oak and black locust hardwood and applied the modified biosorbents for removal of copper and zinc ions from aqueous solution. Marchetti et al. (2000b) extracted wood meal (*Picea abies*) with a toluene-ethanol mixture and applied the modified material as adsorbent for cadmium ions in solution. These authors reported an enhancement in metal sorption capacities and ability of these biosorbents to be further modified by grafting with polyfunctional organic acids and other modifying agents. Literature search revealed that Argun et al. (2009) modified pine bark using the following organic solvents tetra ethylene glycol, chloroform, acetone, ethanol, diethyl ether and glycol for toxic metal adsorption.

2.4.5 Grafting or coupling reactions

Grafting or graft co-polymerization involves attachment of a known functional group onto biosorbent surface to increase its pollutant binding capabilities. Grafting results in covalent attachment of side chains onto the main polymer backbone. Grafting can be initiated by chemical, photo-chemical, enzymatic, plasma-induced or high-energy ionizing radiation-induced methods (Bhattacharya and Misra, 2004). During grafting, oxygen removal is necessary since it is an efficient inhibitor of radical polymerization (Wojnárovits et al., 2010). The properties of the grafted co-polymer depend on the type of monomer used for grafting, the level of grafting, the length and distribution of the grafted chains (Wang and Xu, 2006). Ofomaja et al. (2012) showed that high grafting efficiency of acrylic acid onto Fenton's treated pine cone powder reduced biosorbent surface area due to higher density of the polymer chain on the biosorbent surface. Argun et al. (2009) reported grafting of pine bark with polyacrylamide and its application in the removal of Cd^{2+}, Pb^{2+}, Cu^{2+} and Ni^{2+} ions from aqueous solution.

2.4.6 Cross-linking modification

Cross-linking occurs when a reagent (cross-linking agent) introduces linkages between different polymer chains. The cross-linking agent can link the polymer chains (cross-linking step) and/or itself (self-polymerization step). Cross-linking causes a reduction in segment mobility and results in formation of a three-dimensional network by interconnection of

several polymer chains. Extend of reticulation determines solubility of the matrix in water and organic solvents (Crini, 2005). Shiftan et al. (2000) reported that cross-linking of polysaccharide-based materials is not homogenous and a high cross-linking density makes the material to become amorphous. Cross-linking density is controlled by the cross-linker concentration, duration of cross-linking procedure and temperature among other parameters. The cross-linked polymers are obtained by reticulation using bi- or polyfunctional cross-linking agents such as diisocyanates, carboxylic acids, ethylene glycol diglycidyl diether, gluteraldehyde, benzoquinone, maleic anhydride, phosphorus oxychloride or epichlorohydrin (Crini, 2005).

A number of novel cross-linking procedures have been reported. Güven et al. (1999) and Pekel et al. (2004) applied radiation to induce cross-linking of polysaccharides. Radiation treatment (ionizing radiation, gamma rays or electron beam) has merits over traditional cross-linking techniques. Cross-linking agents (or initiators) are not necessary and the reaction can be initiated at room temperature (Crini, 2005). In radiation treatment, cross-linking density is controlled by irradiation time (absorbed dose) and the reactions can be initiated in liquid and solid state whereas chemical treatment can only take place in liquids. However, cross-linking has both its advantages and limitations.

2.4.6.1 Advantages of cross-linking

Some merits of reticulating polysaccharide chains using polyfunctional cross-linkers have been discussed below:

- Reagents used are relatively cheaper and are available in a variety of configurations and structures with different properties.
- Cross-linked materials show insolubility in acidic and alkaline mediums as well as in organic solvents.
- Cross-linking results in polymers which are more resistant to low pH, high temperature and shear.
- Cross-linked materials retain their original properties (though the crystallinity changes) and are not affected by acidic or basic solutions. This is important for a biosorbent that can be used at different pH values.

- Cross-linking reduces crystallinity in the polymer and this influences its biosorption capabilities as it may improve the accessibility to the biosorption sites.

- Cross-linked materials show faster kinetics and improved diffusion properties. Since their cross-linking units exhibit hydrophilic character, the materials have a high swelling capacity in water. This swelling ability expands their diffusion networks facilitating faster pollutant diffusion.

- Cross-linked polysaccharides show good biosorption capabilities which can be improved by grafting different functions onto the polymer backbone resulting in increased density of biosorption sites. Introduction of new functional groups on the cross-linked polymer network causes an increase in surface polarity and hydrophilic character. This improves the removal of polar adsorbates and target pollutant selectivity.

- The cross-linked materials are usually regenerated easily via solvent extraction or washing.

2.4.6.2 Limitations of cross-linked materials

Despite their excellent biosorption capabilities, cross-linked polymer networks have not found wide-spread industrial use. A myriad of reasons are responsible for the failure to implement this technology at the industrial scale:

- Although cross-linking improves polysaccharide resistance towards acid, alkali and chemicals, it causes a reduction in hydrophilic nature, chain flexibility resulting in reduction of the chelating groups accessibility and mobility. This results in a decrease in biosorption capacity.

- Degree of cross-linking needs to be made as low as possible as it affects number of accessible sorption sites on the biosorbent and diffusion of pollutants thus affecting selectivity success.

- Reaction conditions need manipulation to suppress self-polymerization of the polyfunctional cross-linkers.

- Most cross-linking agents are neither safe nor environmentally friendly, for example, glutaraldehyde (a dialdehyde) contains cytotoxic chemical species and is a known neurotoxin (Berger et al., 2004).

2.5 BIOSORPTION

Biosorption (or bioadsorption) represents biotechnological innovation involving the removal of metal ion and organic pollutants through passive binding to biomass from an aqueous solution (Volesky, 2001). It is a novel approach, competitive, effective, non-hazardous and relatively inexpensive (Rafatullah et al., 2009). Biosorption, unlike bioaccumulation (based on active metabolic transport) is independent of cell metabolism as it is based upon physicochemical interactions between pollutants and surface functional groups. The major advantages of biosorption over conventional treatment methods include: low cost, high efficiency (can effectively sequester pollutants from dilute complex solutions), minimization of chemical or biological sludge, no additional nutrient requirement, regeneration of biosorbents and possibility of metal recovery from the sorbing biomass (Jalali et al., 2002; Basha and Murthy, 2007). Research into biosorption processes has increased over the years due to its potential application in environmental protection and/or recovery of precious or strategic metals (Volesky, 2007). The processes of biological metal binding have also been useful in biohydrometallurgy and biogeochemistry (Chojnacka, 2010). A major limitation of biosorption is the short life time of the biosorbent in comparison with commercial adsorbents (Bailey et al., 1999; Gadd, 2009)

2.5.1 Factors affecting biosorption

Interaction between metal pollutants and biosorbent functional groups is not only depended on nature of the biosorbent but also on the solution chemistry. The sorption capacity of the biosorbents strongly depends on experimental conditions such as solution pH, initial concentration of pollutant, temperature, biomass concentration, surface area (particle size), contact time (or residence time), competing ions (effluent composition), solubility of adsorbate in wastewater, affinity of solute for adsorbent and the hydrophobic character in the biosorption system (Bailey et al., 1999; Barkakati, et al., 2010).

2.5.1.1 pH of medium.

The most important variable affecting biosorption is solution pH (Aksu, 2005; Ho, 2005; Ofomaja and Naidoo, 2011b). Ucun et al. (2003) reported an increase from 6.73 to 53.6 % of lead ion sorption as solution pH increased from 2.0 to 4.0 using pine cone biomass. Solution pH determines protonation or deprotonation (magnitude of surface negative charge) of sorption sites and thus determines the availability of the site to the sorbate. Binding sites are available to metal ions only in deprotonated state (Ofomaja and Ho, 2007a). For pH values greater than the pK_a of the functional groups, sorption sites are mainly in dissociated form and can exchange H^+ ions with metal ions in solution. At pH values lower than pK_a of these groups complexation phenomenon can occur, especially for carboxylic groups (Fourest and Volesky, 1996). Binding sites (or cation exchange capacity) can be determined by potentiometric, volumetric, microscopic and spectroscopic techniques (Naja et al., 2006; Volesky, 2007). Solution pH also affects the speciation and biosorption availability of the sorbate (Ofomaja and Ho, 2007a). At high pH, metal ions can precipitate out of solution as metal hydroxides thus distorting the biosorption process (Argun and Dursun, 2008). By changing the pH, it is possible to release pollutants from the binding site (desorption). This property is used for the recovery of metal ions and/or regeneration of the biosorbent. Therefore, pH influences metal speciation in solution and surface charge of biomaterials (Ofomaja and Ho, 2007a).

2.5.1.2 Initial concentration of pollutant

It creates a concentration gradient necessary to overcome all mass transfer resistances of the pollutant between the bulk solution and surface of sorbent. Therefore, a higher initial concentration of pollutant may improve the biosorption process (Aksu, 2005). Jianlong et al. (2000) observed that the equilibrium sorption capacity of the activated sludge increased with increasing initial pollutant (pentachlorophenol) concentration up to 0.5 mg/dm^3. Aksu and Yener (2001) also observed that the equilibrium sorption capacity of the dried activated sludge for phenol, *o*-chlorophenol and *p*-chlorophenol increased with increase in initial pollutant concentration up to 500 mg/dm^3. The authors suggested that the increase of biosorption capacity with the increase in pollutant concentration maybe due to higher probability of collisions between pollutant and sorbent with sufficient sorption sites.

2.5.1.3 Temperature.

Changes in temperature affect a number of factors in biosorption of heavy metal ions. These include: (1) stability of metal ion species initially placed in solution, (2) stability of metal-biosorption complex depending on the biosorption sites, (3) cell wall configuration of the biosorbent, and (4) ionization of chemical moieties on the biosorbent (Sağ and Kutsal, 2000).

2.5.1.4 Weight of biomass.

An increase in biomass weight should result in a concomitant increase in pollutant uptake or pollutant removal efficiency due to the increase in sorption sites as the biomass species surface area increases. Brandt et al. (1997) showed that the adsorption capacity increased significantly with decreasing microbial biomass (*Mycobacterium chlorophenolicium* PCP-1) weight in the low pollutant (pentachlorophenol) concentration range (below 0.5 g/dm^3). Researchers have proposed that an increase in biomass weight leads to interference between the binding sites due to high cell density. Fourest and Roux (1992) also noted that zinc uptake decreased when microbial biomass *(Rhizopus arrhizus)* weight increased. Jianlong et al. (2000) obtained similar result using activated sludge for bioadsorption of pentachlorophenol. The researchers invalidated the above hypothesis by Brandt et al. (1997) and suggested that reduction in adsorption capacity is due to pollutant shortage in solution. This causes some biomass binding sites to remain unsaturated.

2.5.2 Mechanism of biosorption

Lin and Juang (2009) reported that the chemical nature of pollutant, solution conditions and biosorbent surface properties determine the mechanism of binding by biomass. Ho and Ofomaja (2007b) also reported that acidic organic functional groups present on agricultural by-products provide sites on which pollutant sequestration can take place or which other moieties can be reacted with for possible enhancement of pollutant uptake efficiency. Pollutants are attracted and bound to sorbent surface by a complex process determined by several mechanisms involving adsorption by physical forces, ion-exchange, complexation, chelation, adsorption on surface and pores, chemisorption and entrapment in inter and intrafibrillar capillaries (Basso et al., 2002). Figure 2.3 shows some of the possible mechanisms of biosorption.

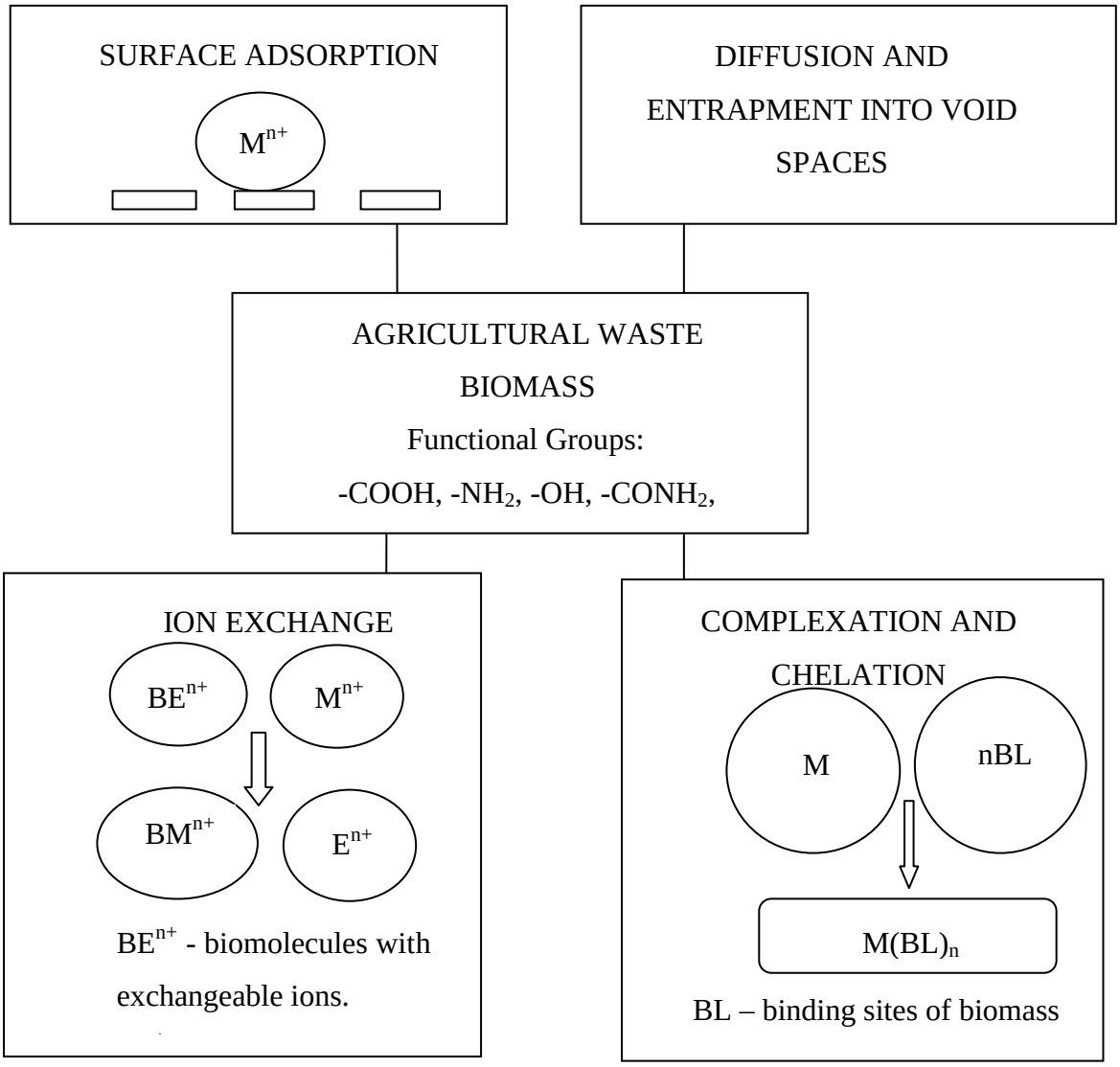

Figure 2.3 Mechanisms for biosorption.

2.6 DESORPTION

Desorption is the reverse of adsorption and refers to the detachment of pollutant species from a sorption site. Desorption experiments are important in elucidation of the adsorption mechanism, applicability in industry and possibility of metal recovery (Volesky, 2001). Desorption characteristics of an adsorbent can be determined by extracting adsorbed metal ions using different solvents. If the adsorbed metal ion can be desorbed by water, the attachment of the metal ion onto the adsorbent is by weak physical interactions. If a strong acid or alkali (such as HC*l* or NaOH) solution desorbs the metal ion, attachment of metal ion to adsorbent is by ion-exchange. When acetic acid can desorb the attached metal ions the

adsorption is believed to be by chemisorption (Pholosi et al., 2013). The desorbing agent should remove all sorbate from biomass by low volume of solution and not alter the sorptive properties of the biosorbent so that it can be used in the subsequent biosorption cycle (Chojnacka, 2010).

2.7 PINE CONE BIOMASS

Pine cone, is an agricultural by-product from pine plantations grown for the timber, wood pulp and paper industry. Pines are softwood trees in the genus *Pinus*, in the family Pinaceae, order Pinales, class Pinopsida, division Pinophyta and kingdom Plantae. There are about 115 species of pine which are native to the Northern Hemisphere (Ryan, 1999). Pines are evergreen, coniferous, resinous trees growing 3-80 m tall, with the majority of species reaching 15-45 m. They are mostly monoecious; having the male (microsporangium) and female (megasporangium) cones on the same tree, though a few species are sub-dioecious with individuals predominantly, but not wholly, single sex. At maturity, the cones open to release seeds depending on their dispersal mechanism. The scales of the mature cone are composed of epidermal and sclerechyma cells which contain cellulose, hemicelluloses, lignin, rosin (mixture of resin acids) and tannins in their cell walls which contain polar functional groups such as alcohols, aldehydes, ketones, carboxylic, phenolic and ether groups (Robbins et al., 1957; Sakagami et al., 1992). These functional groups form active sites for sorption of pollutants. Pine cones have not been used to their full potential and are usually discarded after seed release or left to decay on the forest floor. Their use in biosorption of micropollutants might reduce their environmental disposal problem, produce an alternative cost effective wastewater decontamination biosorbent and earn additional income for pine plantations.

2.7.1 Chemical composition of pine cone

Elemental analysis of virgin pine cone on a percentage dry basis is shown in Tables 2.3 as determined by Brebu et al. (2010).

Table 2.3 Elemental analysis of pine cone (% on dry weight basis).

Carbon	**Hydrogen**	**Nitrogen**	**Sulphur**	***Oxygen**
42.62	5.56	0.76	0.05	51.05

*Calculated by difference

The ultimate analysis presented in Table 2.3 shows very low values for nitrogen and sulphur, indicating that protein content of pine cone is low. Carbon content of 42.62 % confirms polysaccharide nature of pine cone. The results show presence of a large amount of oxygenated groups on pine cone due to high oxygen content of 51.05 %.

The main constituents of pine cone have been determined on a percentage dry basis by Brebu et al. (2010) and are presented in Table 2.4 below.

Table 2.4 Main constituents of pine cone (% on dry weight basis).

Lignin	**Hemicelluloses**	**Cellulose**	**Extractives**
24.9	37.6	32.7	4.8

Table 2.4 shows that pine cone is mainly composed of lignin, hemicelluloses and cellulose. The extractives include resin acids, tannins, simple sugars and other soluble organic substances (Micales et al., 1994). Some of these extractives have been found to have medicinal effects (Nagata et al., 1990).

2.7.1.1 Lignin

Lignin is a branched, three-dimensional, complex polymer that occurs in plant cell walls. The molecule has apparent infinite molecular weight and is covalently linked with xylans in the case of hardwoods and galactoglucomannans in softwoods (Dermibas, 2008). It consists of both aliphatic and aromatic constituents, built mainly with *p*-hydroxycinnamyl alcohols with different degrees of methoxylation (also called monolignols or phenylpropanoids) (Chuaqui et al., 1993). Structure of lignin is not known completely but various molecular models have been proposed (Faulon and Hatcher, 1994). Lignin offers structural and mechanical support to plant cells.

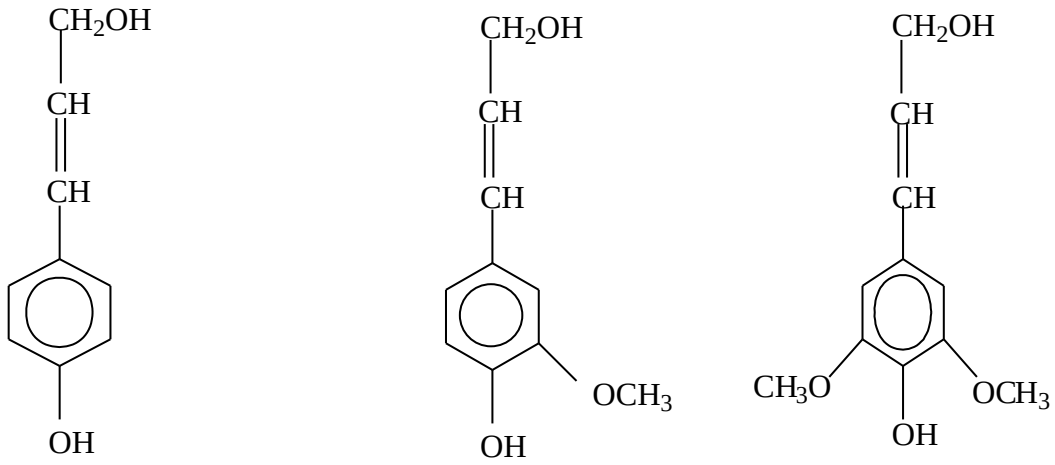

p-cumaril alcohol coniferil alcohol sinapil alcohol

Figure 2.4 Main phenylpropane units forming lignin.

Figure 2.4 shows the main phenylpropane units which are linked together by ring-ring, side chain-side chain and ring-side chain bonds forming a complex three-dimensional structure of lignin. This makes lignin to be highly insoluble and unreactive towards common chemical reagents. Sequence of the repeating monomer units is not homogenous as lignin lacks a primary structure. Figure 2.5 shows structure of lignin.

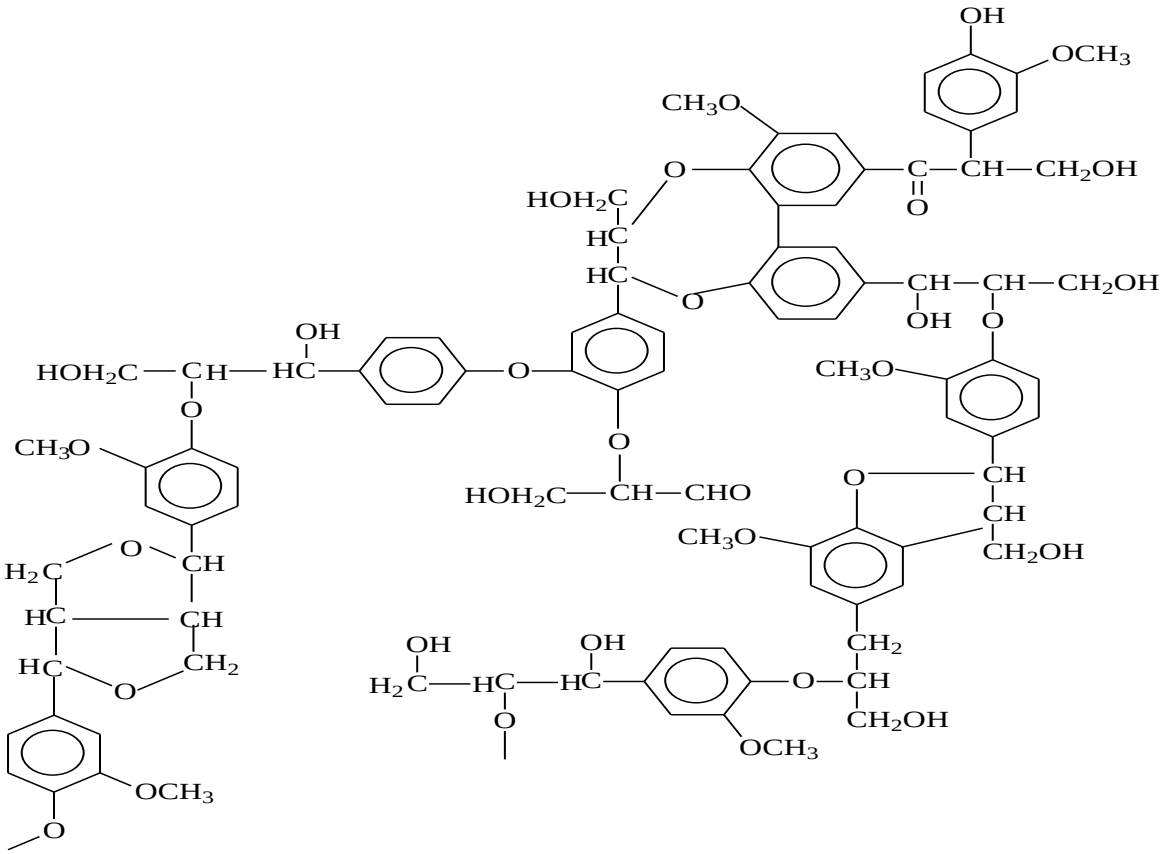

Figure 2.5 Lignin showing lack of primary structure.

2.7.1.2 Cellulose

Cellulose is a carbohydrate homopolymer consisting of β-D-glucopyranose (anhydroglucose) monomer units joined together by β-1.4-glycosidic linkages forming cellobiose dimmer units (Gurgel et al., 2008; Qin et al., 2008). Unlike starch, the glucose units in cellulose are oriented with $–CH_2OH$ groups alternating above and below the plane of rings thus producing long and un-branched chains. The absence of side chains allows cellulose molecules to form organized, stacked structures. The linear cellulose chains are linked by inter- and intra-chain hydrogen bonds making it highly crystalline and insoluble. Cellulose chains can be oriented in parallel and in antiparallel conformation; the two forms are called cellulose I and II respectively (Takács et al., 2000). Figure 2.6 shows a simplified diagram showing structure of cellulose.

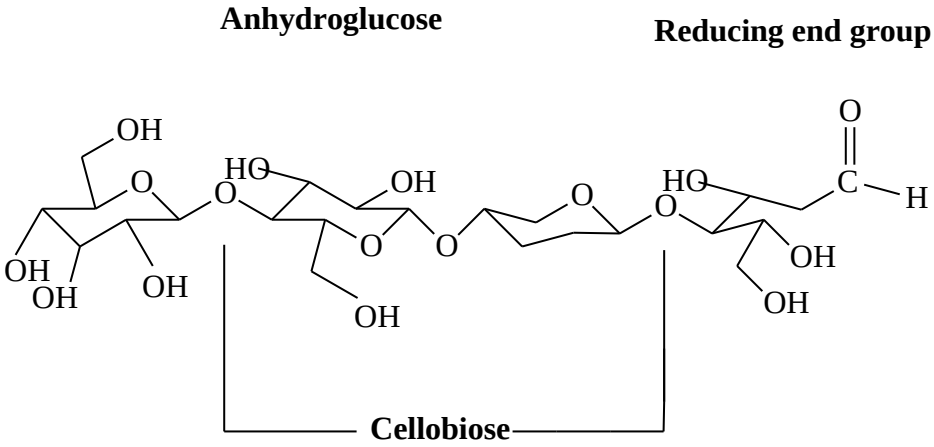

Figure 2.6 The structure of cellulose. Anhydroglucose is the monomer of cellulose, cellobiose is the dimmer (Dermibas, 2008).

2.7.1.3 Hemicelluloses

Hemicelluloses are a group of plant-derived heteropolysaccharides with much lower polymerization degree as compared to cellulose. They possess five- and six-member rings. They contain side chains which prohibit formation of intermolecular hydrogen bonds and the stacking conformation making them amorphous and thus more reactive and soluble in dilute acids, in comparison to cellulose. Hemicelluloses have different sugar monomers but all have two structural features in common which bear importantly on their biological function. (1) They have straight, flat β-1.4-linked backbones. Any side chains attached to the backbone are short, usually just one sugar long and stick out to the sides of the backbone. (2) All have some structural feature which prevents the chains from extended self-aggregation of the type

which exists between the β-1.4-linked glucan chains of cellulose. Most common hemicelluloses are xylan, glucuronoxylan, arabinoxylan, glucomannan, galactoglucomannan and xyloglucan. Figure 2.7 shows a simplified structure of galactoglucomannan.

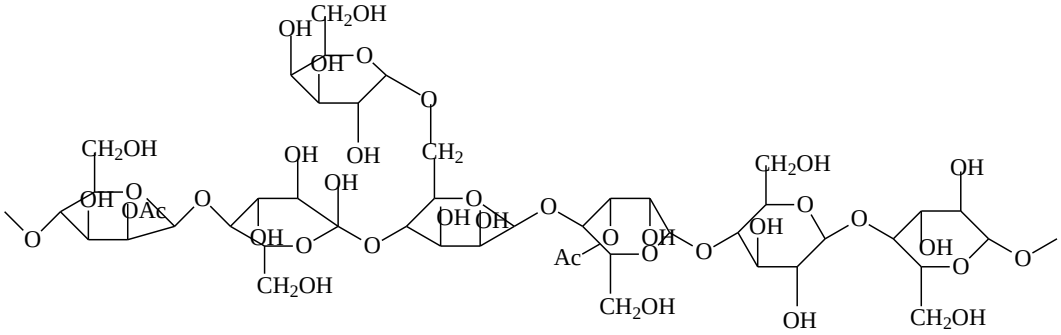

Figure 2.7 Structure of galactoglucomannan.

2.7.2 Use of pine cone as biosorbent

Pine cone is a waste product in pine plantations. When used as a biosorbent, pine cone has shown that it is able to sequester a large amount of pollutant species in a short time. For example, Ucun and co-workers (2003) achieved equilibrium of Cu^{2+} removal by pine cone powder in 20 minutes; Malkoc (2006) achieved equilibrium for Ni^{2+} uptake using pine cone powder biosorbent in about 7 minutes.

Pine cone is polyfunctional due to its lignocellulosic nature and can be chemically derivatized to change the types and amounts of surface functional groups, pore structure and other surface properties to improve its bioadsorption capabilities. Due to its polyfunctionality, a number of researchers have managed to apply it for metal and dye removal from aqueous solution (Nuhoglu and Oguz, 2003; Can et al., 2006; Akar et al., 2007; Ofomaja et al., 2009; Aksakal and Ucun, 2010).

A major drawback in its application as biosorbent is due to colouration of treated water due to presence of organic components such as phenolic groups of lignin, sugars and tannins which leach into treated water increasing chemical oxygen demand (Argun et al., 2008). Another disadvantage is resin acid content of pine cone (isopimaric acid, dehydroabietic acid, abietic acid) which may cause toxicity in the treated water (Ofomaja and Naidoo, 2011b). A number of researchers have used thermal and/or chemical modification of pine cone powder to avoid leaching of volatile and soluble organics into treated water and improve its adsorption

capabilities. For example, Argun and Dursun (2008) modified pine cone using Fenton's reagent/oxidation (Fe^{2+}/H_2O_2) and applied it for Cd^{2+} removal from aqueous solution, Pholosi et al. (2013) used solvent extraction (toluene-ethanol mixture) to modify pine cone and applied it for Pb^{2+} removal from aqueous solution, Ofomaja and Naidoo (2011a) applied base modification (using calcium hydroxide) of pine cone and applied it for Cu^{2+} removal from aqueous solution, Ofomaja et al. (2012) modified pine cone by grafting of acrylic acid and applied the prepared biosorbent for methylene blue removal from aqueous solution, Samarghandi et al. (2009) carbonized the cones to produce a highly porous sorbent and applied it for methyl orange removal from aqueous solution.

2.8 CROSS-LINKING AGRICULTURAL WASTE BIOMASS USING A DIISOCYANATE

Agricultural waste being lignocellulosic, is polyfunctional and possesses reactive hydroxyl functions. However, it has been established that most reagents do not form bonds with the hydroxyl component, but simply bulk the void spaces within the plant material (Elvy et al., 1995). Some of the most important reactions of lignocelluloses include etherification, esterification, acetalization and oxidation (Qiu et al., 2012). This research aims to cross-link Fenton treated pine cone using 1.6-hexamethylene diisocyanate and apply it for the removal of 2-nitrophenol from aqueous solution as it has never been reported in literature.

Chemical modification with diisocyanates presents some unique properties due to: (1) relatively high reaction rates; (2) reactions take place easily under mild ambient conditions (Valodkar and Thakore, 2010); (3) absence of a myriad of secondary products; and (4) chemical stability of urethane moiety in most inorganic or organic solutions (Siqueira et al., 2010) and at low pH (ester and amide linkages easily reversed) since most industrial wastewaters are discharged at low pH (Ofomaja et al., 2012). The gellation reaction (formation of urethane linkage or carbamate ester) is catalysed either by amine compounds like 1.4-diazabicyclo[2.2.2]octane (DABCO), dimethylcyclohexylamine (DMCHA), dimethylethanolamine (DMEA) or organometallic compounds/complexes based on Hg, Pb, Sn, Bi and Zn and needs an inert organic solvent to prevent conversion of diisocyanates into the substituted ureas and carbon dioxide due to the side reaction with water which also reduces cross-linking density (Wolff et al.,1952; Wegener et al., 2001). Amines act as Lewis base catalysts by complexing the hydroxyl functions whereas organometallic compounds

especially organotin compounds like dibutyltin (IV) dilaurate (DBTDL) which are more active than amine compounds function as Lewis acid catalysts by complexing with the diisocyanate (Blank et al., 1999; Wegener et al., 2001). Aliphatic diisocyanates like hexamethylene diisocyanate (HMDI) are mostly used as cross-linkers since both isocyanate functions are equivalent unlike their aromatic counterparts, due to steric and inductive effects of substituents (Kothandaraman and Nasar, 1993). Aromatic diisocyanates like toluene diisocyanate (TDI) and diphenylmethane diisocyanate (MDI) are also more difficult to handle because of their high reactivity to water (Noble, 1997).

2.9 MODELLING OF BIOSORPTION EXPERIMENTAL DATA

Researchers often determine the potential of biosorbents by kinetic models and biosorption isotherms. The time dependence of biosorption systems is established first followed by modelling of biosorption isotherm (Basha and Murthy, 2007).

2.9.1 Kinetics of adsorption

The experimental data is analysed using kinetic parameters to establish the mechanism and efficiency of the adsorption process. Adsorption reaction orders are studied using different kinetic models including pseudo-first-order, pseudo-second-order, intraparticle diffusion models etc. Reaction order of adsorption systems based on solution concentration has also been investigated (Sud et al., 2008). Adsorption and desorption are both dependent on time. Predicting the rate at which adsorption takes place is an important factor in adsorption system design and evaluation of adsorbent. The rate of desorption is also important in design and regeneration of adsorbent. Hence, it is of paramount importance to determine the adsorption and desorption kinetics and compute the parameters characterising the transport of adsorbate within adsorbents (Azizian, 2004). Development of adsorption kinetics is important in surface chemistry, from formulation of adsorption/desorption mechanisms to more complex situations such as catalysis and corrosion.

2.9.1.1 Pseudo-first-order rate equation

This rate equation is the most widely used to investigate adsorption kinetics and was proposed by Lagergren (1898). It is represented as:

$$\frac{dq}{dt} = k_f (q_e - q) \tag{2.2}$$

Where, q_e (mg/g) and q (mg/g) are the adsorption capacity at equilibrium and time t respectively and k_f (min^{-1}) is the rate constant. On integration and applying the following boundary conditions: $q = 0$ at $t = 0$ and $q = q_e$ at $t = t$, Equation (2.2) becomes:

$$\log(q_e - q) = \log q_e - \frac{k_f t}{2.303} \tag{2.3}$$

The adsorption rate constant k_f is computed from a linear plot of $\log(q_e - q)$ against t.

2.9.1.2 Pseudo-second-order rate equation

This model was developed by Ho and McKay (1999) to describe the adsorption of pollutants onto adsorbents. It is based on the assumption that the adsorption process involves chemisorption mechanism. The rate expression is represented as:

$$\frac{dq}{dt} = k_s (q_e - q)^2 \tag{2.4}$$

Where, q_e and q (mg/g) are the adsorption capacities at equilibrium and time t respectively and k_s (g/mg/min) is the rate constant. The integrated form at boundary conditions $q = 0$ at $t = 0$ and $q = q_e$ at $t = t$, becomes:

$$\frac{t}{q} = \frac{1}{k_s q_e^2} + \frac{t}{q_e} \tag{2.5}$$

Values of q_e and k_s are computed from a linear plot of t/q against t. The initial adsorption rate can be expressed as q/t, when t approaches zero. This is expressed as:

$$h = k_s q_e^2 \tag{2.6}$$

Where, *h* is the initial adsorption rate and is expressed in mg/g.min. The advantages of the pseudo-second-order rate equation are that the biosorption capacity, pseudo-second-order rate constant and the initial biosorption rate can all be calculated from the equation without knowing any parameter beforehand (Ho, 2004).

2.9.1.3 Intraparticle diffusion model

This diffusion model was developed by Weber and Morris (1963) to determine the mechanism involved in the adsorption process. A process is diffusion-controlled if its controlling step is the rate at which the components diffuse towards each other. This model is expressed as:

$$q_t = k_d t^{1/2} + I \tag{2.7}$$

Where, q_t (mg/g) is adsorption capacity at time t (min) and k_d (mg/g.min^2) is the intraparticle diffusion rate constant. A straight line plot of q_t versus $t^{1/2}$ will give I as the intercept. The boundary layer effect is strongly depended on value of I.

2.9.1.4 Bangham's model

The Bangham model shows if pore diffusion is the only controlling step (Barkakati et al., 2010). It is represented as:

$$\log\left\{\log\left(\frac{c_b}{c_b - q_t m}\right)\right\} = \log\left(\frac{k_0 m}{2.303V}\right) + \sigma \log t \tag{2.8}$$

Where, C_b (mg/dm^3) is the initial adsorbate concentration, q_t (mg/g) is adsorption capacity at any time t (min), m (g) is the amount of adsorbent, V (dm^3) is the solution volume and k_0 (dm^3/g) and σ (<1) are the Bangham's constants.

2.9.1.5 Boyd's diffusivity model

It is based on diffusion through the boundary layer (Boyd et al., 1947). The simplified form of the equation is shown as:

$$\ln\left[\frac{1}{1-F^2(t)}\right] = \frac{\pi^2 D_e t}{R_a^2} \qquad (2.9)$$

Where, $F(t) = q_t/q_e$ is the fractional uptake at time t, D_e (m^2/s) is the rate constant and R_a (m) is radius of adsorbent particle which is assumed to be spherical. Value of D_e is obtained from a linear plot of $ln[1/\{1-F^2(t)\}]$ versus t.

2.9.1.6 Elovich kinetic model

The model describes adsorption kinetics based on chemisorptions mechanism. The equation is shown as:

$$\frac{dq}{dt} = \alpha \exp(-\omega q) \qquad (2.10)$$

Chien and Clayton (1980) simplified the Elovich equation by assuming $\alpha\omega t >> 1$ and applying the boundary conditions $q = 0$ at $t = 0$ and $q = q$ at $t = t$, the equation gives:

$$q = \frac{1}{\omega}\ln(\alpha\omega) + \frac{1}{\omega}\ln t \qquad (2.11)$$

Where, q (mg/g) is the adsorption capacity at time t (min), α is the initial adsorption rate (mg/g.min) and ω is the desorption constant (g/mg). Equation (2.11) can be rearranged as:

$$q = A_1 + B_1 \ln t \qquad (2.12)$$

Where, $A_1 = ln(\alpha\omega).1/\omega$ and $B_1 = 1/\omega$. From a straight line plot of q against $\ln t$, the values of A_1 and B_1 can be determined.

2.9.1.7 Ritchie kinetic model

The model was developed as an alternative to the Elovich equation by Ritchie (1977) and is shown as:

$$\frac{1}{q} = \frac{1}{k_r q_e t} + \frac{1}{q_e} \qquad (2.13)$$

Where, k_r (1/min) is the rate constant, q (mg/g) shows adsorption capacity at time t (min) and q_e (mg/g) is adsorption capacity at equilibrium. A linear plot of *1/q* versus *1/t* gives magnitudes of q_e and k_r from the intercept and slope.

2.9.2 Equilibrium studies

The fitting of experimental equilibrium adsorption data to adsorption isotherm equations is an integral aspect of data analysis since the isotherm equations describe how pollutants interact with the adsorbent and are used to predict and compare adsorption performance (Kinniburgh, 1986; Basha and Murthy; 2007). The analysis of isotherm data is integral in development of an equation which accurately fits the results and could be used for design and operation of adsorption equipment for wastewater treatment (Yang and Al-Duri, 2005; Reddy et al., 2011). Adsorption isotherms show the relations at constant temperature between equilibrium concentrations of the adsorbate on the solid phase and in the liquid phase (Deniz et al., 2011). A number of equilibrium isotherm models have been proposed in terms of three fundamental approaches: (1) kinetic considerations, (2) thermodynamics, and (3) potential theory (Foo and Hameed, 2010). They can be classified as two parameter, three parameter and multilayer isotherm models. Freundlich (Freundlich, 1906) and Langmuir (Langmuir, 1918) models (two-parameter models) are the most commonly preferred isotherms. Other two-parameter models include: Temkin (Temkin and Pyzhev, 1940), Dubinin-Radushkevich (Dubinin and Radushkevich, 1947), Halsey (Halsey, 1948) and Flory-Huggins (Horsfall and Spiff, 2005). The two parameter models are usually used due to their simplicity which makes them easy to linearize (Basha and Murthy, 2007). Linearization of the equations allows for the fitting of experimental data and determination of the isotherm parameters. The three-parameter isotherm models include: Redlich-Petersen (Redlich and Petersen, 1959), Hill (Hill, 1910), Sips (Sips, 1948), Tóth (Tóth, 1971), Radke-Prausnitz (Radke and Prausnitz, 1972), Khan (Khan et al., 1997) and Koble-Corrigan (Koble and Corrigan, 1952). Multilayer adsorption isotherms include: Brunauer-Emmet-Teller (Brunauer et al., 1938), Frenkel-Halsey-Hill (Hill, 1952) and McMillan-Teller (McMillan and Teller, 1951). The isotherms show the adsorptive capability of the adsorbent, enabling the evaluation of mechanistic pathways and parameters

to be improved, which are important in optimising the adsorption process (Abdullah et al., 2009). Most commonly used equilibrium adsorption isotherms are presented below.

2.9.2.1 Langmuir isotherm

The model proposes monolayer adsorption onto a homogenous surface (Langmuir, 1918). It is based on the following basic assumptions: (1) monolayer adsorption, (2) adsorption takes place at a finite number of adsorption sites, (3) each site only accommodates one adsorbate molecule, (4) all sites are identical and energetically equivalent, and (5) there is no interaction and steric hindrance between molecules adsorbed on neighbouring sites. The general form of the Langmuir equation is:

$$q_e = \frac{q_m K_L C_e}{1 + K_L C_e} \tag{2.14}$$

Where, q_e is the equilibrium adsorption capacity (mg/g), C_e is the equilibrium concentration of the adsorbate (mg/dm^3), the Langmuir constants: q_m (mg/g) and K_L (dm^3/mg) show the monolyer coverage capacity and adsorption energy parameter respectively. When linearized, Equation (2.14) becomes:

$$\frac{C_e}{q_e} = \frac{1}{q_m K_L} + \frac{C_e}{q_m} \tag{2.15}$$

Plotting C_e/q_e against C_e gives a linear relationship with slope $1/q_m$ and intercept $1/(q_m K_L)$.

2.9.2.2 Freundlich isotherm

This isotherm model describes multilayer adsorption onto a heterogeneous surface with interaction between adsorbed molecules (Freundlich, 1906). The Freundlich expression is shown as:

$$q_e = K_F C_e^{1/n} \tag{2.16}$$

Where, C_e is equilibrium adsorbate concentration in mg/dm^3 and q_e is amount of adsorbate adsorbed in mg/g. K_F ((mg/g)/(mg/dm^3)^n) and n are the Freundlich equation parameters. n is indicative of the energy or intensity of the adsorption and suggests the favourability and capacity of the adsorbent-adsorbate system. According to the theory, $n > 1$ represents favourable adsorption conditions and indicates adsorption capacity at a given temperature. Equation (2.16) is linearized into:

$$\log q_e = \log K_F + \frac{1}{n}\log C_e \tag{2.17}$$

A plot of *log* q_e versus *log* C_e of the linearized Equation (2.17) gives a straight line whose gradient and intercept are used to find values of the constant K_F and exponent *1/n*.

2.9.2.3 Temkin isotherm

The Temkin and Pyzhev (1940) isotherm model explains chemisorption between the adsorbate and adsorbent. The model assumes that the heat of adsorption decreases linearly with the coverage. The equation works better for gas phase equilibria. Its original form is:

$$q_e = \frac{RT}{b}\ln\left(K_T C_e\right) \tag{2.18}$$

And after linearization gives:

$$q_e = B_l \ln K_T + B_l \ln C_e \tag{2.19}$$

where, $B_l = RT/b$, b (mol/kJ) is the Temkin isotherm constant, K_T (dm^3/mg) is equilibrium binding constant, q_e (mg/g) is the adsorption capacity and C_e (mg/dm^3) is the equilibrium adsorbate concentration, T (K) is temperature and R (8.314 × 10^{-3} kJ/mol/K) is the ideal gas constant. The linear plot of q_e versus *ln* C_e in Equation (2.19) gives the isotherm parameters, b and K_T which are calculated from the slope and intercept.

2.9.2.4 Dubinin-Radushkevich isotherm

Dubinin and Radushkevich (1947) developed the model which proposes that the sorption curves are related to porosity of the adsorbents. The Dubinin-Radushkevich equation is:

$$q_e = Q_D \exp\left(-B\varepsilon^2\right) \tag{2.20}$$

And its linearized form is:

$$\ln q_e = \ln Q_D - B\varepsilon^2 \tag{2.21}$$

Where, Q_D (mg/g) is the D-R isotherm constant and ε (kJ/mol) is the Polanyi potential. The Polanyi potential ε is represented as:

$$\varepsilon = RT \ln\left(1 + \frac{1}{C_e}\right) \tag{2.22}$$

R is the ideal gas constant (8.314×10^{-3} kJ/mol/K) and T (K) is temperature. B (mol^2/kJ^2) is related to mean free energy of sorption E (kJ/mol) and is represented as:

$$E = \frac{1}{\sqrt{2B}} \tag{2.23}$$

Q_D is determined from the linear plot of $ln\ q_e$ versus ε^2 using Equation (2.21).

2.9.2.5 Redlich-Peterson isotherm

Redlich and Peterson (1959) formulated an isotherm equation with three parameters that incorporates the features of both the Langmuir and Freundlich isotherms as follows:

$$q_e = \frac{K_R C_e}{1 + a_R C_e^{\beta}} \tag{2.24}$$

Where $0 < \beta \leq 1$. When $\beta = 1$, the equation gives the Langmuir form:

$$q_e = \frac{K_R C_e}{1 + a_R C_e} \tag{2.25}$$

When $\beta = 0$, the equation follows Henry's Law:

$$q_e = \frac{K_R C_e}{1 + a_R} \tag{2.26}$$

Equation (2.25) may be rearranged into:

$$K_R \frac{C_e}{q_e} - 1 = a_R C_e^{\beta} \tag{2.27}$$

This equation can be expressed in linear form as:

$$\ln\left[K_R \frac{C_e}{q_e} - 1 \right] = \ln a_R + \beta \ln C_e \tag{2.28}$$

Where, a_R $(dm^3/mg)^{\beta}$ and K_R (dm^3/mg) are isotherm constants and β is an exponent. It is difficult to determine the three unknown Redlich-Petersen constants by a linear plot of $ln[K_R(C_e/q_e) - 1]$ against $ln\ C_e$. Therefore, the three parameters can be determined using non-linear regression. It approaches the Freundlich model at high concentrations and is in concurrence with the low concentration limit of the Langmuir equation, giving a hybrid mechanism of adsorption which departs from ideal monolayer adsorption (Chin et al., 2012).

2.9.2.6 Hills isotherm

This three-parameter model views adsorption as a cooperative phenomenon, with adsorbed molecules influencing affinity of adsorbent at other binding sites (Ringot et al., 2007). The Hill equation is represented as:

$$q_e = \frac{q_{\max} C_e^{n_H}}{K_D + C_e^{n_H}} \tag{2.29}$$

And can be linearized as:

$$\ln\left(\frac{q_e}{q_{\max} - q_e}\right) = n_H \ln C_e - \ln K_D \tag{2.30}$$

Where, q_{max} is the Hill isotherm maximum uptake saturation (mg/g), K_D is the Hill constant (mg/dm^3), n_H is the Hill cooperativity coefficient, q_e is the adsorption capacity (mg/g) and C_e is the equilibrium adsorbate concentration (mg/dm^3). According to the model three possibilities in binding are possible:

(1) $n_H > 1$, positive cooperativity;

(2) $n_H = 1$, non-cooperative and;

(3) $n_H < 1$, negative cooperativity.

2.9.2.7 Brunauer-Emmett-Teller isotherm

Brunauer-Emmett-Teller isotherm is widely used in gas-solid equilibria. It was developed to describe multilayer adsorption systems (Brunauer et al., 1938). Its equation is:

$$q_e = \frac{q_s C_{BET} C_e}{(C_s - C_e)\left[1 + (C_{BET} - 1)(C_e / C_s)\right]} \tag{2.31}$$

Where, C_{BET} is the BET isotherm constant (dm^3/mg), C_s is the adsorbate monolayer saturation concentration (mg/dm^3), q_s is the theoretical isotherm saturation capacity (mg/g) and q_e is the equilibrium adsorption capacity (mg/g). As $C_{BET} >> 1$ and also $C_{BET}(C_e/C_s) >> 1$, Equation (2.31) is simplified as:

$$q_e = \frac{q_s}{1 - (C_e / C_s)} \tag{2.32}$$

When linearized Equation (2.31) becomes:

$$\frac{C_e}{q(C_s - C_e)} = \frac{1}{q_s C_{BET}} + \frac{(C_{BET} - 1)}{q_s C_{BET}} \frac{C_e}{C_s} \quad (2.33)$$

The BET isotherm parameters can be elucidated from a plot of $C_e/q_e(C_s - C_e)$ against C_e/C_s..

2.9.3 Thermodynamic analysis

Values of thermodynamic parameters such as free energy change, entropy change and enthalpy change are important as they show the spontaneity, feasibility, enthalpy and nature of the sorption process (Reddy et al., 2012). The free energy change of the sorption reaction can be obtained from the following expression:

$$\Delta G^0 = -RT \ln K_c \quad (2.34)$$

Where, ΔG^0 is free energy change of sorption (kJ/mol), R is the ideal gas constant (8.314 J/mol/K), T shows temperature (K) and K_c is the equilibrium constant (C_s/C_e). Negative values of ΔG^0 suggest that the sorption process is spontaneous. The values of enthalpy and entropy changes of sorption can be determined using the Van't Hoff equation:

$$\ln K_c = -\frac{\Delta H^0}{RT} + \frac{\Delta S^0}{R} \quad (2.35)$$

Where, ΔH^0 (kJ/mol) is change in enthalpy and ΔS^0 (kJ/mol/K) denotes entropy change. Plot of $ln\ K_c$ against $1/T$ gives a linear relationship with slope $(-\Delta H^0/R)$ and intercept $(\Delta S^0/R)$. Positive values for ΔH^0 and ΔS^0 show that the sorption process is endothermic and reflects increasing randomness at the solid/solution interface during biosorption. The activation energy can be determined using the Arrhenius equation:

$$\ln k_s = \ln A - \frac{E_a}{RT} \quad (2.36)$$

Where, A is the Arrhenius factor and E_a is the activation energy (kJ/mol) which can be estimated from gradient of a straight line plot of $ln\ k_s$ against $1/T$. Low activation energies (5-50 kJ/mol) suggest physisorption, while higher activation energies (60-800 kJ/mol) are characteristic of chemisorption (Deniz et al., 2011).

2.9.4 Error functions

Two error functions will be used to verify and substantiate the goodness of fit between experimental and modelled data. They are the coefficient of determination and the percentage variance. Error functions are used as a guideline to measure the accuracy of a mathematical model.

2.9.4.1 Coefficient of determination

The coefficient of determination, r^2 represents the proportion of variance in the dependent variable that can be explained by the regression line. $0 \leq r^2 \leq 1$, with zero indicating that 0% of the variation of the dependent variable (q_e) has been explained by the regression equation (Ofomaja et al., 2010). The coefficient of determination, r^2 was calculated using the following equations:

$$r^2 = \frac{S_{xy}^2}{S_{xx} S_{yy}} \tag{2.37}$$

Where, S_{xx} is the sum of squares of X:

$$S_{xx} = \sum_{i=1}^{n} X_i^2 - \frac{\sum_{i=1}^{n} X_i}{n} \tag{2.38}$$

Where, S_{yy} is the sum of squares of Y:

$$S_{yy} = \sum_{i=1}^{n} Y_i^2 - \frac{\sum_{i=1}^{n} Y_i}{n} \tag{2.39}$$

Where, S_{xy} is the sum of squares of X and Y:

$$S_{xy} = \sum_{i=1}^{n} X_i Y_i^2 - \frac{\left(\sum_{i=1}^{n} X_i\right)\left(\sum_{i=1}^{n} Y_i\right)}{n} \quad (2.40)$$

2.9.4.2 Percentage variable error

Percentage variance or percentage variable error shows the ratio of the absolute variation to the base value. An absolute variation is the difference between the modelled adsorption capacity ($q_{e,m}$ in mg/g - calculated from the models) and the experimental adsorption capacity value (q_e in mg/g) also known as the base value. The following equation can be used to elucidate the percentage variance (% var or % variance) values:

$$\%\,\text{var} = \frac{100}{n} \sum_{i=1}^{n} \left(\frac{q_{e,m} - q_e}{q_e} \right) \quad (2.41)$$

The larger the % variance, the greater the variation between the modelled and experimental adsorption capacities.

2.10 CONCLUSION

Substantial research has been done to investigate the biosorptive capability of agricultural wastes in both their natural and modified form. Literature search revealed that chemical modification of pine cone powder using polyfunctional cross-linkers to improve its biosorption capabilities has not been attempted. It is the aim of this research to synthesize a hydrophobic biosorbent via Fenton treatment and cross-linking using HMDI and explore its ability to remove 2-nitrophenol from aqueous solution as this has not yet been attempted.

2.11 REFERENCES

1. ABDULLAH, M.A., CHIANG, L. and NADEEM, M. (2009) Comparative evaluation of adsorption kinetics and isotherms of a natural product removal by Amberlite polymeric adsorbents, *Chemical Engineering Journal*. 146(3), pp. 370-376.
2. ACAR, F.N. and MALKOC, E. (2004) The removal of Cr(VI) from aqueous solutions by *Fagus Orientalis L*, *Bioresource Technology*. 94(1), pp. 13-15.
3. ADERHOLD, D., WILLIAMS, C.J. and EDYVEAN, R.G.J. (1996) The removal of heavy-metal ions by seaweeds and their derivatives, *Bioresource Technology*. 58(1), pp. 1-6.
4. AHLUWALIA, S.S. and GOYAL, D. (2005) Removal of heavy metals by waste tea leaves from aqueous solution, *Engineering in Life Sciences.* 5(2), pp. 158-162.
5. AHMED, M.N. and RAM, R.N. (1992) Removal of basic dye from wastewater using silica as adsorbent, *Environmental Pollution.* 77, pp. 79-86.
6. AHN, D-H., CHANG, W-S. and YOON, T-I. (1999) Dyestuff wastewater treatment using chemical oxidation, physical adsorption and fixed bed biofilm process, *Process Biochemistry*. 34(5), pp. 429-439.
7. AKAR, T., OZCAN, A.S., TUNALI, S. and OZCAN, A. (2007) Biosorption of a textile dye (Acid blue 40) by cone biomass of *Thuja orientalis*: Estimation of equilibrium, thermodynamic and kinetic parameters, *Bioresource Technology.* 99(8), pp. 3057-3065.
8. AKSAKAL, O. and UCUN, H. (2010) Equilibrium, kinetic and thermodynamic studies of the biosorption of textile dye (Reactive Red 195) onto *Pinus sylvestris L*, *Journal of Hazardous Materials.* 181(1-3), pp. 666-672.
9. AKSU, Z. (2005) Application of biosorption for the removal of organic pollutants: A review, *Journal of Process Biochemistry.* 40(3-4), pp. 997–1026.
10. AKSU, Z., KUTSAL, T., GÜN, S., HACIOSMANOĞLU, N. and GHOLAMINEJAD, M. (1991) Investigation of biosorption of Cu (II), Ni (II) and Cr (VI) ions to activated sludge bacteria, *Environmental Technology*. 12(10), pp. 915-921.

11. AKSU, Z., SAG, Y. and KUTSAL, T. (1990) A comparative study of the adsorption of chromium (VI) ions to *C.vulgaris* and *Z.ramigera*, *Environmental Technology*. 11(1), pp. 33-40.

12. AKSU, Z., SAG, Y. and KUTSAL, T. (1992) The biosorption of copper by *C.vulgaris* and *Z.ramigera*, *Environmental Technology.* 13(6), pp. 579-586.

13. AKSU, Z. and YENER, J.A. (2001) A comparative adsorption/biosorption study of mono-chlorinated phenols onto various sorbents, *Waste Management*. 21(8), pp. 695-702.

14. ALINNOR, I.J. 2007. Adsorption of heavy metal ions from aqueous solution by fly ash, *Fuel*. 86(5-6), pp. 853-857.

15. ALTUNDOGAN, H.S., ARSLAN, N.E. and TUMAN, F. (2007) Copper removal from aqueous solutions by sugar beet pulp treated by NaOH and citric acid, *Journal of Hazardous Materials.* 149(2), pp. 432-439.

16. ARGUN, M.E., DURSUN, S., OZDEMIR, C. and KARATAS, M. (2007) Heavy metal adsorption by modified oak sawdust: thermodynamics and kinetics, *Journal of Hazardous Materials.* 141(1), pp. 77-85.

17. ARGUN, M.E. and DURSUN, S. (2008) A new approach to modification of natural adsorbent for heavy metal adsorption, *Bioresource Technology*. 99(7), pp. 2516-2527.

18. ARGUN, M.E., DURSUN, S., KARATAS, M. and GÜRÜ, M. (2008) Activation of pine cone using Fenton oxidation for Cd (II) and Pb (II) removal, *Bioresource Technology*. 99(18), pp. 8691-8698.

19. ARGUN, M.E., DURSUN, S. and KARATAS, M. (2009) Removal of Cd (II), Pb (II), Cu (II) and Ni (II) from water using modified pine bark, *Desalination*. 249(2), pp. 519-527.

20. ATIA, A., DONIA, A.M., ABOU-EL-ENEIN, S.A. and YOUSIF, A.M. (2003) Studies on uptake behavior of Cu (II) and Pb (II) by amine chelating resins with different textural properties, *Separation & Purification Technology*. 33(3), pp. 295-301.

21. AWWAD, A.M., and SALEM, N.M. (2012) Biosorption of copper (II) and lead (II) ions from aqueous solutions by modified loquat (*Eriobotrya japonica*) leaves (MLL), *Journal of Chemical Engineering and Materials Science*. 3(1), pp. 7-17.

22. AZIZ, H.A., ADLAN, M.N. and ARIFFIN, K.S. (2008) Heavy metals (Cd, Pb, Zn, Ni, Cu and Cr(III)) removal from water in Malaysia: post treatment by high quality limestone, *Bioresource Technology*. 99(6), pp. 1578-1583.

23. AZIZIAN, S. (2004) Kinetic models of sorption: a theoretical analysis, *Journal of Colloid and Interface Science*. 276(1), pp. 47-52.

24. BACKHAUS, W.K., KLUMPP, E., NARRES, H.D. and SCHWUGER, M.J. (2001) Adsorption of 2.4-dichlorophenol on montmorillonite and silica: influence of non-ionic surfactants, *Journal of Colloid Interface Science*. 242, pp. 6-13.

25. BAILEY, S.E., OLIN, T.J., BRICKA, R.M. and ADRIAN, D.D. (1999) A review of potentially low-cost sorbents for heavy metals, *Water Research.* 33(11), pp. 2469-2479.

26. BANAT, I.M., NIGAM, P., SINGH, D. and MARCHANT, R. (1996) Microbial decolourization of textile-dye-containing effluents: a review, *Bioresource Technology*. 58(3), pp. 217-227.

27. BAO, M.L., GRIFFINI, O., SANTIANNI, D., BARBIERI, K., BURRINI, D. and PANTANI, F. (1999) Removal of bromate ion from water using granular activated carbon, *Water Research.* 33(13), pp. 2959-2970.

28. BARAKAT, M.A. (2011) New trends in removing heavy metals from industrial wastewater, *Arabian Journal of Chemistry.* 4(4), pp. 361-377.

29. BARAL, A. and ENGELKEN, R.D. (2002) Chromium-based regulations and greening in metal finishing industries in the USA, *Environmental Science Policy*. 5(2), pp. 121-133.

30. BARKAKATI, P., BEGUM, A., LAL DAS, M. and RAO, P.G. (2010) Adsorptive separation of *Ginsenoside* from aqueous solution by polymeric resins: Equilibrium, kinetic and thermodynamic studies, *Chemical Engineering Journal*. 161(1-2), pp. 34-45.

31. BASHA, S. and MURTHY, Z.V.P. (2007) Kinetic and equilibrium models for biosorption of Cr (VI) on chemically modified seaweed, *Cystoseira indica*, *Process Biochemistry*. 42(11), pp. 1521-1529.

32. BASSO, M.C., CERRELLA, E.G. and CUKIERMAN, A.L. (2002) Lignocellulosic materials as potential biosorbents of trace toxic metals from wastewater, *Industrial & Engineering Chemistry Research.* 41(15), pp. 3580-3585.

33. BELE, M., KODRE, A., ARČ, I., GRDADOLNIK, J., PEJOVNIK, S. and BESENHARD, J.O. (1998) Adsorption of cetytrimethylammonium bromide on carbon black from aqueous solution, *Carbon.* 36(7-8), pp. 1207-1212.

34. BELL, J., PLUMB, J.J., BUCKLEY, C.A. and STUCKEY, D.C. (2000) Treatment and decolorization of dyes in an anaerobic baffled reactor, *Journal of Environmental Engineering*. 126(11), pp. 1026-1032.

35. BERGER, J., REIST, M., MAYER, J.M., FELT, O., PEPPAS, N.A. and GURNY, R. (2004) Structure and interactions in covalently and ionically cross-linked chitosan hydrogels for biomedical applications, *European Journal of Pharmaceutics and Biopharmaceutics*. 57(1), pp. 19-34.

36. BHATNAGAR, A. and SILLANPÄÄ, M. (2010) Utilization of agro-industrial and municipal waste materials as potential adsorbents for water treatment-A review, *Chemical Engineering Journal*. 157(2-3), pp. 277-296.

37. BHATTACHARYA, A. and MISRA, B.N. (2004) Grafting: a versatile means to modify polymers: Techniques, factors and applications, *Progress in Polmer Science*. 29(8), pp. 767-814.

38. BLANK, W.J., HE, Z.A. and HESSELL, E.T. (1999) Catalysis of the isocyanate-hydroxyl reaction by non-tin catalysts, *Progress in Organic Coatings*. 35(1-4), pp. 19-29.

39. BOYD, G.E., ADAMSON, A.W. and MYERS, L.S. (1947) The exchange adsorption of ions from aqueous solutions on organic zeolites: II Kinetics, *Journal of American Chemical Society*. 69(11), pp. 2836-2848.

40. BRANDT, S., ZENG, A-P. and DECKWER W-D. (1997) Adsorption and desorption of pentachlorophenol on cells of *Mycobacterium chlorophenolicium* PCP-1, *Biotechnology & Bioengineering*. 55, pp. 480-491.

41. BREBU, M., UCAR, S., VASILE, C. and YANIK, J. (2010) Co-pyrolysis of pine cone with synthetic polymers, *Fuel*. 89(8), pp. 1911-1918.

42. BRUNAUER, S., EMMETT, P.H. and TELLER, E. (1938) Adsorption of gases in multimolecular layers, *Journal of American Chemical Society*. 60, pp. 309-319.

43. CAN, M.Y., KAYA, Y. and ALGUR, O.F. (2006) Response surface optimization of the removal of nickel from aqueous solution by cone biomass of *Pinus sylvestris, Bioresource Technology*. 97(14), pp. 1761-1765.

44. CELIK, A. and DEMIRBAS, A. (2005) Removal of heavy metal ions from aqueous solutions via adsorption onto modified lignin from pulping wastes, *Energy Sources*. 27(12), pp. 1167-1177.

45. CELIS, R., CARMEN, H.M. and CORNEJO, J. (2000) Heavy metal adsorption by functionalized clays, *Environmental Science & Technology*. 34(21), pp. 4593-4599.

46. CHIN, L.S., CHEUNG, W.H., ALLEN, S.J. and McKAY, G. (2012) Error analysis of adsorption isotherm models for acid dyes onto bamboo derived activated carbon, *Chinese Journal of Chemical Engineering*. 20(3), pp. 535-542.

47. CHANG, C., CHAU, L., HU, W., WANG, C. and LIAO, J. (2008) Nickel hexacyanoferrate multilayers on functionalized mesoporous silica supports for selective sorption and sensing of cesium, *Microporous and Mesoporous Materials*. 109(1-3), pp. 505–512.

48. CHERN, J-M. and CHIEN, Y-W. (2002) Adsorption of nitrophenol onto activated carbon: isotherms and breakthrough curves, *Water Research.* 36(3), pp. 647-655.

49. CHIEN, S.H. and CLAYTON, W.R. (1980) Application of Elovich equation to the kinetics of phosphates release and sorption in soils, *Soil Science Society of America Journal*. 44(2), pp. 265-268.

50. CHOJNACKA, K. (2010) Biosorption and bioaccumulation – The prospects of practical applications, *Environmental International.* 36(3), pp. 299-307.

51. CHOY, K.K.H., PORTER, J.F. and McKAY, G. (2004) Intraparticle diffusion in single and multicomponent acid dye adsorption from wastewater onto carbon, *Chemical Engineering Journal.* 103(1-3), pp. 135-145.

52. CHUAQUI, C.A., RAJAGOPAL, S., KOVÁCS, A., STEPANIK, T., MERRITT, J., GYöRGY, I., WHITEHOUSE, R. and EWING, D. (1993) Radiation-induced effects in lignin model compounds: a pulse and steady-state radiolysis study, *Tetrahedron.* 49(43), pp. 9689-9698.

53. CRINI, G. (2005) Recent developments in polysaccharide-based materials used as adsorbents in wastewater treatment, *Progress in Polymer Science*. 30(4), pp. 778-783.

54. CRINI, G. (2006) Non-conventional low-cost adsorbents for dye removal: A review, *Bioresource Technology*. 97(9), pp. 1061-1085.

55. DABROWSKI, A. (2001) Adsorption, from theory to practice, *Advances in Colloid and Interface Science*. 93(1-3), pp. 135-224.

56. DAS, N., VIMALA, R. and KARTHIKA, P. (2008) Biosorption of heavy metals – An overview, *Indian Journal of Biotechnology.* 7(2), pp. 159-169.

57. DAVIS, T.A., VOLESKY, B. and MUCCI, A. (2003) A review of the biochemistry of heavy metal biosorption by brown algae, *Water Research.* 37(18), pp. 4311-4330.

58. DENIZ, F., KARAMAN, S. and SAYGIDEGER, S.D. (2011) Biosorption of a model basic dye onto *Pinus brutia* Ten: Evaluating of equilibrium, kinetic and thermodynamic data, *Desalination.* 270(1-3), pp. 199-205.

59. DEMIRBAS, A. (2008) Heavy metal adsorption onto agro-based waste materials: A review, *Journal of Hazardous Material.* 157(2-3), pp. 220–229.

60. DHAKAL, R.P., GHIMIRE, K.N. and INOUE, K. (2005) Adsorptive separation of heavy metals from an aquatic environment using orange waste, *Hydrometallurgy*. 79(3-4), pp. 182-190.

61. DIMITROVA, S.V. (1996) Metal sorption on blast-furnace slag, *Water Research.* 30(1), pp. 228-232.

62. DUBININ, M.M. and RADUSHKEVICH, L.V. (1947) Equation of the characteristic curve of activated charcoal, *Proceedings of the Academy of Sciences (USSR)*. 55, pp. 331-333.

63. ELLIS, J. and KORTH, W. (1993) Removal of geosmin and methylisoborneol from drinking water by adsorption on ultrastable zeolite-Y, *Water Research.* 27(4), pp. 535-539.

64. EL SEOUD, O.A., FIDALE, L.C., RUIZ, N., D'ALMEIDA, M.L.O. and FROLLINI, E. (2008) Cellulose swelling by protic solvents: which properties of the biopolymer and the solvent matter, *Cellulose*. 15(3), pp. 371-392.

65. ELVY, S.B., DENNIS, G.R. and LOO-TECK, N.G. (1995) Effect of coupling agent on the physical properties of wood-polymer composites, *Journal of Materials Processing Technology*. 48(1-4), pp. 365-372.

66. FAULON, J. and HATCHER, P.G. (1994) Is there any order in the structure of lignin, *Energy & Fuels.* 8(2), pp. 402-407.

67. FOO, K.Y. and HAMEED, B.H. (2010) Insights into the modelling of adsorption isotherm systems, *Chemical Engineering Journal.* 156(1), pp. 2-10.

68. FÖLDVARY, C.M., TAKÁCS, E. and WOJNÁROVITS, L. (2003) Effect of high-energy radiation and alkali treatment on the properties of cellulose, *Radiation Physics & Chemistry*. 67(3-4), pp. 505-508.

69. FOUREST, E. and ROUX, J-C. (1992) Heavy metal biosorption by fungal mycelia by-products: mechanisms and influence on pH, *Applied Microbiology and Biotechnology*. 37(3), pp. 399-403.

70. FOUREST, E. and VOLESKY, B. (1996) Contribution of sulfonate groups and alginate to heavy metal biosorption by the dry biomass of *Sargassum fluitans*, *Environmental Science & Technology*. 30(1), pp. 277-282.

71. FREUNDLICH, H. (1906) Uber die adsorption in losungen, *Zeitschrift fur Physikalische Chemie (Leipzig)*. 57A, pp. 385-470.

72. FRIBERG, L.T. (1985) The rationale of biological monitoring of chemicals – with special reference metals, *American Industrial Hygiene Association Journal*. 46(11), pp. 633-642.

73. FU, Y. and VIRARAGHAVAN, T. (2001) Fungal decolourization of wastewaters: a review, *Bioresource Technology*. 79(3), pp. 251-262.

74. GABALLAH, I., GOY, D., ALLAIN, E., KILBERTUS, G. and THAURONT, J. (1997) Recovery of copper through decontamination of synthetic solutions using modified barks, *Metallurgical and Materials Transactions*. B 28(1), pp. 13–23.

75. GABALLAH, I. and KILBERTUS, G. (1998) Recovery of heavy metal ions through decontamination of synthetic solutions and industrial effluents using modified barks, *Journal of Geochemical Exploration*. 62(1-3), pp. 241-286.

76. GADD, G.M. (2009) Biosorption: critical review of scientific rationale, environmental importance and significance for pollution treatment, *Journal of Chemical Technology & Biotechnology*. 84(1), pp. 13-28.

77. GARDEA-TORRESDEY, J.L., GONZALEZ, J.H., TIEMANN, K.J., RODRIGUEZ, O. and GAMEZ, G. (1998) Phytofiltration of hazardous cadmium, chromium, lead and zinc ions by biomass of *Medicago sativa* (alfalfa), *Journal of Hazardous Materials*. 57(1-3), pp. 29-39.

78. GARG, V.K., GUPTA, R., YADAV, A.B. and KUMAR, R. (2003) Dye removal from aqueous solution by adsorption on treated sawdust, *Bioresource Technology*. 89(2), pp. 121-124.

79. GARG, V.K., AMITA, M., KUMAR, R. and GUPTA, R. (2004) Basic dye (methylene blue) removal from simulated wastewater by adsorption using Indian Rosewood sawdust: a timber industry waste, *Dyes and Pigments*. 63(3), pp. 243-250.

80. GARG, U.K., KAUR, M.P., GARG, V.K. and SUD, D. (2007) Removal of hexavalent chromium from aqueous solutions by agricultural waste biomass, *Journal of Hazardous Materials*. 140(1-2), pp. 60-68.

81. GASSAN, J. and BLEDZKI, A.K. (1999) Possibilities for improving the mechanical properties of jute/epoxy composites by alkali treatment of fibres, *Composites Science and Technology*. 59(9), pp. 1303-1309.

82. GHODBANE, I. and HAMDAOUR, O. (2008) Removal of Hg(II) from aqueous media using eucalyptus bark: kinetic and equilibrium studies, *Journal of Hazardous Materials*. 160(2-3), pp. 301-309.

83. GHOUL, M., BACQUET, M. and MORCELLET, M. (2003) Uptake of heavy metals from synthetic aqueous solutions using modified PEI-silica gels, *Water Research*. 37(4), pp. 729-734.

84. GRELUK, M. and HUBICKI, Z. (2010) Kinetics, isotherm and thermodynamic studies of Reactive Black 5 removal by acid acrylic resins, *Chemical Engineering Journal*. 162(3), pp. 919-926.

85. GURGEL, L.V.A., JÚNIOR, O.K., GIL, R.P.F and GIL, L.F. (2008) Adsorption of Cu (II), Cd (II) and Pb (II) from aqueous single metal solutions by cellulose and mercerized cellulose chemically modified with succinic anhydride, *Bioresource Technology*. 99(8), pp. 3077-3083.

86. GÜVEN, O., SEN, M., KARADAĞ, E. and SARAYDIN, D. (1999) A review on the radiation synthesis of copolymeric hydrogels for adsorption and separation purposes, *Radiation Physics & Chemistry*. 56(4), pp. 381-386.

87. HACHEM, K., ASTIER, C., CHALEIX, V., FAUGERON, C., KRAUSZ, P., KAID-HARCHE, M. and GLOAGUEN, V. (2012) Optimization of lead and cadmium binding by oxidation of biosorbent polysaccharide moieties, *Water, Air & Soil Pollution.* 223(7), pp. 3877-3885.

88. HALSEY, G. (1948) Physical adsorption on non-uniform surfaces, *Journal of Chemical Physics*. 16(10), pp. 931-937.

89. HAMERLINCK, Y. (1994) Purification of industrial effluent using granular activated carbon and reactivation, *Filtration & Separation.* 31(6), pp. 637-641.

90. HILL, A.V. (1910) The possible effects of the aggregation of the molecules of haemoglobin on its dissociation curves, *Journal of Physiology*. 40, pp. 4-7.

91. HILL, T.L. (1952) Theory of physical adsorption, *Advances in Catalysis*. 4, pp. 211-258.

92. HO, Y.S. (2004) Pseudo-isotherms using a second order kinetic expression constant, *Journal of the International Adsorption Society*. 10(2), pp. 151-158.

93. HO, Y.S. (2005) Effect of pH on lead removal from water using tree fern as the sorbent, *Bioresource Technology*. 96(11), pp. 1292-1303.

94. HO, Y.S. and McKAY, G. (1999) Pseudo-second order model for sorption processes, *Process Biochemistry*. 34(5), pp. 451-465.

95. HO, Y.S. and McKAY, G. (2003) Sorption of dyes and copper ions onto biosorbents, *Process Biochemistry*. 38(7), pp. 1047-1061.

96. HO, Y.S. and OFOMAJA, A.E. (2006) Biosorption thermodynamics of cadmium on coconut copra meal as biosorbent, *Biochemical Engineering Journal*. 30(2), pp. 117-123.

97. HORIKOSHI, T., NAKAJIMA, A. and SAKAGUCHI, T. (1981) Studies on the accumulation of heavy metal elements in biological systems XIX. Accumulation of uranium by microorganisms, *Applied Microbiology & Biotechnology*. 12(2), pp. 90-96.

98. HORSFALL, M. and SPIFF, A.I. (2005) Equilibrium biosorption study of Al^{3+}, Co^{2+} and Ag^{+} in aqueous solutions by fluted pumpkin *(Telfairia occidentalis)* waste biomass, *Acta Chimica Slovenica.* 52, pp. 174-181.

99. HOSEA, M., GREENE, B., MCPHERSON, R., HENZL, M., ALEXANDER, M.D. and DARNALL, D.W. (1986) Accumulation of elemental gold on alga *Chlorella vulgaris*, *Inorganica Chimica Acta*. 123(3), pp. 161-165.

100. HU, Z., LEI, L., LI, Y. and NI Y. (2003) Chromium adsorption on high-performance activated carbons from aqueous solution, *Separation & Purification Technology*. 31(1), pp. 13-18.

101. IZANLOO, H. and NASSERI, S. (2005) Cadmium removal from aqueous solutions by ground pine cone, *Iranian Journal of Environmental Health Science and Engineering*. 2(1), pp. 33-42.

102. JAIN, A.K., GUPTA, V.K., BHATNAGAR, A. & SUHAS. (2003) Utilization of industrial waste products as adsorbents for the removal of dyes, *Journal of Hazardous Materials*. 101(1), pp. 31-42.

103. JALALI, R., GHAFOURIAN, H., ASEF, Y., DAVARPANAH, S.J. and SEPEHR, S. (2002) Removal and recovery of lead using nonliving biomass of marine algae, *Journal of Hazardous Materials.* 92(3), pp. 253-262.

104. JIANLONG, W., YI, Q., HORAN, N. and STENTIFORD, E. (2000) Bioadsorption of pentachlorophenol (PCP) from aqueous solution by activated sludge biomass, *Bioresource Technology*. 75(2), pp. 151-161.

105. KAPOOR, A. and VIRARAGHAVAN, T. (1995) Fungal biosorption - an alternative treatment option for heavy metal bearing wastewaters: a review, *Bioresource Technology*. 53(3), pp. 195-206.

106. KARTEL, M.T., KUPCHIK, L.A. and VEISOV, B.K. (1999) Evaluation of pectin binding of heavy metal ions in aqueous solutions, *Chemosphere*. 38(11), pp. 2591-2596.

107. KASPRZYK-HORDERN, B. (2004) Chemistry of alumina, reactions in aqueous solution and its application in water treatment, *Advances in Colloid and Interface Science.* 110(1-2), pp. 19-48.

108. KHAN, A.R., ATAULLAH, R. and AL HADDAD, A. (1997) Equilibrium adsorption studies of some aromatic pollutants from dilute aqueous solutions on activated carbon at different temperatures, *Journal of Colloid and Interface Science*. 194(1), pp. 154-165.

109. KHAN, S.A. (1992) Ion exchange and adsorption behavior of natural clays and hydrated metal oxides. Pakistan: University of the Punjab Lahore. (Thesis – DPhil) pp. 14.

110. KHOTIMCHENKO, M., KOVALEV, V. and KHOTIMCHENKO, Y. (2007) Equilibrium studies of sorption of lead (II) ions by different pectin compounds, *Journal of Hazardous Materials.* 149(3), pp. 693-699.

111. KINNIBURGH, D.G. (1986) General purpose adsorption isotherms, *Enviromental Science & Technology*. 20(9), pp. 895-904.

112. KJELLSTROM, T., SHIROISHI, K. and ERWIN, P.E. (1977) Urinary beta./sub 2/-microglobulin excretion among people exposed to cadmium in the general environment, *Environmental Research.* 13, pp. 318-344.

113. KOBLE, R.A. and CORRIGAN, T.E. (1952) Adsorption isotherms for pure hydrocarbons, *Industrial and Engineering Chemistry*. 44(2), pp. 383-387.

114. KONGSRICHAROERN, N. and POLPRASERT, C. (1996) Chromium removal by a bipolar electro-chemical precipitation process, *Water Science and Technology*. 34(9), pp. 109-116.

115. KOTHANDARAMAN, H. and NASAR A.S. (1993) The thermal dissociation of phenol-blocked toluene diisocyanate crosslinkers, *Polymer.* 34(3), pp. 610-615.

116. KRYSZTAFKIEWICZ, A., BINKOWSKI, S. and JESIONOWSKI, T. (2002) Adsorption of dyes on a silica surface, *Applied Surface Science.* 199(1-4), pp. 31-39.

117. KUŠIĆ, H., BOŽIĆ, A.L. and KOPRIVANAC, N. (2007) Fenton type processes for minimization of organic content in colored wastewaters: Part 1: Processes optimization, *Dyes & Pigments*. 74(2), pp. 380-387.

118. KUYUKAC, K. (1990) Feasibility of biosorbents application. In: Volesky, B., *ed*. Biosorption of Heavy Metals. Florida: CRC Press. pp 371-378.

119. LAGERGREN, S. (1898) Zur theorie der sogenannten adsorption gelöster stoffe, *Kungliga Svenska Vetenskapsakademiens Handlingar*. 24(4), pp. 1-39.

120. LANGMUIR, I. (1918) The adsorption of gases on plane surfaces of glass, mica and platinum, *Journal of American Chemical Society.* 40(9), pp. 1361-1403.

121. LAPARA, T.M., KONOPKA, A., NAKATSU, C.H. and ALLENMAN, J.E. (2000) Thermophilic aerobic wastewater treatment in continuous-flow bioreactors, *Journal of Environmental Engineering.* 126(8), pp. 739-744.

122. LATA, H., GARG, V.K. and GUPTA, R.K. (2007) Removal of basic dye from aqueous solution by adsorption using Parthenium hysterophorus: An agricultural waste, *Dyes and Pigments*. 74(3), pp. 653-658.

123. LEE, K.B., GU, M.B. and MOON, S.H. (2003) Degradation of 2,4,6-trinitrotoluene by immobilized horseradish peroxidase and electrogenerated peroxidase, *Water Research.* 37(5), pp. 983-992.

124. LEE, J-M., KIM, M-S., HWANG, B., BAE, W. and KIM, B-W. (2003) Photodegradation of acid red 114 dissolved using a photo-Fenton process with TiO_2, *Dyes and Pigments.* 56(1), pp. 59-67.

125. LEYVA-RAMOS, R., BERNAL-JACOME, L.A. and ACOSTA-RODRIGUEZ, I. (2005) Adsorption of cadmium (II) from aqueous solution on natural and oxidized corncob, *Separation and Purification Technology*. 45(1), pp. 41-49.

126. LI, X., TANG, Y., XUAN, Y., LIU, Z.Y. and LUO, F. (2007) Study on the preparation of orange peel cellulose adsorbents and biosorption of Cd^{2+} from aqueous solution, *Separation and Purification Technology*. 55(1), pp. 69-75.

127. LIN, S-H. and JUANG, R-S. (2002) Removal of free and chelated Cu^{2+} ions from water by a non-dispersive solvent extraction process, *Water Research*. 36, pp. 3611-3619.

128. LIN, S-H. and JUANG, R-S. (2009) Adsorption of phenol and its derivatives from water using synthetic resins and low-cost natural adsorbents: A review, *Journal of Environmental Management.* 90(3), pp. 1336-1349.

129. LOUKIDOU, M.X., MATIS, K.A., ZOUBOULIS, A.I. and LIAKOPOULOU-KYRIAKIDOU, M. (2003) Removal of As (V) from wastewaters by chemically modified fungal biomass, *Water Research.* 37(18), pp. 4544-4552.

130. LOW, K.S., LEE, C.K. and MAK, S.M. (2004) Sorption of copper and lead by citric acid modified wood, *Wood Science and Technology.* 38(8), pp. 629-640.

131. LÓPEZ, E., SOTO, B., ARIAS, M., NÚÑEZ,A., RUBINOS, D. and BARRAL, M.T. (1998) Adsorbent properties of red mud and its use for wastewater treatment, *Water Research.* 32(4), pp. 1314-1322.

132. LU, D., CAO, Q., LI, X., CAO, X., LUO, F. and SHAO, W. (2008) Kinetics and equilibrium of Cu (II) adsorption onto chemically modified orange peel cellulose biosorbents, *Hydrometallurgy*. 95(1-2), pp. 145-152.

133. MAEKAWA, E. and KOSHIJIMA, T. (1984) Properties of 2.3-dicarboxy cellulose combined with various metallic ions, *Journal of Applied Polymer Science.* 29, pp. 2289-2297.

134. MALKOC, E. (2006) Ni (II) removal from aqueous solutions using cone biomass of *Thuja orientalis, Journal of Hazardous Materials.* 137(2), pp. 899-908.

135. MALKOC, E. and NUHOGLU, Y. (2003) The removal of Cr (VI) from synthetic wastewater by *Ulothrix zonata, Fresenius Environmental Bulletin.* 12(4), pp. 376-381.

136. MARCHETTI, V., CLEMENT, A., LOUBINOUX, B. and GERARDIN, P. (2000a) Decontamination of synthetic solutions containing heavy metals using chemically modified sawdust bearing polyacrylic acid chains, *Journal of Wood Science*. 46(4), pp. 331-333.

137. MARCHETTI, V., CLEMENT, A., GERARDIN, P. and LOUBINOUX, B. (2000b) Synthesis and use of esterified sawdust bearing carboxyl group for removal of cadmium (II) from water, *Wood Science and Technology*. 34(2), pp. 167-173.

138. MARSHALL. W.E. and JOHNS, M.M. (1996) Agricultural by-products as metal adsorbents: sorption properties and resistance to mechanical abrasion, *Journal of Chemical Technology & Biotechnology*. 66(2), pp. 192-198.

139. MARSHALL, W.E., WARTELLE, D.E., BOLER, D.E., JOHNS, M.M. and TOLES, C.A. (1999) Enhanced metal adsorption by soybean hulls modified with citric acid, *Bioresource Technology*. 69(3), pp. 263-268.

140. MARTÍNEZ, N.S.S., FERNÁNDEZ, J.F., SEGURA, X.F. and FERRER, A.N. (2003) Pre-oxidation of an extremely polluted industrial wastewater by the Fenton's reagents, *Journal of Hazardous Materials.* B101, pp. 315-322.

141. McMILLAN, W.G. and TELLER, E. (1951) The assumptions of the BET theory, *Journal of Physical Chemistry*. 55(1), pp. 17-20.

142. METEŠ, A., KOVAČEVIČ, D., VUJEVIČ, D. and PAPIČ, S. (2004) The role of zeolites in wastewater treatment of printing inks, *Water Research.* 38(14-15), pp. 3373-3381.

143. MICALES, J.A., HAN, J.S., DAVIS, J.L. and YOUNG, R.A. (1994) Chemical composition and fungitoxic activities of pine cone extractives. *In:* Llewellyn, G.C., Dashek, W.V., O'Rear, C.E., *eds*., Biodeterioration Research 4: Mycotoxins, wood decay, plant stress, biocorrosion and general biodeterioration: Proceedings of 4th meeting of the Pan American Biodeterioration Society, 1991 August 20-25; as an electronic symposium. New York: Plenum Press. pp. 317-332.

144. MIN, S.H., HAN, J.S., SHIN, E.W. and PARK, J.K. (2004) Improvement of cadmium ion removal by base treatment of juniper fiber, *Water Research*. 38(5), pp. 1289-1295.

145. MOHAN, D. and PITTMAN, C.U. (2007) Arsenic removal from water/wastewater using adsorbents - A critical review, *Journal of Hazardous Materials*. 142(1-2), pp. 1-53.

146. MONTANHER, S.F., OLIVEIRA, E.A. and ROLLEMBERG, M.C. (2005) Removal of metal ions from aqueous solutions by sorption onto rice bran, *Journal of Hazardous Materials.* B 117(2-3), pp. 207-211.

147. NAGATA, K., SALAGAMI, H., HARADA, H., MONOYAMA, M., ISHIHAMA, A. and KONNO, K. (1990) Inhibition of influenza virus infection by pine cone antitumor substances, *Antiviral Research.* 13(1), pp. 11-21.

148. NAJA, G., MUSTIN, C., VOLESKY, B. and BERTHELIN, J. (2006) Stabilization of the initial potential for a metal-based potentiometric titration study of a biosorption process, *Chemosphere*. 62(1), pp. 163-170.

149. NING, R.Y. (2002) Arsenic removal by reverse osmosis, *Desalination.* 143(3), pp. 237-241.

150. NOBLE, K-L. (1997) Waterborne polyurethanes, *Progress in Organic Coatings*. 32(1-4), pp. 131-136.

151. NORDBERG, G.F. (1974) Health hazards of environmental cadmium pollution, *AMBIO*. 3(2), pp. 55-66.

152. NUHOGLU, Y., MALKOC, E., GÜRSES, A. and CANPOLAT, N. (2002) The removal of Cu (II) from aqueous solutions by *Ulothrix zonata*, *Bioresource Technology*. 85(3), pp. 331-333.

153. NUHOGLU, Y. and OGUZ, E. (2003) Removal of copper (II) from aqueous solutions by biosorption on the cone biomass of *Thuja orientalis, Process Biochemistry*. 38(11), pp. 1627-1638.

154. OFOMAJA, A.E. and HO, Y.S. (2007a) Effect of pH on cadmium biosorption by coconut copra meal, *Journal of Hazardous Materials.* 139(2), pp. 356-362.

155. OFOMAJA, A.E. and HO, Y.S. (2007b) Equilibrium sorption of anionic dye from aqueous solution by palm kernel fibre as sorbent, *Dyes and pigments*. 74(1), pp. 60-66.

156. OFOMAJA, A.E. and NAIDOO, E.B. (2011a) Kinetic modeling of the interaction between Cu (II) and calcium hydroxide treated pine cone powder, *Journal of the Taiwan Institute of Chemical Engineers.* 42(3), pp. 480-485.

157. OFOMAJA, A.E. and NAIDOO, E.B. (2011b) Biosorption of copper from aqueous solution by chemically activated pine cone: A kinetic study, *Chemical Engineering Journal.* 175, pp. 260-270.

158. OFOMAJA, A.E., NAIDOO, E.B. and MODISE, S.J. (2009) Removal of copper (II) from aqueous solution by pine and base modified pine cone powder as biosorbent, *Journal of Hazardous Materials*. 168(2-3), pp. 909-917.

159. OFOMAJA, A.E., NAIDOO, E.B. and MODISE, S.J. (2010a) Dynamic studies and pseudo-second order modeling of copper (II) biosorption onto pine cone powder, *Desalination*. 251(1-3), pp. 112-122.

160. OFOMAJA, A.E., NAIDOO, E.B. and MODISE, S.J. (2010b) Biosorption of copper (II) and lead (II) onto potassium hydroxide treated pine cone powder, *Journal of Environmental Management*. 91(8), pp. 1674-1685.

161. OFOMAJA, A.E., NGEMA, S.L. and NAIDOO, E.B. (2012) The grafting of acrylic acid onto biosorbents: Effect of plant components and initiator concentration, *Carbohydrate Polymers*. 90(1), pp. 201-209.

162. OFOMAJA, A.E., PHOLOSI, A. and NAIDOO, E.B. (2013) Kinetics and competitive modeling of cesium biosorption onto chemically modified pine cone powder, *Journal of the Taiwan Institute of Chemical Engineers*. 44(6), pp. 943-951.

163. OKOLO, B., PARK, C. and KEANE, M.A. (2000) Interaction of phenol and chlorophenols with activated carbon and synthetic zeolites in aqueous media, *Journal of Colloid Interface Science*. 226(2), pp. 308-317.

164. PAGLIUCA, A. and MUFTI, G.J. (1990) Lead poisoning: an age old problem, *British Medical Journal.* 300(6728), pp. 830.

165. PAPADOPOULOS, A.N., MILITZ, H. and PFEFFER, A. (2010) The biological behaviors of pine wood modified with linear chain carboxylic acid anhydrides against soft rot fungi, *International Biodeterioration & Biodegradation*. 64(5), pp. 409-412.

166. PEARCE, C.I., LLOYD, J.R. and GUTHRIE, J.T. (2003) The removal of color from textile wastewater using whole bacterial cells: a review, *Dyes and Pigments*. 58(3), pp. 179-196.

167. PEDERSEN, A.J. (2003) Characterization and electrolytic treatment of wood combustion fly ash for the removal of cadmium, *Biomass & Bioenergy*. 25(4), pp. 447-458.

168. PEKEL, N., YOSHII, F., KUME, T. and GÜVEN, O. (2004) Radiation cross-linking of biodegradable hydroxypropylmethylcellulose, *Carbohydrate Polymers*. 55(2), pp. 139-147.

169. PEREIRA, M.F.R., SOARES, S.F., ORFAO, J.M.J. and FIGUEIREDO, J.L. (2003) Adsorption of dyes on activated carbons: influence of surface chemical groups, *Carbon*. 41(4), pp. 811-821.

170. PEREZ-CANDELA, M., MARTIN-MARTINEZ, J.M. and TORREGROSA-MACIA, R. (1995) Chromium (VI) removal with activated carbons, *Water Research.* 29(9), pp. 2174-2180.

171. PHOLOSI, A., OFOMAJA, A.E. and NAIDOO, E.B. (2013) Effect of chemical extractants on the biosorptive properties of pine cone powder: Influence on Pb (II) removal mechanism, *Journal of Saudi Chemical Society*. 17(1), pp. 77-86.

172. QIN, C., SOYKEABKAEW, N., XIUYUAN, N. and PEIJS, T. (2008) The effect of fibre volume fraction and mercerization on the properties of all-cellulose composites, *Carbohydrate Polymers.* 71(3), pp. 458-467.

173. QIU, X., TAO, S., REN, X. and HU, S. (2012) Modified cellulose films with controlled permeatability and biodegradability by crosslinking with toluene diisocyanate under homogenous conditions, *Carbohydrate Polymers*. 88(4), pp. 1272-1280.

174. RADKE, C.J. and PRAUSNITZ, J.M. (1972) Adsorption of organic solutes from dilute aqueous solution of activated carbon, *Industrial and Engineering Chemistry Fundamentals*. 11(4), pp. 445-451.

175. RAFATULLAH, M., SULAIMAN, O., HASHIM, R. and AHMAD, A. (2009) Adsorption of methylene blue on low-cost adsorbents: A review, *Journal of Hazardous Materials*. 177(1-3), pp. 70-80.

176. REDDAD, Z., GERENTE, C., ANDRES, Y., THIBAULT, J.F. and LE CLOIREC, P. (2003) Cadmium and lead adsorption by natural polysaccharide in MF membrane reactor: experimental analysis and modeling, *Water Research.* 37(16), pp. 3983-3991.

177. REDDY, D.H.K., RAMANA, D.K.V., SESHAIAH, K. and REDDY, A.V.R. (2011) Biosorption of Ni (II) from aqueous phase by *Moringa oleifera* bark, a low cost biosorbent, *Desalination.* 268(1-3), pp. 150-157.

178. REDDY, D.H.K., SESHAIAH, K., REDDY, A.V.R. and LEE. S.M. (2012) Optimization of Cd (II), Cu (II) and Ni (II) biosorption by chemically modified *Moringa oleifera* leaves powder, *Carbohydrate Polymers*. 88(3), pp. 1077-1086.

179. REDLICH, O. and PETERSON, D.L. (1959) A useful adsorption isotherm, *Journal of Physical Chemistry*. 63(6), pp. 1024.

180. RENGARAJ, S., YEON, K-H. and MOON, S-H. (2001) Removal of chromium from water and wastewater by ion exchange resins, *Journal of Hazardous Materials*. B 87 (1-3), pp. 273-287.

181. RINGOT, D., LERZY, B., CHAPLAIN, K., BONHOURE, J-P., AUCLAIR and LARONDELLE, Y. (2007) In vitro biosorption of ochratoxin A on the yeast industry

by-products: Comparison of isotherm models, *Bioresource Technology*. 98, pp. 1812-1821.

182. RITCHIE, A.G. (1977) Alternative to the Elovich equation for the kinetics of adsorption of gases on solids, *Journal of the Chemical Society*. 73, pp. 1650-1653.

183. ROBBINS, W.W., WEIER, T.E. and STOCKING, C.R. (1957) Botany-An Introduction to Plant Science, *Soil Science*. 84(2), pp. 180.

184. ROBINSON, T., CHANDRAN, B. and NIGAM, P. (2002) Studies on desorption of individual textile dyes and a synthetic dye effluent from dye-adsorbed agricultural residues using solvents, *Bioresource Technology*. 84(3), pp. 299-301.

185. ROWBOTHAM, A.L., LEVY, L.S. and SHUKER, L.K. (2000) Chromium in the environment: an evaluation of exposure of the UK general population and possible adverse health effects, *Journal of Toxicology and Environmental Health, Part B: Critical Reviews.* 3(3), pp. 145-178.

186. RYAN, M.G (1999) The Complete Pine, *BioScience.* 49(12), pp. 1023-1024.

187. SAĞ, Y. and KUTSAL, T. (2000) Determination of the biosorption heats of heavy metal ions on *Zoogloea ramigera* and *Rhizopus arrhizus, Biochemical Engineering Journal.* 6(2), pp. 145–151.

188. SAKAGAMI, H., TAKEDA, M., KAWAZOE, Y., NAGATA, K., ISHIHAMA, A., UEDA, M. and YAMAZAKI, S. (1992) Anti-influenza virus activity of a lignin fraction from cone of *Pinus parviflora* Sieb. et Zucc, *In Vivo.* 6(5), pp. 491-495.

189. SALIPIRA K.L., MAMBA B.B., KRAUSE R.W., MALEFETSE T.J. and DURBACH S.H. (2008) Cyclodextrin polyurethanes polymerized with carbon nanotubes for the removal of organic pollutants in water, *Water SA*. 34(1), pp. 113-118.

190. SAMARGHANDI, M.R., HADI, M., MOAYEDI, S. and ASKARI, F.B. (2009) Two-parameter isotherms of methyl orange sorption by pine cone derived activated carbon, *Iranian Journal of Environmental Health Science & Engineering*. 6(4), pp. 285-294.

191. SCIBAN, M., KLASNJA, M. and SKRBIC, B. (2006) Modified hardwood sawdust as adsorbent of heavy metal ions from water, *Wood Science and Technology*. 40(3), pp. 217-227.

192. SHEN, H. and WANG, Y-T. (1994) Biological reduction of chromium by *E.coli*, *Journal of Environmental Engineering.* 120(3), pp. 560-571.

193. SHIFTAN, D., RAVENELLE, F., MATEESCU. M.A. and MARCHESSAULT, R.H. (2000) Change in the V/B polymorph ratio and T_1 relaxation of epichlorohydrin cross-linked high amylose starch excipient, *Starch-Stärke*. 52(6-7), pp. 186-195.

194. SIPS, R. (1948) Combined form of Langmuir and Freundlich equations, *Journal of Chemical Physics.* 16, pp. 490-495.

195. SIQUEIRA, G., BRAS, J. and DUFRESNE, A. (2010) New process of chemical grafting of cellulose nanoparticles with a long chain isocyanate, *Langmuir.* 26(1), pp. 402-411.

196. SOTELO, J.L., OVEJERO, G., DELGADO, J.A. and MARTINEZ, I. (2002) Comparison of adsorption equilibrium and kinetics of four chlorinated organics from water onto GAC, *Water Research.* 36(3), pp. 599-608.

197. SUD, D., MAHAJAN, G. and KAUR, M.P. (2008) Agricultural waste material as potential adsorbent for sequestering heavy metal ions from aqueous solutions - A review, *Bioresource Technology*. 99(14), pp. 6017-6027.

198. SUN, Q. and YANG, L. (2003) The adsorption of basic dyes from aqueous solution on modified peat-resin particle, *Water Research.* 37(7), pp. 1535-1544.

199. TAKÁCS, E., WOJNÁROVITS, L., FöLDVÁRY, CS., HARGITTAI, P., BORSA, J. and SAJÓ, I. (2000) Effect of combined gamma-irradiation and alkali treatment on cotton-cellulose, *Radiation Physics & Chemistry*. 57(3-6), pp. 399-403.

200. TEMKIN, M.I. and PYZHEV, V. (1940) Kinetics of ammonia synthesis on promoted iron catalysts, *ActaPhysiochimica (URSS)*. 12, pp. 327-356.

201. THEOPHANIDES, T. and ANASTASSOPOULOU, J. (2002) Copper and carcinogenesis, *Critical Reviews in Oncology/Hematology.* 42(1), pp. 57-64.

202. TÓTH, J. (1971) State equations of the solid gas interface layer, *Acta Chimica Academiae Scientiarum Hungaricae*. 69, pp. 311-317.

203. TSEZOS, M. and REMOUDAKI, E. (1997) Recent advances in the mechanistic understanding of metal mobility and interaction with microbial biomass, *Research in Microbiology.* 148(6), pp. 515-517.

204. UCUN, H., BAYHAN, Y.K., KAYA, Y., CAKICI, A. and ALGUR, O.F. (2003) Biosorption of lead (II) from aqueous solution by cone biomass of *Pinus sylvestris*, *Desalination*. 154(3), pp. 233-238.

205. VALODKAR, M. and THAKORE, S. (2010) Isocyanate crosslinked reactive starch nanoparticles for thermo-responsive conducting applications, *Carbohydrate Research.* 345(16), pp. 2354-2360.

206. VAN DER BRUGGEN, B. and VANDECASTEELE, C. (2003) Removal of pollutants from surface water and groundwater by nanofiltration: overview of possible applications in the drinking water industry, *Environmental Pollution.* 122(3), pp. 435-445.

207. VAUGHAN, T., SEO, C.W. and MARSHALL, W.E. (2001) Removal of selected metal ions from aqueous solution using modified corncobs, *Bioresource Technology*. 78(2), pp. 133-139.

208. VIEIRA, R.H.S.F. and VOLESKY, B. (2000) Biosorption: a solution to pollution, *International Microbiology.* 3(1), pp. 17-24.

209. VOLESKY, B. (2001) Detoxification of metal-bearing effluents. Biosorption for the next century, *Hydrometallurgy*. 59(2-3), pp. 203-216.

210. VOLESKY, B. (2007) Biosorption and me, *Water Research.* 41(18), pp. 4017-4029.

211. VYMAZAL, J. (1990) Uptake of lead, chromium, cadmium and cobalt by *Cladophora glomerata, Bulletin of Environmental Contamination and Toxicology*. 44(3), pp. 468-472.

212. WALLING, C. (1975) Fenton's reagent revisited, *Accounts of Chemical Research.* 8(4), pp. 125-131.

213. WAN NGAH, W.S. and HANAFIAH, M.A.K.M. (2008) Removal of heavy metal ions from wastewater by chemically modified plant wastes as adsorbents: a review, *Bioresource Technology*. 99(10), pp. 3935-3948.

214. WANG, L.K., VACCARI, D.A., LI, Y. and SHAMMAS, N.K. (2004) Chemical precipitation. *In*: Wang, L.K., Hung, Y.T., Shammas, N.K., *eds.*, Physicochemical Treatment Processes, Vol 3, New Jersey: Humana Press. pp. 141-198.

215. WANG, L.L. and XU, Y.S. (2006) γ-radiation-induced graft copolymerization of ethyl acrylate onto hydroxypropyl methylcellulose, *Macromolecular Materials & Engineering*. 291(8), pp. 950-961.

216. WANG, S. and PENG, Y. (2010) Natural zeolites as effective adsorbents in water and wastewater treatment, *Chemical Engineering Journal*. 156(1), pp. 11-24.

217. WARTELLE, L.H. and MARSHALL, W.E. (2000) Citric acid modified agricultural by-products as copper ion adsorbents, *Advances in Environmental Research*. 4(1), pp. 1–7.

218. WEBER, W.J. and MORRIS, J.C. (1963) Kinetics of adsorption on carbon from solution, *Journal of Sanitary Engineering Division (ASCE),* 89, pp. 31-59.

219. WEGENER, G., BRANDT, M., DUDA, L., HOFMANN, J., KLESCZEWSKI, B., KOCH, D., KUMPF, R.J., ORZESEK, H., PIRKL, H-S., SIX, C., STEINLEIN, C. and WEISBECK, M. (2001) Trends in industrial catalysis in the polyurethane industry, *Applied Catalysis A: General*. 221(1-2), pp. 303-335.

220. WEISS, B. and LANDRIGAN, P.J. (2000) The developing brain and the environment: an introduction, *Enviromental Health Perspectives.* 108(3), pp. 373-374.

221. WILPISZEWSKA, K. and SPYCHAJ, T. (2007) Chemical modification of starch with hexamethylene diisocyanate derivatives, *Carbohydrate Polymers*. 70(3), pp. 334-340.

222. WING, R.E. (1996a) Corn fiber citrate: preparation and ion-exchange properties, *Industrial Crops and Products.* 5(4), pp. 301-305.

223. WING, R.E. (1996b) Starch citrate: preparation and ion exchange properties, *Starch*. 48(7-8), pp. 275-279.

224. WOJNÁROVITS, L., FöLDVÁRY, Cs.M. and TAKÁCS, E. (2010) Radiation-induced grafting of cellulose for adsorption of hazardous water pollutants: A review, *Radiation Physics & Chemistry*. 79(8), pp. 848-862.

225. WOLFF, I.A., WATSON, P.R. and RIST, C.E. (1952) Polysaccharide aryl carbamates. II. Nuclear substituted tricarbanilates of corn starch, corn amylase and amylopectin, *Journal of American Chemical Society*. 74(12), pp. 3061-3063.

226. WONG, K.K., LEE, C.K., LOW, K.S. and HARON, M.J. (2003) Removal of copper and lead by tartaric acid modified husk from aqueous solutions, *Chemosphere*. 50(1), pp. 23-28.

227. XUAN, Z., TANG, Y., LI, X., LIU, Y. and LUO, F. (2006) Study on the equilibrium, kinetics and isotherm of biosorption of lead ions onto pretreated chemically modified orange peel, *Biochemical Engineering Journal*. 31(2), pp. 160-164.

228. YANG, X. and AL-DURI, B. (2005) Kinetic modelling of liquid-phase adsorption of reactive dyes on activated carbon, *Journal of Colloid and Interface Science*. 287, pp. 25-34.

229. YAVUZ, Ö., ALTUNKAYNAK, Y. and GÜZEL, F. (2003) Removal of copper, nickel, cobalt and manganese from aqueous solution by kaolinite, *Water Research*. 37(4), pp. 948-952.

230. ZHANG, L., ZHAO, L., YU, Y. and CHEN, C. (1998) Removal of lead from aqueous solution by non-living *Rhizopus nigricans, Water Research*. 32(5), pp. 1437-1444.

231. ZHOU, J.L. and BANKS, C.J. (1993) Mechanism of humic acid color removal from natural waters by fungal biomass biosorption, *Chemosphere*. 27(4), pp. 607-620.

232. ZHOU, D., ZHANG, L., ZHOU, J. and GUO, S. (2004) Cellulose/chitin beads for adsorption of heavy metals in aqueous solution, *Water Research*. 38(11), pp. 2643-2650.

233. ZHU, B., FAN, T. and ZHANG, D. (2008) Adsorption of copper ions from aqueous solution by citric acid modified soybean straw, Journal of Hazardous Materials. 153(1-2), pp. 300-308.

3 EXPERIMENTAL PROCEDURES

3.1 INTRODUCTION

This chapter is divided into four sections. The first section explains the sample preparation which involved thermal and Fenton's reagent oxidation of the raw pine cone biomass.

The second section involves the optimization procedures for the cross-linking reaction between 1.6-hexamethylene diisocyanate (HMDI) and the Fenton treated pine cone biomass using Fourier transform infrared instrumentation. Weight percent gain calculations were done to determine extend/degree of the cross-linking reaction. The section also deals with the characterization of the prepared hydrophobic biomaterial composite using thermogravimetric analysis, X-ray diffraction, scanning electron microscope, electron dispersive spectroscopy and Brunauer-Emmett-Teller surface area to confirm the success of HMDI cross-linking modification of the pine cone biomass.

The third section deals with surface properties of the pine cone biomass, before and after the modification techniques. Experiments to determine acidic groups and pH_{pzc} are also presented.

The fourth section describes the application of pine cone biosorbents (Raw, Raw-HMDI, Fenton treated and Fenton treated-HMDI) in the removal of 2-nitrophenol from aqueous solution using the batch adsorption technique. Equilibrium and kinetic experiments are presented to investigate the adsorption process.

3.2 SAMPLE COLLECTION AND PREPARATION

3.2.1 Sample collection

The cones were collected from pine trees in Vanderbijlpark, Gauteng province in South Africa. The cones were washed and heated in a thermostatic oven at 80 °C for 48 hours to remove impurities and some volatile organics like resin acids without destroying the pine cone matrix. The pine cone scales were peeled and crushed to a powder using a pulveriser and sieved. Particles between 45 and 90 µm were then used for analysis.

3.2.2 Modification of pine cone sample

3.2.2.1 Theory of Fenton modification of biomass

Hydrogen peroxide-ferrous ion system (H_2O_2/Fe^{2+}), known as Fenton's reagent is known to destroy plant organic constituents and pigments along with resin acids present in pine cone which are likely to colour the purified water and increase total organic carbon, chemical and biological oxygen demand (Ahn et al., 1999; Argun et al, 2008). Addition of Fenton's reagent in strong acid to plant biomass results in a complex redox reaction (Walling and Kato, 1971) involving the following Equations (3.1-3.3):

$$Fe^{2+} + H_2O_2 \rightarrow Fe^{3+} + OH^- + HO^{\cdot} \quad (3.1)$$

$$RH + HO^{\cdot} \rightarrow H_2O + R^{\cdot} \quad (3.2)$$

$$R\cdot + O_2 \rightarrow ROO\cdot \rightarrow \text{decomposed} \quad (3.3)$$

3.2.2.2 Fenton oxidation of pine cone

Fenton's reagent was prepared by accurately measuring 303 cm^3 of 30 % H_2O_2 and 6.993 g of Fe^{2+} as $FeSO_4.7H_2O$ which were separately placed in 1000 cm^3 volumetric flasks containing distilled water. The pH of Fe^{2+} was adjusted to between 3 and 4.5 with 0.1 mol/dm^3 H_2SO_4. An Adwa AD8000 pH meter, supplied by Labmark (Romania) was used for the pH measurements. In a 2000 cm^3 three-necked round-bottomed flask with a nitrogen inlet and magnetic stirrer, 250 cm^3 of Fe^{2+} and 100 g of pine cone powder were mixed and heated at 50 °C for 30 minutes. To this mixture, 250 cm^3 of the prepared H_2O_2 was added and the heating programme continued for a further 30 minutes. The resulting bleached/oxidised mixture was filtered under suction with a Whatman™ filter paper and the residue was washed with distilled water until filtrate was clear. The Fenton oxidised pine cone biomass was then oven dried for 8 hours at 80 °C and changes in surface properties determined using Fourier transform-infrared spectroscopy (FTIR), thermogravimetric analysis (TGA), X-ray diffraction (XRD), scanning electron microscopy (SEM), electron dispersive spectroscopy (EDX) and Brunauer-Emmett-Teller (BET) surface area determination techniques before being used in the cross-linking reaction.

3.2.3 Cross-linking of Fenton treated pine cone biomass with hexamethylene diisocyanate

3.2.3.1 Theory of cross-linking Fenton treated pine cone with a diisocyanate

The reaction of lignocellulosic based materials with diisocyanates requires the initial activation of the biomass (Gafurov et al., 1970; Rozman et al., 2001). The activating agent causes a swelling of the biomass to allow access of the hexamethylene diisocyanate (HMDI) cross-linker to the matrix surface. Fenton oxidised pine cone powder (0.1 g) was dispersed in anhydrous hexane (10 cm^3), in which dibutyltin dilaurate (1 cm^3) was added as catalyst in a 250 cm^3 three-necked round-bottomed flask with a magnetic stirrer and an inlet for N_2 gas. The mixture was heated in a reflux set up at 50 °C for 15 minutes to complete the process of activation. This reaction has been shown to cause a redistribution of the hydrogen bonds in lignocelluloses (Gavurov et al., 1970). A separate volume of HMDI (2.5 cm^3) was dissolved in anhydrous hexane (10 cm^3), this has been shown to produce easier reaction of lignocellulosic materials and the dominant transverse bond formation without homopolymer production (Gafurov et al., 1970). It was then added drop wise to the activated pine cone biomass. The mixture was heated under reflux in a nitrogen atmosphere for 1 hour with continuous stirring. The HMDI modified Fenton treated pine cone biosorbent produced was rinsed with fresh hexane several times, followed by drying in a thermostatic oven at 80 °C for 8 hours.

3.2.3.2 Proposed reaction pathway for cross-linking of pine cone using a diisocyanate

Since pine cone is lignocellulosic, it should be feasible to cross-link the biomass using a diisocyanate forming hydrophobic urethane linkages (Noble, 1997) as shown in the proposed reaction pathway in Figure 3.1:

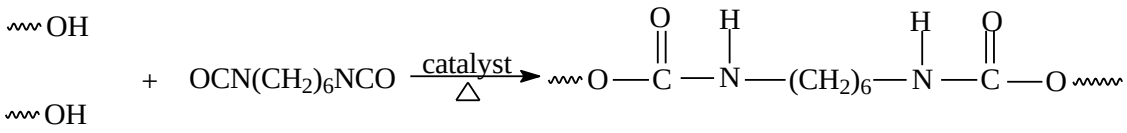

Figure 3.1 Schematic illustrations showing proposed cross-linking of pine cone using HMDI.

3.2.3.3 Optimization of mass of Fenton treated pine cone biomass

Accurately weighed amounts (0.1 g, 0.2 g, 0.3 g, 0.4 g and 0.5 g) of Fenton treated pine cone were placed in separate 250 cm^3 three-necked round-bottomed flasks, each with a magnetic stirrer. The procedure for the biomass activation and cross-linking described in 3.2.3.1 was followed. Changes to the surface properties of modified biosorbent were determined using FTIR to confirm cross-linking of pine cone biomass using HMDI and select the optimum mass of Fenton treated pine cone for this reaction.

3.2.3.4 Optimization of HMDI cross-linker

Fenton treated pine cone samples (0.2 g) were weighed and separately placed in five 250 cm^3 three-necked round-bottomed flasks, each with a magnetic stirrer. The procedure described in 3.2.3.1 was followed with carefully measured volumes of HMDI cross-linker (2.5 cm^3, 3.5 cm^3, 4.5 cm^3, 5.5 cm^3 and 6.5 cm^3). Changes to the surface properties of modified biosorbent were determined using FTIR to confirm cross-linking of pine cone biomass using HMDI and select the optimum volume of HMDI cross-linker for this reaction.

3.2.3.5 Optimization of dibutyltin dilaurate catalyst

Carefully weighed four samples of Fenton treated pine cone (0.2 g) were separately placed in 250 cm^3 three-necked round bottomed flasks and activated using the procedure described in 3.2.3.1 but with catalyst volumes of 1 cm^3, 1.5 cm^3, 2.5 cm^3 and 4 cm^3. The cross-linking procedure as in 3.2.3.1 was also followed using HMDI (3.5 cm^3) together with the characterization in order to choose the optimum catalyst volume for this reaction.

3.2.3.6 Optimization of cross-linking temperature

The same procedure (using a catalyst volume of 1.5 cm^3) as in 3.2.3.5 was followed in the activation and cross-linking of the Fenton treated pine cone but using 30 °C, 50 °C, 70 °C and 90 °C as the cross-linking temperatures in different experiments. FTIR was used to confirm cross-linking of the cone biomass.

3.2.3.7 Optimization of cross-linking time

The same procedure (at 50 °C) as in 3.2.3.6 was followed in the activation and cross-linking of the Fenton treated pine cone but using 1 hour, 2 hours, 3 hours and 4 hours as the cross-

linking times in different experiments. The same characterization technique (FTIR) was used to confirm the cross-linking of the biomass.

3.2.4 Cross-linking of Raw and Fenton treated pine cone

Accurately weighed amounts of Raw and Fenton treated pine cone (0.2 g) were placed in two separate 250 cm^3 three-necked round-bottomed flasks, each with a magnetic stirrer. The procedures as in 3.2.3.6 were followed with the cross-linking mixture being refluxed under nitrogen atmosphere for 4 hours with continuous stirring. Weight percent gain calculations together with FTIR instrumentation was used to confirm and determine extend of cross-linking of pine cone biomass using HMDI.

3.3 CHARACTERIZATION OF PINE CONE BIOMASS

3.3.1 Fourier-Transform Infra-Red spectroscopy

Fourier-transform infrared (FTIR) spectroscopy was used to study the functional groups of the pine cone biomass and the changes in functional groups observed due to different treatments and chemical derivatization (Sim et al., 2012). The FTIR spectra provide qualitative and semi-quantitative information suggesting the presence and absence of lignocellulosic compounds (Li et al., 2010). The analysis was done using a Perkin-Elmer (USA) FTIR Spectra 400 spectrometer in the range 650-4000 cm^{-1}.

3.3.2 Thermogravimetric Analysis

Thermogravimetric analysis (TGA) determines weight loss as a function of temperature. It was used to determine the changes to the pine cone matrix due to the different chemical treatments since each kind of biomass has a characteristic pyrolysis behaviour which is explained based on its individual component characteristics (Raveendran et al. 1996). The cone samples were subjected to pyrolysis from 30 – 700 °C in a N_2/air atmosphere at a heating rate of 10 $°C.min^{-1}$ using a Perkin-Elmer (USA) Simultaneous Thermal Analyzer 6000 instrument. An empty crucible was used as reference.

3.3.3 X-Ray Diffraction spectroscopy

X-ray diffraction (XRD) was conducted to identify the chemical composition and crystallographic structure of the raw and modified pine cone biomass. An X'Pert PRO X-ray diffractometer (PANalytical, PW3040/60 XRD; CuKα anode; λ = 0.154 nm) was used to obtain the XRD patterns. The samples were placed in an aluminium holder and scanned at 45 kV and 40 mA from 10 ° to 120 ° 2θ, the exposure time for each sample was 20 minutes and a step size of 0.02 °. The Debye-Scherrer equation (Burton et al., 2009) was used to determine particle sizes of the prepared biosorbents:

$$d = \frac{0.89\lambda}{\beta \cos\theta} \qquad (3.4)$$

Where, d = particle size (nm),

λ = 0.154 nm (CuKα),

$\beta = \frac{FWHM}{360\ X\ 2\pi}$ (FWHM = Full Width at Half Maximum),

θ = half of 2θ (centre of peak).

3.3.4 Scanning Electron Microscopy

Scanning electron microscopy (SEM) was used to observe the microstructure and surface morphology of treated and untreated pine cone biomass (Ouajai and Shanks, 2005). The SEM images were obtained on a Cerl-Zeiss-Sigma instrument (Germany) that uses a tungsten filament source. The samples were Pd-Au coated and imaging was done at 5 kV and 150× magnification.

3.3.5 Electron Dispersive Spectroscopy (EDX)

Elemental analysis was done on the raw and modified pine cone samples using a Cerl-Zeiss-Sigma instrument (Germany). The samples were Pd-Au coated before analysis in order to improve their surface conductivity.

3.3.6 Brunauer-Emmett-Teller Surface Area

Sample surface area, pore volume and pore size were determined by N_2 adsorption at -196 ^oC using a Tristar 3000 analyzer coupled to a VacPrep 061 degassing unit. Both instruments were supplied by Micromeritics Instrument Corporation (Australia).

3.3.7 Weight Percent Gain Determination

Weight percent gain (WPG) calculations were done to determine extend/degree of cross-linking due to the reaction between HMDI and the pine cone biomass (Raw and Fenton treated). The WPG values were calculated as follows (Rozman et al., 2001):

$$WPG = \frac{W_1 - W_0}{W_0} \times 100 \qquad (3.5)$$

Where, W_1 is the weight of oven-dried HMDI-modified pine cone biomass (after rinsing with hexane) and W_0 is the weight of oven-dried unmodified pine cone biomass.

3.4 SURFACE PROPERTIES

3.4.1 Determination of acid groups on pine cone surface

3.4.1.1 Theory

Acidic oxygen surface functional groups on raw, Fenton oxidised, HMDI cross-linked Fenton oxidised and HMDI cross-linked raw pine cone biomass were determined by the acid-base titration method proposed by Boehm (1994). The titration works on the principle that oxygen groups on material surfaces have different acidities, hence can be neutralised by bases of different strengths (Oickle et al., 2010). The total acid sites matching phenolic, lactonic and carboxylic groups were neutralised using a 0.1 $mol.dm^{-3}$ NaOH solution. Lactonic and carboxylic sites were neutralised using a 0.05 $mol.dm^{-3}$ Na_2CO_3 solution while carboxylic sites were neutralised by a 0.1 $mol.dm^{-3}$ $NaHCO_3$ solution. The difference between the consumption of bases can be used to identify and quantify the types of oxygen surface groups present on the pine cone sample (Goertzen et al., 2010). Therefore, by taking the difference, the magnitude of each acidic function on the pine cone surface was determined as follows:

(1) mmoles of NaOH reacted – mmoles of Na_2CO_3 reacted = mmoles of phenolics

(2) mmoles of Na_2CO_3 reacted – mmoles of $NaHCO_3$ reacted = mmoles of lactones

(3) mmoles of $NaHCO_3$ reacted = mmoles of carboxyl groups

3.4.1.2 Experimental

To a series of 100 cm^3 volumetric flasks containing 50 cm^3 of either NaOH or Na_2CO_3 or $NaHCO_3$ solutions, 0.1 g samples of raw (Raw) or Fenton treated or HMDI cross-linked Fenton oxidised (Fenton treated-HMDI) or HMDI cross-linked raw (Raw-HMDI) pine cone powder were separately added. The flasks were immediately closed to prevent dissolution of CO_2 which ends up reacting with water forming carbonic acid, causing the pH to shift (Goertzen et al., 2010). The volumetric flasks were agitated at 100 revolutions per minute (rpm) on a shaker for 120 hours. A 10 cm^3 aliquot of the reaction base from each volumetric flask was then pipetted out and titrated with a 0.1 mol/dm^3 HC*l* solution using phenolphthalein and bromocresol green indicators to detect the end point. The titration was carried out in triplicates.

3.4.2 pH at point zero charge

The solid addition method (Lataye et al., 2006) was used to determine the pH_{pzc} of the Raw, Fenton treated, Fenton treated-HMDI and Raw-HMDI pine cone powder. To a series of 100 cm^3 volumetric flasks, 45 cm^3 of 0.01 mol/dm^3 KNO_3 solution were transferred. The pH_i values of the solutions were roughly adjusted between pH 2 to 12 by addition of either 0.1 mol/dm^3 HC*l* or NaOH on a pH meter with constant stirring. Total volume of the solution in each flask was made up to 50 cm^3 by addition of KNO_3 solution of the same strength. The pH_i of the solutions were accurately noted, and 0.1 g of either Raw or Fenton treated or Fenton treated-HMDI or Raw-HMDI pine cone powder were added to each volumetric flask, which was then immediately closed. The suspensions were allowed to equilibrate for 48 hours on a shaker operating at 100 rpm. The pH_f values of the supernatant were accurately noted and the difference between the initial and final pH values ($\Delta pH = pH_f - pH_i$) were plotted against the pH_i. The point of intersection of the resulting curve at which $\Delta pH = 0$ gave the pH_{pzc}.

3.5 APPLICATION OF PREPARED BIOSORBENT IN POLLUTANT REMOVAL FROM AQUEOUS SOLUTION

3.5.1 Analytical method

At high pH (11-12), the phenolic proton dissociates giving a phenolate anion with an intense yellow colour that can easily be measured spectrometrically (Ofomaja, 2011). The procedure for determination of equilibrium concentrations of 2-nitrophenol after the adsorption process involves mixing equal volumes (2 cm^3) of the 2-nitrophenol sample and 0.5 mol/dm^3 Na_2CO_3 solution (pH 11-12) before analysis with a Perkin-Elmer (USA) Lambda 25 UV-visible (UV-vis) spectrometer. The absorption of the resulting mixture was read at 400 nm wavelength using distilled water as blank.

3.5.2 Effect of solution pH

An accurately weighed amount (0.05 g) of each of the four different pine cone biomass samples (Raw, Raw-HMDI, Fenton treated and Fenton treated-HMDI) was separately placed in six 250 cm^3 conical flasks. To each conical flask, 100 cm^3 of 50 mg/dm^3 (2-nitrophenol) whose pH had each been adjusted to 1, 2, 4, 6, 8 and 10 using 0.1 mol/dm^3 of either HC*l* or NaOH was then separately added. The conical flasks were then agitated at 100 rpm for 1 hour at 299 K and then filtered to stop the adsorption process. The 2-nitrophenol samples were then analysed as described in 3.5.1 to determine the equilibrium concentrations.

3.5.3 Adsorbent dose

The experiments were performed by agitating known masses (0.0125 g, 0.05 g, 0.10 g, 0.15 g and 0.2 g) of the four pine cone biomass samples (Raw, Raw-HMDI, Fenton treated and Fenton treated-HMDI) in 250 cm^3 conical flasks containing 50 mg/dm^3 (2-nitrophenol) at pH 6. The conical flasks were agitated at 100 rpm for 1 hour at 299 K and then filtered. The filtrate was then analysed as described in 3.5.1.

3.5.4 Equilibrium studies

The experiments were done at 299 K, 309 K, 319 K and 329 K. Accurately weighed amounts (0.15 g) of each of the four different pine cone samples (Raw, Raw-HMDI, Fenton treated and Fenton treated-HMDI) were separately placed in five 250 cm^3 conical flasks, each containing 100 cm^3 of either 50 mg/dm^3, 200 mg/dm^3, 300 mg/dm^3, 350 mg/dm^3 or 400 mg/dm^3 (2-nitrophenol) at pH 6. The conical flasks were agitated at 100 rpm for 1 hour. The adsorption process was stopped and concentration of the remaining 2-nitrophenol determined by the procedure described in section 3.5.1.

3.5.5 Effect of initial 2-nitrophenol concentration

The kinetic experiments were conducted using different concentrations of 2-nitrophenol (100 mg/dm^3, 200 mg/dm^3, 300 mg/dm^3 and 400 mg/dm^3) at pH 6. Accurately weighed amounts (0.015 g) of each of the pine cone samples (Raw, Raw-HMDI, Fenton treated and Fenton treated-HMDI) were separately placed in seven 100 cm^3 beakers, each containing 10 cm^3 of 2-nitrophenol and a magnetic stirrer. The beakers were stirred for different time intervals and concentration of 2-nitrophenol was determined using UV-vis spectrometry as described in 3.5.1.

3.6 REFERENCES

1. AHN, D-H., CHANG, W-S. and YOON, T-I. (1999) Dyestuff wastewater treatment using chemical oxidation, physical adsorption and fixed bed biofilm process, *Process Biochemistry*. 34(5), pp. 429-439.
2. ARGUN, M.E., DURSUN, S., KARATAS, M. and GÜRÜ, M. (2008) Activation of pine cone using Fenton oxidation for Cd (II) and Pb (II) removal, *Bioresource Technology*. 99(18), pp. 8691-8698.
3. BOEHM, H.P. (1994) Some aspects of the surface chemistry of carbon black and other carbons, *Carbon*. 32(5), pp. 759-769.
4. BURTON, A.W., ONG, K., REA, T. and CHAN, I.Y. (2009) On the estimation of average crystallite size of zeolites from the Scherrer equation: A critical evaluation of its application to zeolites with one-dimensional pore systems, *Microporous and Mesoporous Materials*. 117, pp. 75-90.
5. GAFUROV, T.G., PILOSOV, M., ADYLOV, A., MANNANOVA, D., SUVOROVA, V., TASHPULATOV, G.V. and USMANOV, V. (1970) The reaction of cellulose with hexamethylene diisocyanate, *Vysokomol soyed*. A12(11), pp. 2515-2519.
6. GOERTZEN, S.L., THÉRIAULT, K.D., OICKLE, A.M., TARASUK, A.C. and ANDREAS, H.A. (2010) Standardization of the Boehm titration. Part I. CO_2 expulsion and end point determination, *Carbon*. 48(4), pp. 1252-1261.
7. LATAYE, D.H., MISHRA, I.M. and MALL, I.D. (2006) Removal of pyridine from aqueous solution by adsorption on bagasse fly ash, *Industrial & Engineering Chemistry Research*. 45(11), pp. 3934-3943.
8. LI, C., KNIERIM, B., MANISSERI, C., ARORA, R., SCHELLER, H.V., AUER, M., VOGEL, K.P., SIMMONS, B.A. and SINGH, S. (2010) Comparison of dilute acid and ionic liquid of switchgrass: Biomass recalcitrance, delignification and enzymatic saccharification, *Bioresource Technology*. 101(13), pp. 4900-4906.
9. NOBLE, K-L. (1997) Waterborne polyurethanes, *Progress in Organic Coatings*. 32(1-4), pp. 131-136.
10. OFOMAJA, A.E. (2011) Kinetics and pseudo-isotherm studies of 4-nitrophenol adsorption onto mansonia wood sawdust, *Industrial Crops and Products*. 33, pp. 418-428.

11. OICKLE, A.M., GOERTZEN, S.L., HOPPER, K.R., ABDALLA, Y.O. and ANDREAS, H.A. (2010) Standardization of the Boehm titration. Part II. Method of agitation, effect of filtering and dilute titrant, *Carbon*. 48(12), pp. 3313-3322.
12. OUAJAI, S. and SHANKS, R.A. (2005) Composition, structure and thermal degradation of hemp cellulose after chemical treatments, *Polymer degradation & Stability*. 89(2), pp. 327-335.
13. RAVEENDRAN, K., GANESH, A and KHILAR, K.C. (1996) Pyrolysis characteristics of biomass and biomass components, *Fuel*. 75(8), pp. 987-998.
14. ROZMAN, H.D., TAN, K.W., KUMAR, R.N. and ABUBAKAR, A. (2001) The effect of hexamethylene diisocyanate modified ALCELL lignin as a coupling agent on the flexural properties of oil palm empty fruit bunch – polypropylene composites, *Polymer International*. 50(5), pp. 561-567.
15. SIM, S.F., MOHAMED, M., LU, N.A.L.M.I., SAFITRI, N., SARMAN, N.S.P. and SAMSUDIN, S.N.S. (2012) Computer-assisted analysis of Fourier Transform Infrared (FTIR) spectra for characterization of various treated and untreated agriculture biomass, *BioResources.* 7(4), pp. 5367-5380.
16. WALLING, C. and KATO, S. (1971) The oxidation of alcohols by Fenton's Reagent. The effect of copper ion, *Journal of the American Chemical Society*. 93(17), pp. 4275-4281.

4 RESULTS AND DISCUSSION (PART 1): CHARACTERIZATION OF HYDROPHOBIC BIOMATERIAL COMPOSITE:

4.1 INTRODUCTION

The chapter is divided into two sections. The first section deals with optimization of the synthesis of the HMDI cross-linked hydrophobic pine cone biosorbent and its characterization using FTIR, TGA, XRD, SEM, EDX and BET surface area. WPG results are also presented and discussed.

The second section discusses surface properties of the pine cone biomass before and after the modification procedures. Types, magnitude of acidic surface groups and pH_{pzc} results are presented and discussed.

4.2 OPTIMIZATION OF SYNTHESIS AND CHARACTERIZATION OF CROSS-LINKED PINE CONE BIOMASS

4.2.1 FTIR spectroscopy

4.2.1.1 FTIR discussion for raw pine cone

The FTIR spectra of raw pine cone in Figure 4.1, indicates presence of organic functional groups characteristic of lignocellulosic biomass. The major peaks due to cellulose include the broad peak observed at 3333.80 cm^{-1} representing hydrogen bonded (O-H) stretching vibration of polymeric compounds (Saygideger et al., 2005; Ghali et al., 2012) namely α-cellulose and phenol hydroxyls. The peak at 2930.54 cm^{-1} is characteristic of C-H stretching vibration from CH_n in cellulose component (Jayaramudu et al., 2010). The 1421.60 cm^{-1} band may be due to the CH_2 symmetric bending present in cellulose (Bessadok et al., 2008; De Rosa et al., 2011). The band at 1370.91 cm^{-1} represents symmetric C-H bending from the methoxyl group (Adel et al., 2010). Peak at 894.37 cm^{-1} is attributed to the β-glycosidic linkages (De Rosa et al., 2010). Absorbance at 807.01 cm^{-1} is due to C-H out-of-plane vibrations (Ouajai and Shanks, 2005).The absorbance at 664.27 cm^{-1} corresponds to C-OH bending deformation (Sgriccia et al., 2008).

The FTIR spectra also reveals functional groups characteristic of lignin. The functions include carbonyls, phenol hydroxyls, aromatic rings and methoxyls (He et al., 2008). The absorption band at 1728.40 cm^{-1} is characteristic of carbonyl (C=O) stretching of unconjugated ketones in lignin and the acetyl groups of hemicelluloses (Abraham et al., 2011; He et al., 2008). The peak at 1607.12 cm^{-1} is characteristic of C-O stretching of lignin (Jayaramudu et al., 2010) and the peak at 1508.93 cm^{-1} represents aromatic C=C stretching vibrations of aromatic rings of lignin (Alemdar and Sain, 2008; Subramanian et al., 2005). The bands at 1450, 1262 and 1021 cm^{-1} are indicative of methoxy ($O\text{-}CH_3$) groups (Suksabye and Thiravetyan, 2012), syringyl ring bending (Shi and Li, 2012) and C-O stretching vibration of secondary alcohol (Qiu et al., 2012) in lignin.

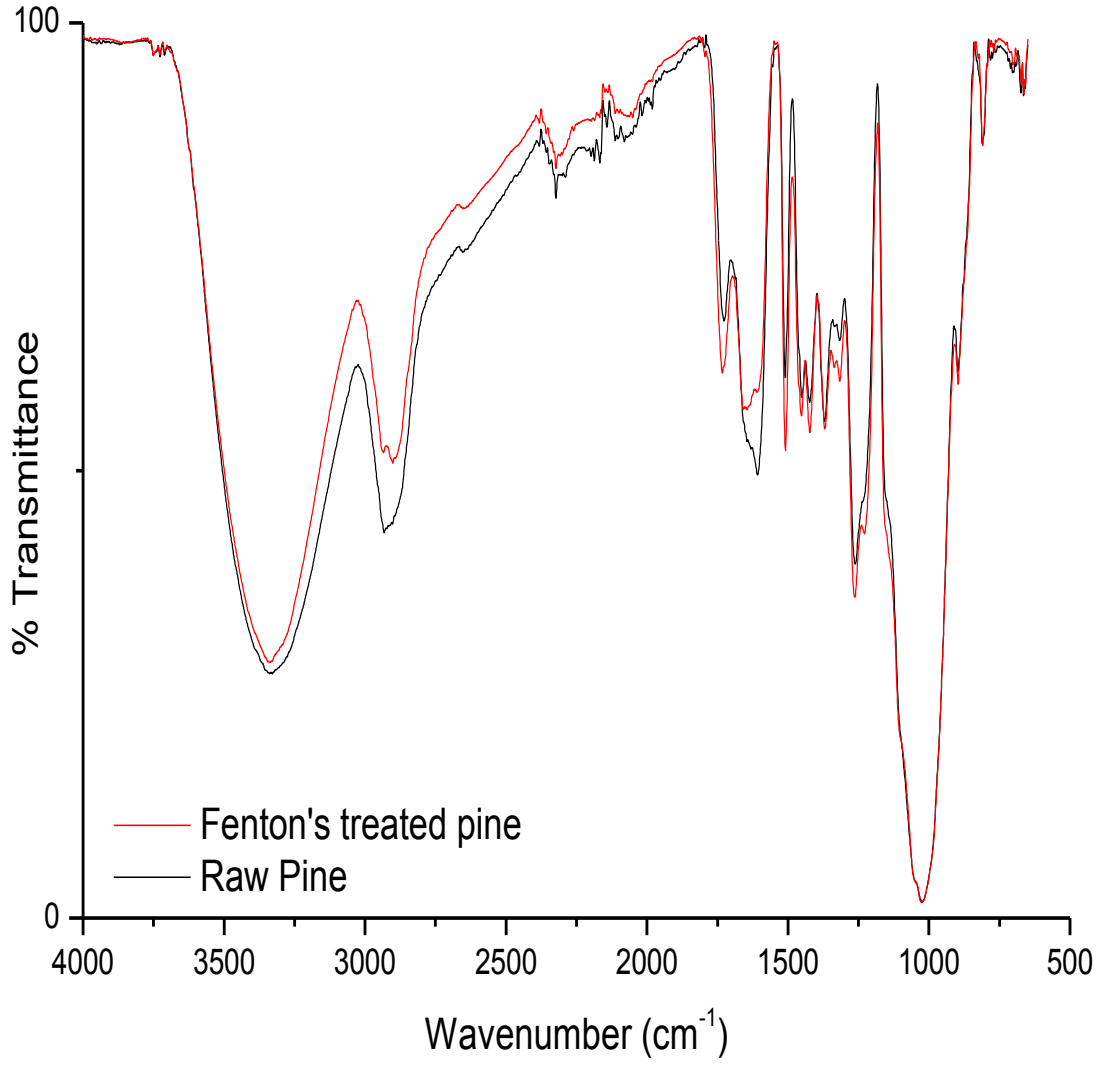

Figure 4.1 FTIR spectra for Raw pine and Fenton treated pine cone

4.2.1.2 FTIR discussion for Fenton treated pine cone

After modification of pine cone with Fenton's reagent the intensity of the broad peak at 3337.70 cm^{-1} decreased as shown in Figure 4.1. Higher percentage of transmittance mean lower amount of functional groups (Argun and Dursun, 2008), this implies a decrease in –OH functional groups which is supported by the following mechanism proposed by Collison and Thielemans (2010):

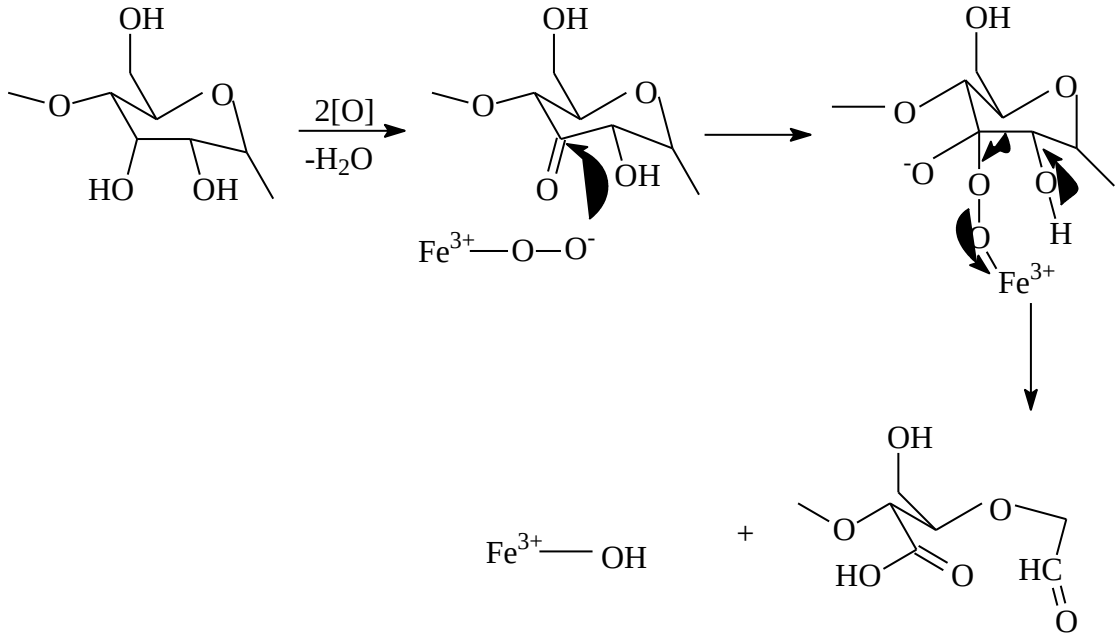

Figure 4.2 Mechanism of the oxidation of sugars by H_2O_2 in presence of water-soluble metal phthalocyanines.

The absorbance at 2927.86 cm^{-1} which is indicative of C-H stretching, is narrower and shorter than for raw pine cone. Decrease in intensity of C-H absorption band shows reduction of hydrocarbon content (Shi and Li, 2012). Since the –OH and CH_n (representing –CH-, $-CH_2-$ and $–CH_3$) intensities decrease, three likely things may have happened: (1) destruction of resin acids by oxidation, (2) the rupture of links between cellulose and lignin, and (3) oxidation and extraction of waxes containing alkyl groups from the pine surface. Absorbance peak at 1731.77 cm^{-1} is more intense in the treated than virgin pine cone showing an increase in C=O groups. This shows that the oxidising agent did manage to oxidise some functions on the lignocellulosic material (He et al., 2008). A decrease in intensity of the C-O peak due to stretching of lignin shows degradation of lignin components due to Fenton treatment. Absorbance band at 1507.19 cm^{-1} which is indicative of aromatic characteristics of lignin increased in intensity for the Fenton treated pine than for the raw pine cone due to removal of

extractives, waxes and other soluble organics. Intensity of absorbance at 1024.04 cm^{-1} did not change showing that oxidation did not take place on the secondary alcohol groups from lignin. The absorption band at 806.40 cm^{-1} which is attributed to an aromatic C-H out-of-plane vibration in lignin decreased in intensity showing that delignification took place (Ouajai and Shanks, 2005). In general, absorption bands shifted which is indicative of changes to lignin and cellulose structure. The intensity and shape evolution of these infrared absorbance bands define the structural changes caused by the Fenton treatment (Colom and Carillo, 2002). FTIR spectrums also show that the Fenton modified pine cone constituents are mainly composed of OH and CO groups which all have affinity for pollutant adsorption (Al-Degs et al., 2006).

4.2.1.3 FTIR discussion for optimisation of synthesis of cross-linked Fenton treated pine cone biosorbent using HMDI

The broad OH peak at 3337 cm^{-1} becomes narrower and shifts to lower wavelengths between 3327-3315 cm^{-1} as the mass of the Fenton treated pine cone is increased from 0.1 to 0.5 g as shown in Figure 4.3. This is due to the carbamate NH bond formed during the nucleophillic reaction between hydroxyl groups on the pine cone and isocyanate groups from HMDI (Islam et al., 2011). The CH and CH_2 peak absorbance around 2900 cm^{-1} becomes narrower, more intense and split into two giving absorbances around 2930 and 2850 cm^{-1} due to asymmetric and symmetric CH_2 stretching (Stenstad et al., 2008). This is evidence of interaction between HMDI cross-linker and pine resulting in addition of six consecutive CH_2 groups from the HMDI cross-linker. A new peak not present in the Fenton treated pine appears around 2265 cm^{-1} in the HMDI cross-linked pine. This is attributed to the N=C=O group (Barikani and Mohammadi, 2007) from the diisocyanate and shows that most of the diisocyanate is only reacting with pine hydroxyl groups at one end. This peak was more intense at 0.2 g than in all the other samples implying that more reaction between the pine and HMDI took place with this mass. The C=O stretching vibration at 1731 cm^{-1} becomes smaller until it disappears with an increase in mass of pine cone and is replaced with a new ureic carbonyl absorption around 1615 cm^{-1} (Qiu et al., 2012) formed in the cross-linking reaction. A new absorbance peak appears around 1570 cm^{-1} due to NH in urethane linkage (Siqueira et al., 2010). These two absorbance peaks at 1615 and 1570 cm^{-1} increased in intensity as mass of pine cone was increased from 0.1 to 0.2 g then became constant with further mass increases from 0.3 to 0.5

g. This shows that the optimum pine cone mass for the cross-linking reaction is 0.2 g. An intense absorbance peak is observed around 1250 cm^{-1} except for a mass of 0.1 g. This peak is due to C=O vibrations of aliphatic polyurethanes (Zha et al., 2008). The peak at 1228 cm^{-1} shifted to lower frequencies around 1213 cm^{-1} and also increased in intensity suggesting an increase in nitrogen content since this peak is due to aliphatic tertiary C-N stretch and corroborates the cross-linking reaction (Sarkar and Adhikari, 2001). Absorption peak around 1024 cm^{-1} decreased in intensity representing reaction between the secondary alcohol groups on lignin with HMDI. Two new peaks are also observed around 770 and 735 cm^{-1} and are due to CH_2 bending vibrations from the added HMDI (Valodkar and Thakore, 2010). The shifts, changes in intensity and shape of the absorbance bands signify changes to the chemical composition of the pine cone due to the cross-linking reaction.

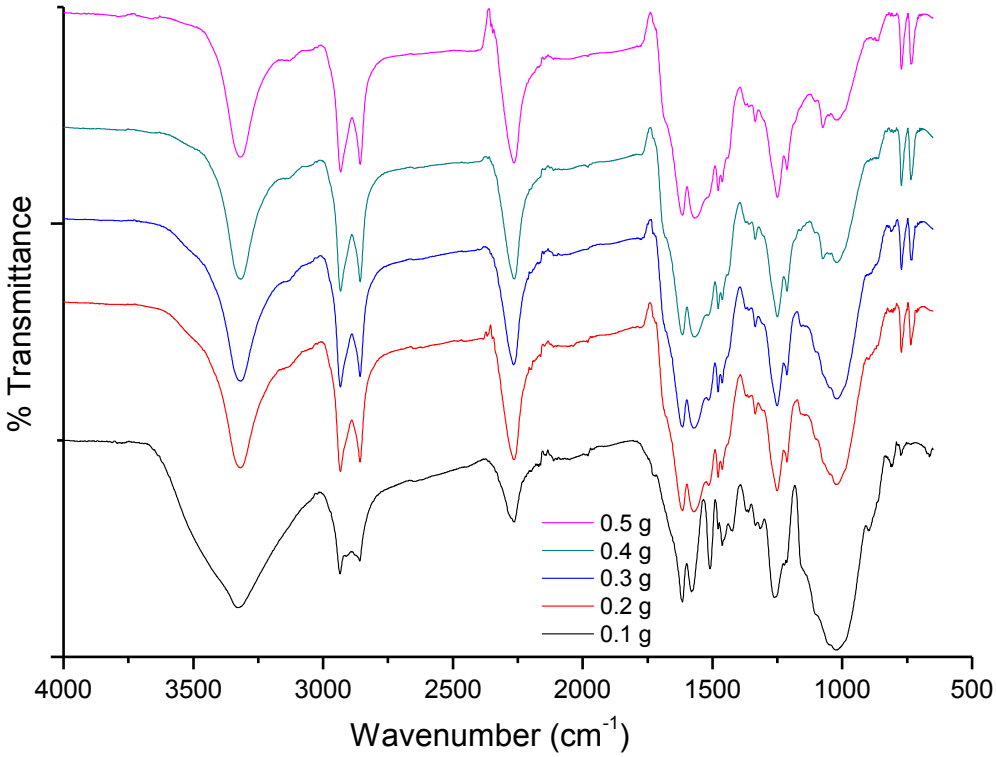

Figure 4.3 FTIR spectra for mass optimization

The FTIR spectrum in Figure 4.4 was obtained during determination of optimum amount of cross-linker needed for the modification reaction. As quantity of HMDI is increased from 2.5, 3.5, 4.5, 5.5 to 6.5 cm^3 no major changes to peak intensities or shape were observed only minor shifts were noted on the absorbance bands. From 3.5 cm^3 HMDI, the urethane C=O

peak around 1730 cm^{-1} (Barikani and Mohammadi, 2007; Valodkar and Thakore, 2010) reappears further proving occurrence of the cross-linking reaction. In light of the above, 3.5 cm^3 was taken as the optimum amount of HMDI needed for the reaction to take place since above this amount no major changes were noted to the chemical composition of the cross-linked pine cone.

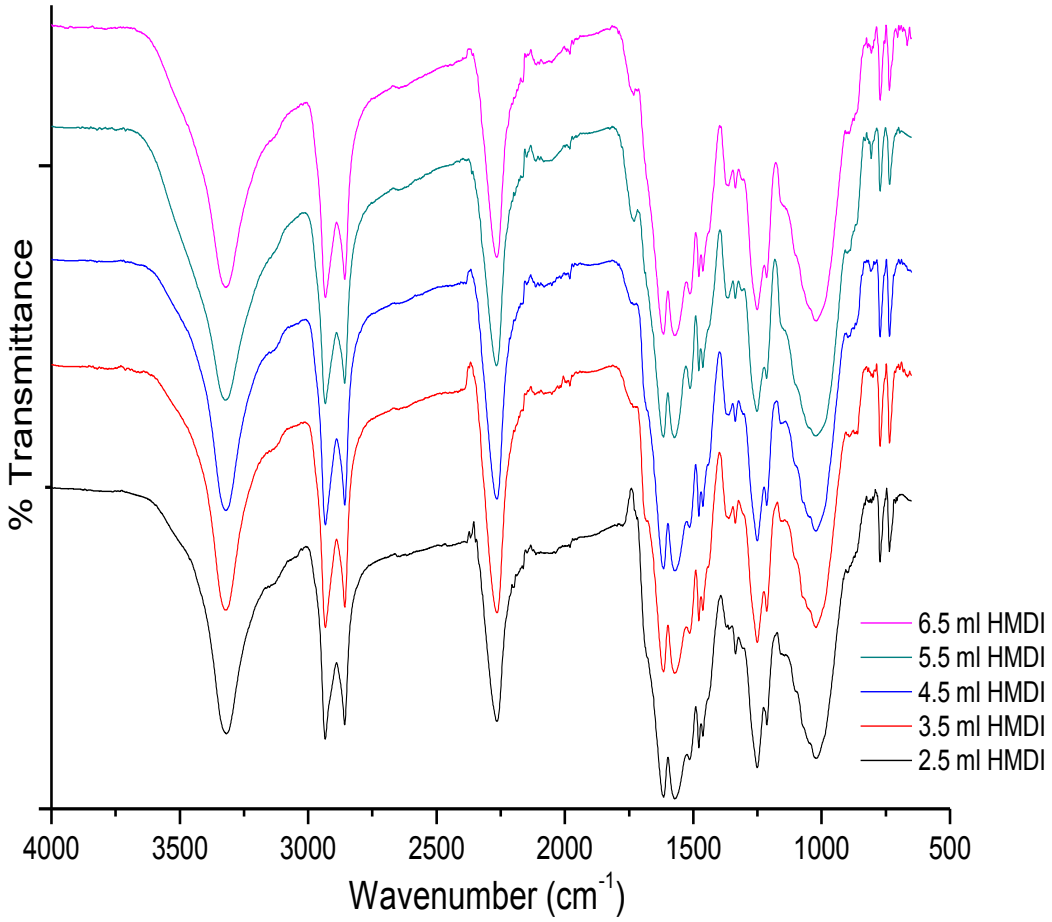

Figure 4.4 FTIR spectra showing optimization of HMDI cross-linker

The FTIR spectra in Figure 4.5 were obtained during optimization of the dibutyltin (IV) dilaurate catalyst. Catalyst volumes of 1, 1.5, 2.5 and 4 cm^3 were used in the optimization experiments. Decrease in intensity of the N=C=O absorption peak around 2265 cm^{-1} was used in choosing the optimum volume of catalyst needed for the reaction as this now represented level of cross-linking of the pine cone. Higher intensity of this peak signifies that the bi-functional cross-linker is only reacting with the pine on one end. Therefore, a catalyst volume of 1.5 cm^3 was chosen as the optimum.

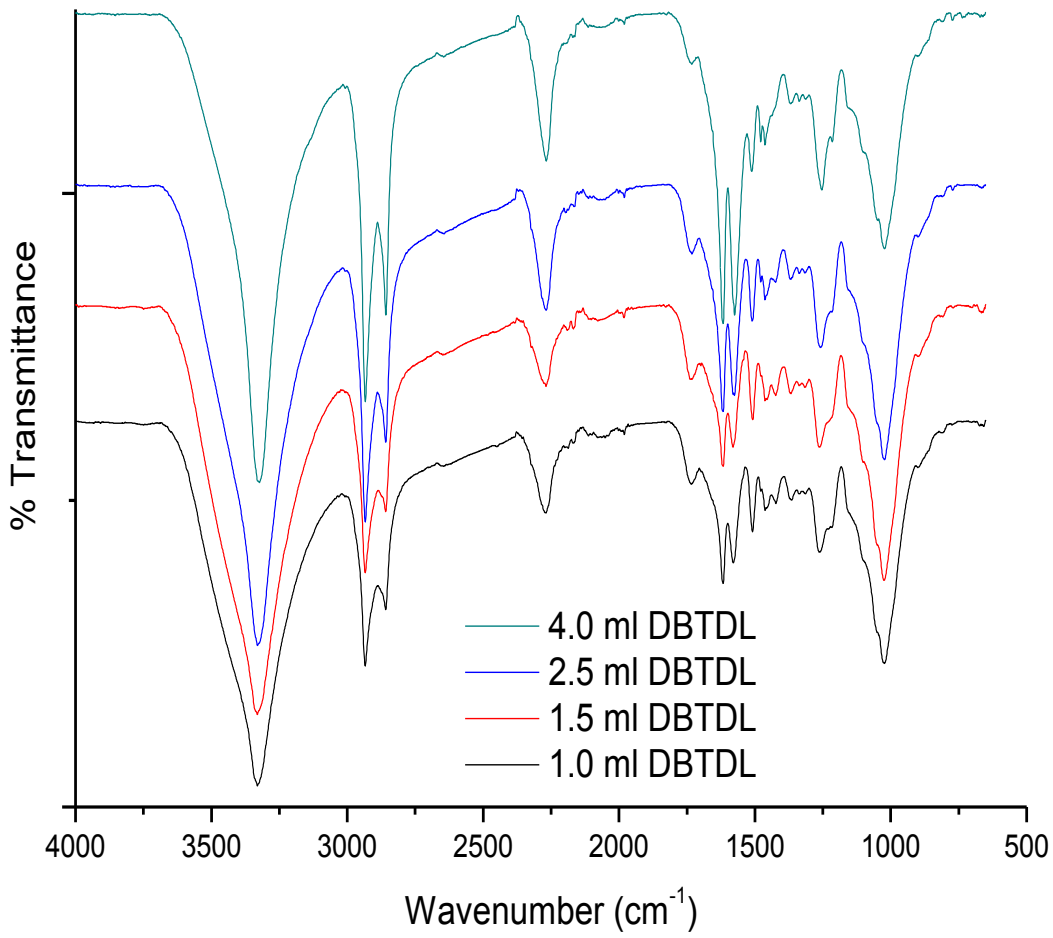

Figure 4.5 FTIR spectra showing optimization of dibutyltin (IV) dilaurate catalyst

The same approach was employed in selection of the optimum temperature from the following temperature ranges; 30, 50, 70 and 90 °C whose FTIR spectra are shown in Figure 4.6. A temperature of 50 °C was chosen as the optimum due to narrowness, high intensity of the NH bond peak at 3329 cm^{-1} and small intensity of the N=C=O peak at 2269 cm^{-1}. The urethane C=O absorption at 1731 cm^{-1} is also well resolved for this temperature. The above stated absorbances show that more cross-linking took place at this temperature. At 70 and 90 °C, some spectral changes were observed which are due to low cross-linking density and destruction of the biological matrix at these higher temperatures. For example, broadening of the absorbance around 3343 cm^{-1} and splitting of the CH_2 peak around 2900 cm^{-1} did not occur at 70 °C showing that not much HMDI had reacted with the OH groups resulting in addition of a hydrocarbon chain across the cross-linked pine cone molecules.

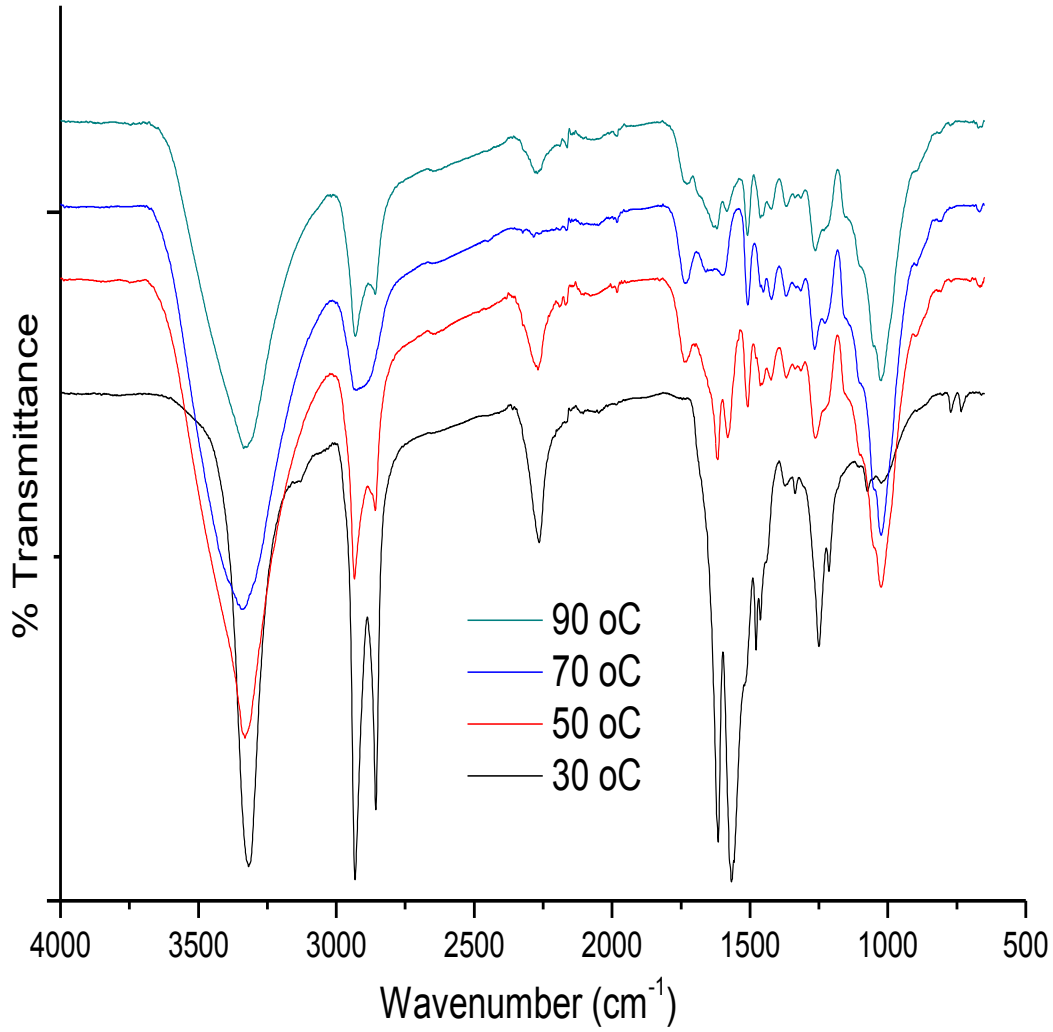

Figure 4.6 FTIR spectra showing temperature optimization for the cross-linking reaction

Time was the last experimental parameter to be optimized. Experiments were conducted at 1, 2, 3 and 4 hours. No major spectral changes emanated as shown in Figure 4.7. A time of 4 hours was chosen as the optimum due to the small absorbance of the N=C=O peak at 2268 cm^{-1} implying more cross-linking of the pine cone with HMDI. The peak did not disappear completely as some few N=C=O groups can get embedded in the pine cone matrix and hence will not be available for reaction due to steric effects.

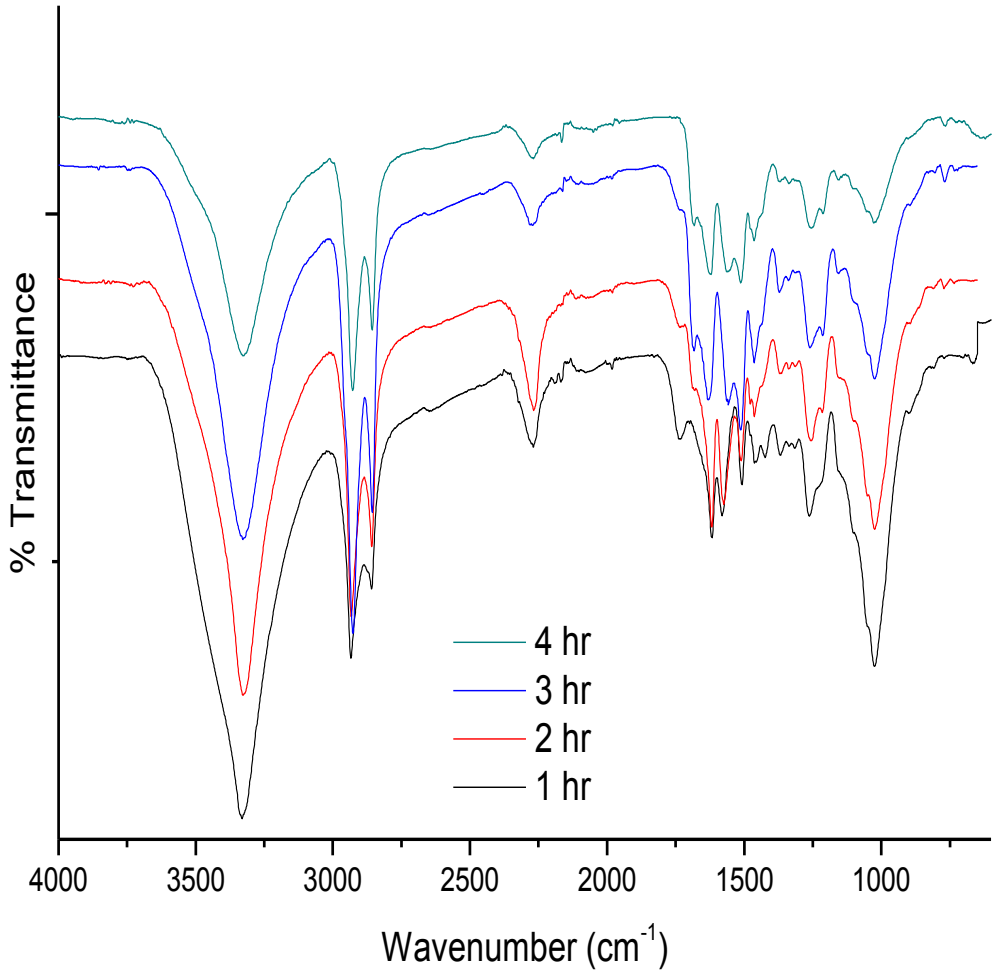

Figure 4.7 FTIR spectra for time optimization of the cross-linking reaction

A comparison of the spectra of cross-linked raw pine and cross-linked Fenton treated pine is shown in Figure 4.8. A few differences were noted. The NH, CH_2 and C=O absorbance peaks around 3328, 2920, 2850 and 1250 cm^{-1} are less intense with the raw than Fenton treated, but the N-C=O peak around 2268 cm^{-1} was more intense for the raw than for Fenton treated pine cone. All this shows that less cross-linking took place between HMDI and virgin pine than with Fenton treated pine. This is because in the treated pine some lignin was degraded as it can hinder the nucleophillic reaction between the isocyanate and hydroxyl groups. Also the Fenton treatment leaches out waxes and other organic extractives thus improving access of HMDI to the pine hydroxyl moieties.

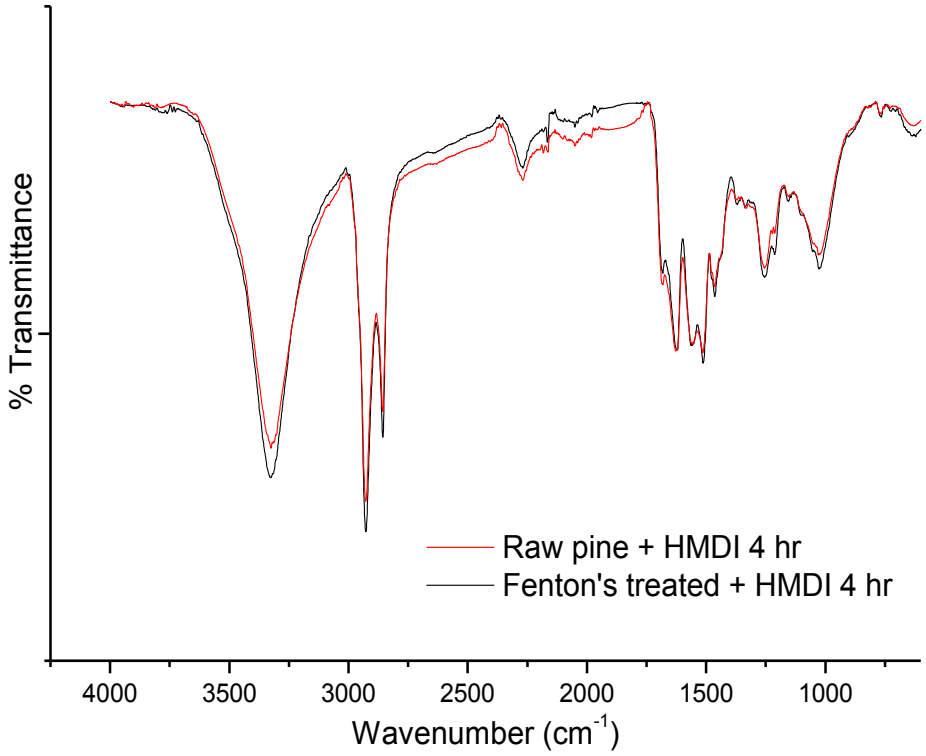

Figure 4.8 FTIR spectra of HMDI cross-linked Raw and Fenton treated pine cone

4.2.2 Thermogravimetric Analysis (TGA) of pine cone biomass

Thermal degradation of the pine cone biomass can be divided into three stages (Idris et al., 2010; Gao et al., 2013): (1) moisture evolution from 30–150 °C, (2) hemicelluloses and cellulose decomposition from 200–350 °C, and (3) lignin decomposition from 160–700 °C as shown in Figures 4.9 and 4.10. The weight losses are focused in the temperature range 200–400 °C.

4.2.2.1 Thermogravimetric Analysis of Raw pine and Fenton treated pine cone

The first stage (30–150 °C) corresponds to evaporation of water, showing the hygroscopic nature of the pine cone biomass surface (Chen and Kuo, 2011). The mass losses during this stage were about 8.75 % for the raw pine and 4.50 % for the Fenton modified pine. This difference in mass losses between the two biosorbents signifies a decrease in surface hydrophilic groups due to the Fe^{2+}/H_2O_2 treatment. It further corroborates information obtained from the FTIR results in figure 4.0, which shows a decrease in hydroxyl functions

(hydrophilic group) after the Fenton treatment. Collison and Thielemans (2010) proposed a reaction mechanism in Figure 4.2, showing oxidation of hydroxyl moieties with the ferrous ion-hydrogen peroxide system which further accounts for the decrease in hydroxyl functional groups after Fenton modification.

The second stage (200–350 °C) is attributed to hemicelluloses and cellulose degradation. It has been shown in several studies that hemicelluloses especially xylans decompose at lower temperatures due to their random and amorphous structure (Raveendran et al., 1996; Órfão et al., 1999; Yang et al., 2004). Hemicelluloses decomposition took place from 200 -310 °C with maximum weight loss rate at 270 °C. Cellulose decomposition took place from 310–350 °C with maximum weight loss rate around 330 °C. Raw pine experienced a mass loss of about 52.25 %, while Fenton treated pine showed a mass loss of about 46.5 % during this second stage. The difference in mass losses can be attributed to rupture of the saccharide rings due to Fenton treatment (Collison and Thielemans, 2010) reducing the quantity of hemicelluloses and cellulose present in the biomass.

The third stage (160–700 °C) is due to lignin degradation. Yang and co-workers (2007), showed that lignin degradation was more difficult and takes place over a wide temperature range since it is heavily cross-linked in three-dimensions and part of its structure consists of benzene rings resulting in slow carbonization (Yang et al., 2004; Gani and Naruse, 2007; Idris et al, 2010). It was also noted that nearly all the Fenton treated pine was decomposed but about 15 % of the raw pine remained undecomposed.

The thermal degradation properties of the pine cone components can be summarised from the easiest to the most difficult, as follows: hemicelluloses > cellulose >>> lignin (Dermibas, 2001). Similar results for the thermal degradation of pine cone biomass were reported by other authors (Singh et al., 2012; Gao et al., 2013).

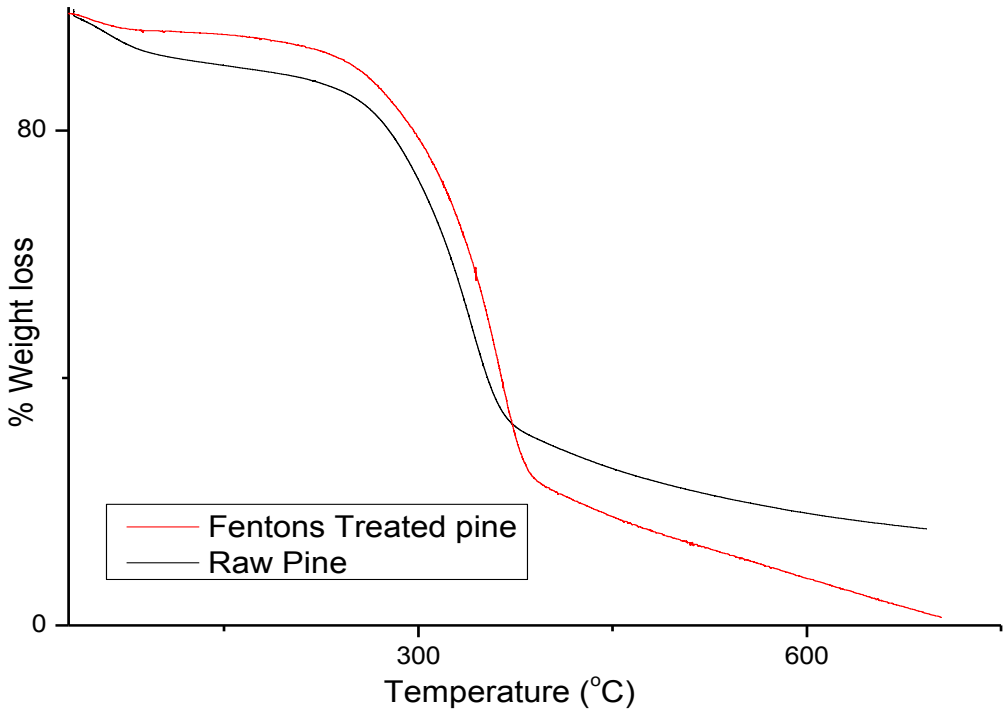

Figure 4.9 TG curves for Raw and Fenton modified pine cone

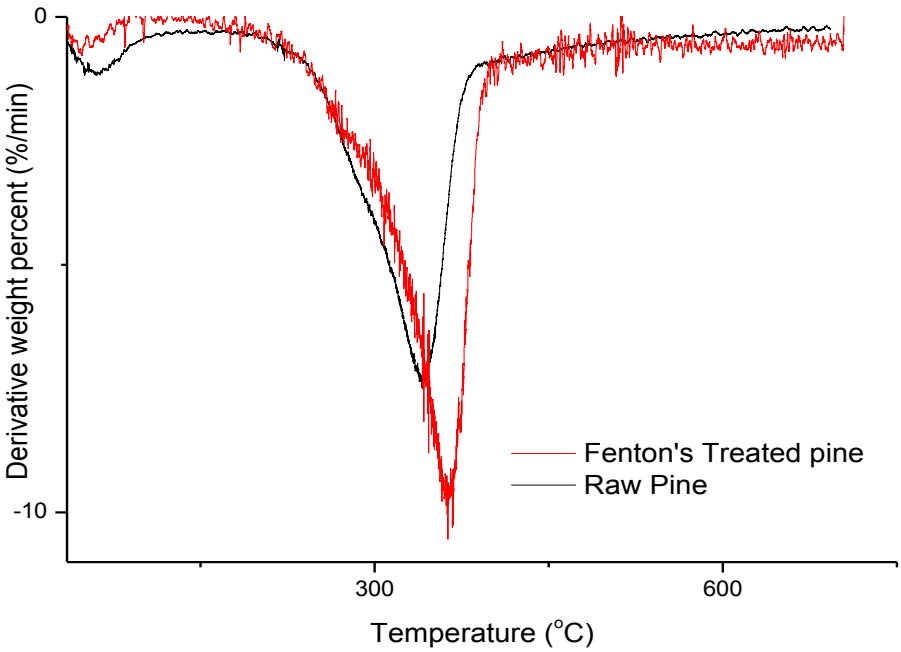

Figure 4.10 Derivative weight percent curves for Raw and Fenton treated pine cone

4.2.2.2 Thermogravimetric Analysis of Raw-HMDI pine and Fenton treated-HMDI pine cone

The HMDI modified pine cone biomass did degrade in three stages as shown in Figures 4.11 and 4.12. The first stage, which is due to evaporation of water from the biomass surface, took place from 30–150 °C, with weight losses of about 2 and 4 % being noted respectively between Fenton treated-HMDI and the Raw-HMDI pine cone. The second stage, signifying decomposition of hemicelluloses and cellulose, occurred from 200–480 °C, with weight losses of about 78 and 75 % between Fenton treated-HMDI and the Raw-HMDI pine cone biomass. The third stage, which is due to lignin degradation, took place between 160–700 °C. Less than 20 % of either Fenton treated-HMDI or Raw-HMDI pine cone biomass remained as residue at the end of the thermal degradation process.

The thermogravimetric curves of Raw-HMDI and Fenton treated-HMDI pine cone show a number of differences to that of Raw pine cone. Firstly, the weight losses due to evaporation of water from the cross-linked pine cone biomass surfaces are lower. This signifies a decrease in hydrophilic character or increase in hydrophobic character due to the diisocyanate cross-linking modification (Qiu et al., 2012). Secondly, the HMDI modified pine cone biomass degraded at higher temperatures than the raw pine cone during the second degradation stage showing an increase in stability due to cross-linking, as it results in extensive covalent bonding (Valodkar and Thakore, 2010). Thirdly, during the second degradation stage, the cross-linked pine cone biomass showed rapid degradation than the raw pine. This is attributed to formation of carbamate esters during the cross-linking reaction, hence the degradation rates of cross-linked biomass approached to polyurethane's (Javni et al., 2000). The fourth difference is that, the second degradation stage is resolved into two sections on the thermograms of the cross-linked pine cone biomass. This can be attributed to the supramolecular structure of cellulose which consists of amorphous and crystalline regions, with the amorphous regions being oxidised at a lower temperature, while the crystalline regions are oxidised at a higher temperature. Qiu and co-workers (2012) published similar TG curves on diisocyanate cross-linked cellulose. In general, the results showed that cross-linking the Raw and Fenton treated pine with HMDI did improve the thermal stability of the pine cone biomass.

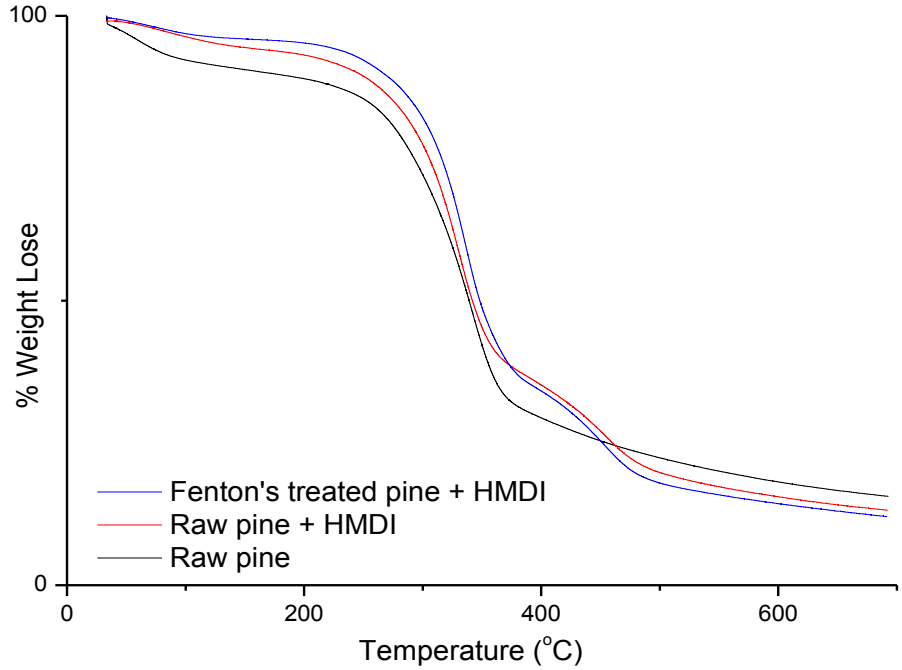

Figure 4.11 TG curves for Raw, Raw-HMDI and Fenton treated-HMDI pine cone.

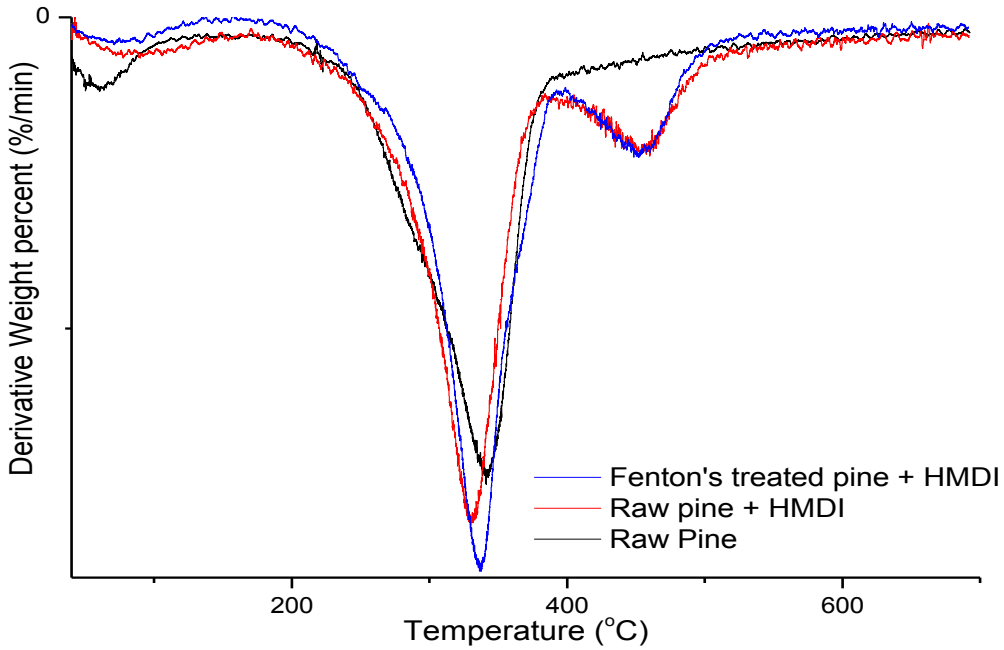

Figure 4.12 Derivative weight percent curves for Raw, Raw-HMDI and Fenton treated-HMDI pine cone.

4.2.3 X-ray diffraction (XRD)

The diffraction patterns for raw pine and Fenton's treated pine are presented in Figure 4.13 and are characteristic of lignocelluloses.

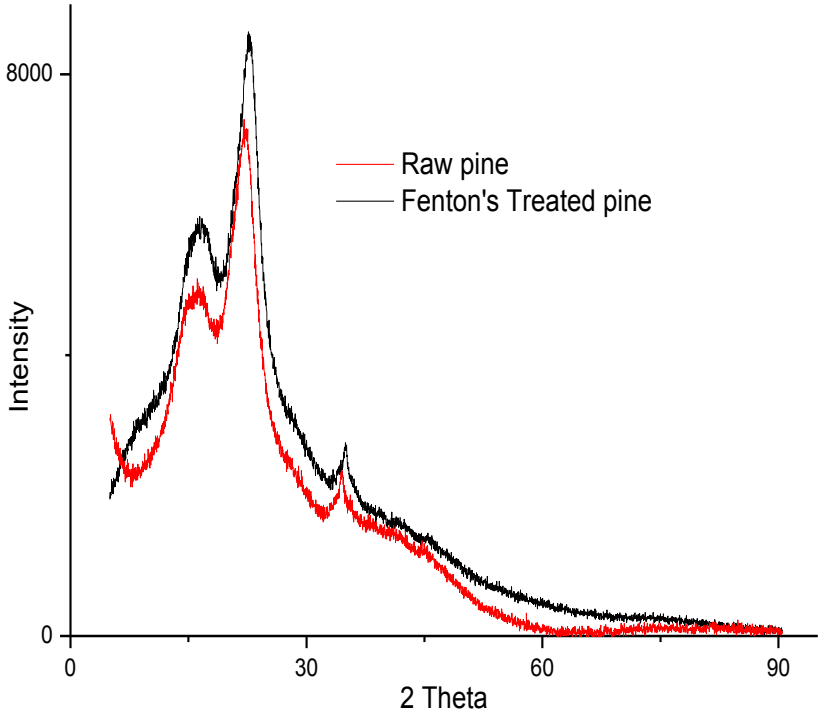

Figure 4.13 XRD diagram of Raw pine and Fenton treated pine.

The diffraction patterns of the Raw pine and Fenton treated pine show three major peaks at 2θ=18°, 22° and 35°. The peak at 2θ=18° represents the amorphous component (cellulose, lignin and hemicelluloses) and that at 2θ=22° represents the crystalline portion of the biomass (cellulose) (Kim et al., 2003). Analysis of the biomass major peaks shows an increase in intensity due to Fenton treatment. This is attributed to leaching of extractives, waxes and resin acids thus increasing magnitude of the lignocellulosic components.

The diffraction diagram in figure 4.14 shows the diffraction patterns for Fenton treated pine and Fenton treated-HMDI pine cone. The diffraction pattern of Fenton treated-HMDI pine only shows two major peaks at 2θ=22° and 35°. Absence of the peak at 2θ=18°, suggest a significant decrease in amorphous content of the biomass due to the cross-linking modification. Scrutiny of the 2θ=22° intensity peaks of the pine cone biomass shows a

decrease in intensity on the Fenton treated-HMDI pine suggesting a decrease in crystallinity due to the reaction between the diisocyanate and hydroxyl groups on cellulose.

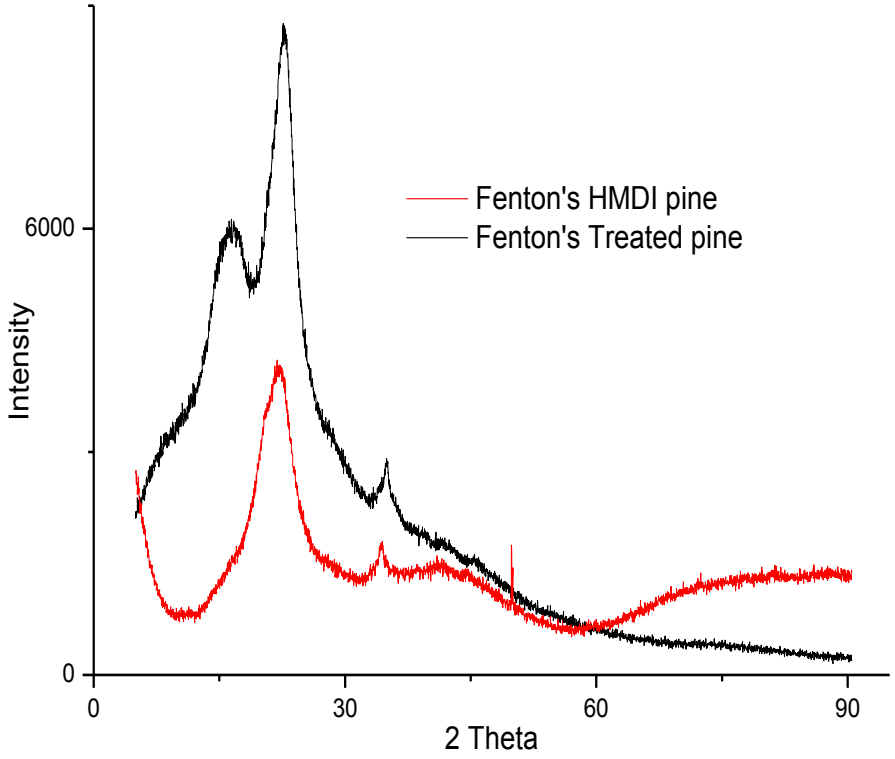

Figure 4.14 XRD patterns of Fenton treated and Fenton treated-HMDI pine cone biomass.

The diffraction patterns for the Raw-HMDI and Fenton treated-HMDI pine cone biomass are presented in Figure 4.15. They both show two major peaks at 2θ=22° and 35° but the crystallinity peak at 2θ=22° is more intense in the Raw-HMDI pine than the Fenton-HMDI pine. This may be attributed to extent of cross-linking with HMDI, since cross-linking reduces crystallinity (Crini, 2005).

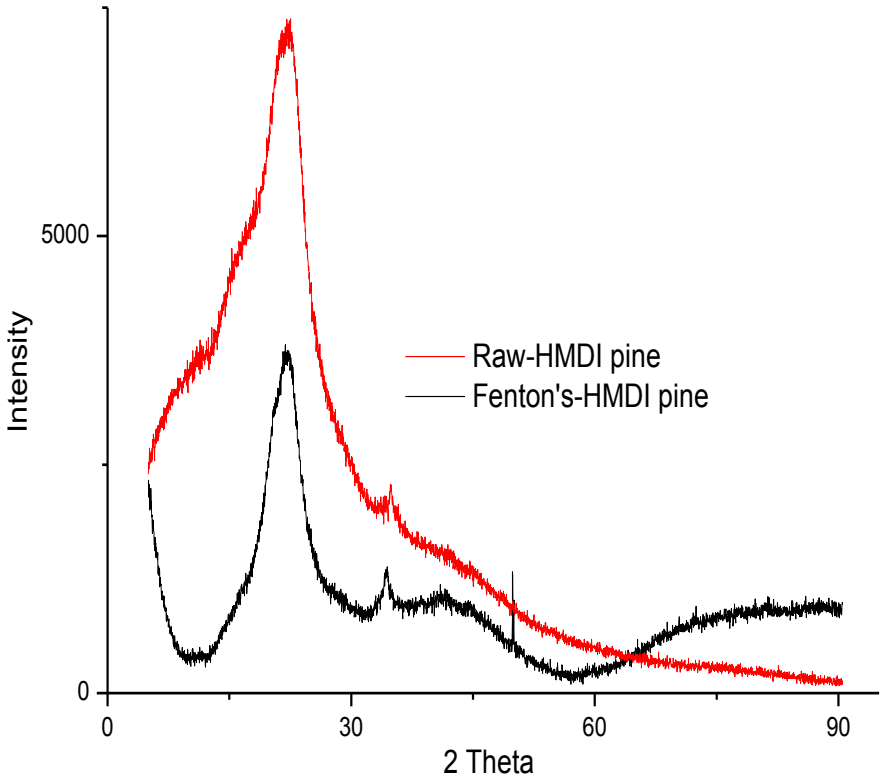

Figure 4.15 X-ray diffractograms of Raw-HMDI and Fenton treated-HMDI pine

The biosorbents particle sizes determined from the XRD patterns by use of the Debye-Scherrer equation are presented in Table 4.1. The Debye-Scherrer equation relates the width of a diffraction peak to the average dimensions of crystalline particles (Burton et al., 2009)

Table 4.1 Particle sizes of the pine cone biosorbents.

	Pine cone biomass			
	Raw	Raw-HMDI	Fenton	Fenton-HMDI
Particle size (nm)	556.71	772.85	377.26	411.71

The particle sizes for the Raw, Raw-HMDI, Fenton treated and Fenton treated-HMDI pine cone biomass are 556.71 nm, 772.85 nm, 377.26 nm and 411.71 nm respectively. The results show a decrease in particle size due to Fenton treatment and an increase in particle size due to the cross-linking modification.

4.2.4 Scanning electron microscopy (SEM)

The surface morphology of the raw and modified pine cone biomass is shown in Figure 4.16 (a)-(d). Surface of raw pine appears rough and has few pores as shown in Figure 4.16 (a). The cone surface appears more porous and coated with a milky layer in Figure 4.16 (b) for the Raw-HMDI pine. After treatment with Fenton's reagent (Figure 4.16 (c)), the cone surface appears to be highly porous. The surface appears smoother and coated with a milky layer in Figure 4.16 (d) after HMDI treatment.

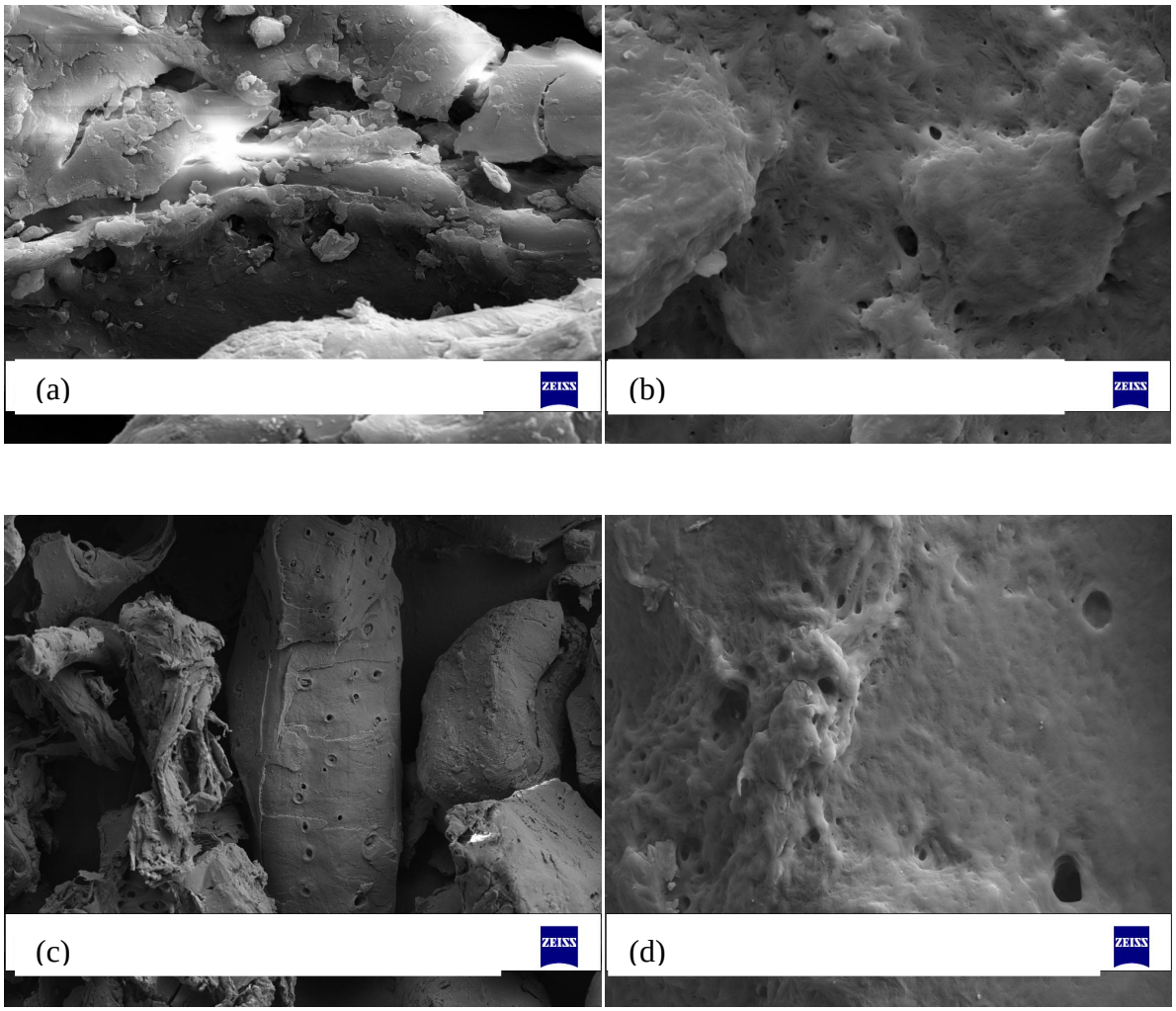

Figure 4.16 SEM images of (a) Raw, (b) Raw-HMDI, (c) Fenton treated and (d) Fenton treated-HMDI pine cone biomass.

The SEM images show that HMDI treatment of raw pine increased its porosity and made the surface to be smooth. This is attributed to the cross-linking reaction. The cross-linking reaction took place in anhydrous hexane as solvent. Other researchers like Pholosi et al.

(2013) have shown that solvents are able to leach out extractives from pine cone thus increasing its porosity. The smoothness on the surface is due to the milky coating which shows that cross-linking took place between the raw pine and HMDI.

Fenton treatment of raw pine increased number of pores on the surface in accordance with previous research done by Argun and Dursun (2008). The researchers showed that Fenton's reagent can degrade organics and leach out extractives from the pine cone biomass. The Fenton treated pine surface became smooth with a milky coating due to the cross-linking reaction with HMDI.

4.2.5 Electron dispersive spectroscopy (EDX)

The elemental analysis results of the cone samples obtained from EDX are presented in Table 4.2. The Raw pine cone had 63.47 % C, 24.96 % O and 1.35 % N, while the Fenton treated pine had 48.03 % C, 25.70 % O and 4.32 % N. The Raw-HMDI pine had 53.56 % C, 22.85 % O and 14.54 % N, whilst Fenton treated-HMDI pine had 49.12 % C, 25.03 % O and 22.43 % N.

Table 4.2 Elemental analysis of raw and modified pine cone

	Weight % (on dry basis)		
	C	O	N
Raw pine	63.47	24.96	1.35
Fenton treated pine	48.03	25.70	4.32
Raw-HMDI pine	53.65	22.85	14.54
Fenton-HMDI pine	49.12	25.03	22.43

*instrument cannot measure % of H present in the pine cone sample

Amount of carbon in Fenton treated pine decreased in comparison to the Raw pine. This can be attributed to leaching of alkyl groups present in extractives, waxes and resin acids due to the oxidation modification. A slight increase in oxygen content was noted between the raw and Fenton's treated pine. This signifies that oxidation of some organic functional groups took place due to the Fenton's reagent treatment. The main difference between the Raw, Fenton treated and the HMDI cross-linked pine cone biomass is in the nitrogen content. This

showed that cross-linking between the pine cone biomass and HMDI took place. The highest percent increase in nitrogen content was on the Fenton treated-HMDI pine cone. This signifies that more cross-linking took place between Fenton treated pine and HMDI than between the raw pine and the diisocyanate. This is attributed to Fenton treatment of the biomass which increased access of the HMDI to the pine cone matrix.

4.2.6 Brunauer-Emmett-Teller (BET) Surface Area

The BET surface area, pore volume and pore size values of the raw and modified pine cone samples are presented in Table 4.3.

Table 4.3 Surface area of raw and Fenton's pine unmodified and modified with HMDI

Sample	Surface area (m^2/g)	Pore volume (cm^3/g)	Pore size (nm)
Raw pine	4.48	0.0203	33.10
Fenton pine	8.43	0.0425	77.38
Raw-HMDI	1.47	0.0021	17.11
Fenton-HMDI	3.22	0.0032	21.23

The Raw pine had a surface area of 4.48 m^2/g, pore volume of 0.0203 cm^3/g and pore size of 33.10 nm. Fenton treated pine showed a surface area of 8.43 m^2/g, pore volume of 0.0425 cm^3/g and pore size of 77.38 nm. The Raw-HMDI pine biosorbent had a surface area of 1.47 m^2/g, pore volume of 0.0021 cm^3/g and pore size of 17.11 nm. Fenton treated-HMDI pine cone exhibited a surface area of 3.22 m^2/g, pore volume of 0.0032 cm^3/g and pore size of 21.23 nm.

Surface area, pore volume and pore size values of Fenton treated pine are much greater than those of raw pine. Previous research by Argun and Dursun (2008) reported similar results. This is attributed to the oxidation modification which results in leaching of extractives (including resin acids and waxes) and rupture of some links within the lignocellulosic matrix. The results also show that the cross-linking modification reduced surface area, pore volume and pore sizes.

4.2.7 Weight percent gain determination (WPG)

The weight percent gain values for the raw and Fenton's treated pine cone biomass after modification with HMDI is presented in Table 4.4.

Table 4.4 Weight percent gain values

	Weight percent gain
Raw pine + HMDI	19.96
Fenton's treated pine + HMDI	24.13

The weight percent gain values of the biomass after modification with HMDI was 19.96 for the raw pine cone and 24.13 for the Fenton treated pine cone. The results show that more cross-linking took place between Fenton treated pine cone and HMDI as shown by the higher weight percent gain value. This can be attributed to effect of Fenton oxidation which leached out extractives, low molecular weight organics and ruptured some links within the lignocellulosic biomass thus increasing access of HMDI to the pine cone matrix and increasing cross-linking density.

4.3 SURFACE PROPERTIES

4.3.1 Determination of acidic surface functional groups on pine cone

The results showing type and quantity of surface oxygen acidic groups on Raw, Fenton oxidised, HMDI cross-linked Fenton oxidised (Fenton treated-HMDI) and HMDI cross-linked raw (Raw-HMDI) pine cone samples are shown in Table 4.5.

Table 4.5 Type and quantity of acidic groups on pine cone surface

	type of acidic functional group on pine cone surface (mmol/g)		
	Phenolic	Lactonic	carboxylic
Raw	2.03	0.21	0.32
Fenton oxidised	4.63	0.13	1.25
Fenton treated-HMDI	3.00	0.25	0.75
Raw-HMDI	2.38	0.10	0.50

The results from Table 4.5 show that Fenton oxidised pine cone had the greatest number of acidic functions due to the oxidative modification process. Its total acidic content is more than twice that of the raw pine cone sample. Fenton's reagent (strong oxidant) treatment of pine cone produces a material which is mainly composed of polymeric OH and COOH groups which all contribute to its high surface acidity (Al-Degs et al., 2006; Collinson and Thielemans, 2010). The Fenton treated-HMDI pine cone has less surface acidic groups than Fenton oxidised pine cone. The decrease in magnitude of surface acidic functions is due to the reactions that occur between the OH and COOH groups and HMDI producing urethane and amide linkages (Noble, 1997; Stankovich et al., 2006):

$$\text{-NCO + OH} \rightarrow \text{urethane}$$
$$\text{-NCO + COOH} \rightarrow \text{amide + } CO_2$$

The raw-HMDI pine cone sample had fewer surface acidic groups than Fenton treated-HMDI pine cone since there was no oxidation of any organic functions. The few acidic groups present were further reduced on reaction with the diisocyanate. Raw pine showed the least amount of presence of surface acidic groups since it mainly consists of hydroxyl groups and a few carboxyl groups on some hemicelluloses.

4.3.2 pH at point zero charge (pH_{pzc})

The pH at point zero charge (pH_{pzc}) is the pH at which the amount of negative charges on biosorbent surface just equals the amount of positive charges (Ofomaja et al., 2009), that is, the pH at which biosorbent surface has net electrical neutrality (Deng et al., 2009). At pH above pH_{pzc} the biosorbent surface is negatively charged and it is positively charged at pH below pH_{pzc}. This knowledge informs about the possible electrostatic interactions between sorbent and sorbate (Fiol et al., 2009).

The pH_{pzc} of the pine cone and modified pine cone samples were observed to be different and the values are presented in Table 4.6. Variations in pH_{pzc} values within the samples can be attributed to the difference in the surface functional groups present on pine cone and modified pine cone (Kumar et al., 2008).

Table 4.6 pH_{pzc} values of pine cone and modified pine cone samples

	Raw	Fenton treated	Fenton-HMDI	Raw-HMDI
pH_{pzc}	7.49	5.40	6.12	6.68

The pH_{pzc} of Raw pine cone powder was found to be 7.49, while those of Fenton treated pine cone, Fenton treated-HMDI pine cone and Raw-HMDI pine cone biomass where observed to be 5.40, 6.12 and 6.68. Decrease in pH_{pzc} from 7.49 for the Raw pine cone to 5.40 for the Fenton treated pine cone can be attributed to: (1) increase in acidic functional groups due to the oxidative modification of the surface and (2) exposure of acidic groups within blocked pores due to the leaching out of plant organic extractives. The increase in pH_{pzc} from 5.40 for the Fenton treated pine cone to 6.12 for the Fenton treated-HMDI pine cone sample can be attributed to a reduction in acidic groups due to the reaction of acidic groups (e.g. carboxylic acids) with the diisocyanate forming urethane and/or amide linkages which reduces the total acidity. An increase in pH_{pzc} from 5.40 on Fenton treated pine cone to 6.68 for the Raw-HMDI pine cone was also noted. The higher increase in the pH_{pzc} value of Raw-HMDI pine over the Fenton treated-HMDI pine can be attributed to the fewer number of acid groups reacting with the diisocyanate in the raw pine as compared with the Fenton treated pine.

4.4 CONCLUSION

The results show successful modification of pine cone biomass by Fenton treatment and cross-linking using HMDI. Optimum conditions for cross-linking of Fenton treated pine cone were determined using FTIR analysis and found to be: 0.2 g pine biomass, 3.5 ml HMDI cross-linker, 50 ml hexane, 1.5 ml dibutyltin dilaurate catalyst, temperature of 50 °C and a reaction time of 4 hours. The synthesized hydrophobic pine cone biosorbent was characterized using analytical instrumentation (FTIR, TGA, XRD, SEM, EDX and BET surface area). Weight percent gain (WPG) computation was done to determine the extent of the cross-linking reaction. The pine surface showed an increase in phenolic, lactonic and carboxylic acid groups due to the modification. The pH_{pzc} showed a decrease due to modification of the pine cone biomass.

4.5 REFERENCE

1. ABRAHAM, E., DEEPA, B., POTHAN, L.A., JACOB, M., THOMAS, S., CVELBAR, U. and ANANDJIWAL, R. (2011) Extraction of nanocellulose fibrils from lignocellulosic fibres: A novel approach, *Carbohydrate Polymers*. 86(4), pp. 1468-1475.
2. ADEL, A.M., ABD EL-WAHAB, Z.H., IBRAHIM, A.A. and AL-SHEMY, M.T. (2010) Characterization of microcrystalline cellulose prepared from lignocellulosic materials. Part 1. Acid catalyzed hydrolysis, *Bioresource Technology*. 101(12), pp. 4446-4455.
3. AHN, D.H., CHANG, W.S. and YOON, T.I. (1999) Dyestuff wastewater treatment using chemical oxidation, physical adsorption and fixed bed biofilm process, *Process Biochemistry*. 34(5), pp. 429-439.
4. AL-DEGS, Y.S., EL-BARGHOUTHI, M.I., ISSA, A.A., KHRAISHEH, M.A. and WALKER, G.M. (2006) Sorption of Zn(II), Pb(II), and Co(II) using natural sorbents: equilibrium and kinetic studies, *Water Research.* 40(14), pp. 2645-2658.
5. ALEMDAR, A. and SAIN, M. (2008) Isolation and characterization of nanofibres from agricultural residues - wheat straw and soy hulls, *Bioresource Technology*. 99(6), pp. 664-671.
6. ARGUN, M.E. and DURSUN, S. (2008) A new approach to modification of natural adsorbent for heavy metal adsorption, *Bioresource Technology*. 99(7), pp. 2516-2527.
7. BARIKANI, M. and MOHAMMADI, M. (2007) Synthesis and characterization of starch-modified polyurethane, *Carbohydrate Polymers*. 68(4), pp. 773-780.
8. BESSADOK, A., MARAIS, S., ROUDESLI, S., LIXON, C. and METAYER, M. (2008) Influence of chemical modifications on water-sorption and mechanical properties of Agave fibres, *Composites: Part A*. 39(1), pp. 29-45.
9. BURTON, A.W., ONG, K., REA, T. and CHAN, I.Y. (2009) On the estimation of average crystallite size of zeolites from the Scherrer equation: A critical evaluation of its application to zeolites with one-dimensional pore systems, *Microporous and Mesoporous Materials*. 117, pp. 75-90.
10. CHEN, W-H. and KUO, P-C. (2011) Isothermal torrefaction kinetics of hemicellulose, cellulose, lignin and xylan using thermogravimetric analysis, *Energy*. 36, pp. 6451-6460.

11. COLLISON, S.R. and THIELEMANS, W. (2010) The catalytic oxidation of biomass to new materials focusing on starch, cellulose and lignin, *Coordination Chemistry Reviews*. 254(15-16), pp. 1854-1870.
12. COLOM, X. and CARILLO, F. (2002) Crystallinity changes in lyocell and viscose-type fibres by caustic treatment, *European Polymer Journal.* 38(11), pp. 2225-2230.
13. CRINI, G. (2005) Recent developments in polysaccharide-based materials used as adsorbents in wastewater treatment, *Progress in Polymer Science*. 30(4), pp. 778-783.
14. DE ROSA, I.M., KENNY, J.M., PUGLIA, D., SANTULLI, C. and SARASINI, F. (2010) Morphological, thermal and mechanical characterization of okra (*Abelmoschus esculentus*) fibres as potential reinforcement in polymer composites, *Composites Science & Technology*. 70(1), pp.116-122.
15. DE ROSA, I.M., KENNY, J.M., MANIRUZZAMAN, M., MONIRUZZAMAN, M., MONTI, M, PUGLIA, D., SANTULLI, C. and SARASINI, F. (2011) Effect of chemical treatments on the mechanical and thermal behaviour of okra (*Abelmoschus esculentus*) fibres, *Composites Science & Technology*. 71(2), pp. 246-254.
16. DENG, H., YANG, L., TAO, G. and DAI, J. (2009) Preparation and characterization of activated carbon from cotton stalk by microwave assisted chemical activation – application in methylene blue adsorption from aqueous solution, *Journal of Hazardous Materials*. 166(2-3), pp. 1514-1521.
17. DERMIBAS, A. (2001) Biomass resource facilities and biomass conversion processing for fuels and chemicals, *Energy Conversion & Management*. 42, pp. 1357-1378.
18. FIOL, N. and VILLAESCUSA, I. (2009) Determination of sorbent point zero charge: usefulness in sorption studies, *Environmental Chemistry Letters*. 7(1), pp. 79-84.
19. GANI, A. and NARUSE, I. (2007) Effect of cellulose and lignin content on pyrolysis and combustion characteristics for several types of biomass, *Renewable Energy*. 32, pp. 649-661.
20. GAO, N., LI, A., QUAN, C., DU, L. and DUAN, Y. (2013) TG-FTIR and Py-GC/MS analysis on pyrolysis and combustion of pine sawdust, *Journal of Analytical and Applied Pyrolysis.* 100, pp. 26-32.
21. GHALI, E.A., MARZOUG, I.B., BAOUBAB, M.H.V. and ROUDESLI, M.S. (2012) Separation and characterization of new cellulosic fibres from the Junctus Acutus L plant, *BioResources*. 7(2), pp. 2002-2018.

22. GOERTZEN, S.L., THÉRIAULT, K.D., OICKLE, A.M., TARASUK, A.C. and ANDREAS, H.A. (2010) Standardization of the Boehm titration. Part I. CO_2 expulsion and end point determination, *Carbon*. 48(4), pp. 1252-1261.
23. HE, Y, PANG, Y., LIU, Y., LI, X. and WANG, K. (2008) Physicochemical characteristics of rice straw pretreated with sodium hydroxide in the solid state for enhancing biogas production, *Energy & Fuels*. 22(4), pp. 2775-2781.
24. IDRIS, S.S., RAHMAN, N.A., ISMAIL, K., ALIAS, A.B., RASHID, Z.A. and ARIS, M.J. (2010) Investigation on thermochemical behavior of low rank Malaysian coal, oil palm biomass and their blends during pyrolysis via thermogravimetric analysis (TGA), *Bioresource Technology*. 101, pp. 4584-4592.
25. ISLAM, M.S., HAMDAN, S., RAHMAN, M.R., JUSOH, I. and AHMED, A.S. (2011) The effect of cross-linker on mechanical and morphological properties of tropical wood material composites, *Materials & Design*. 32(4), pp. 2221-2227.
26. JAVNI, I., PETROVIĆ, Z.S., GUO, A. and FULLER, R. (2000) Thermal stability of polyurethanes based on vegetable oils, *Journal of Applied Polymer Science*. 77(8), pp. 1723-1734.
27. JAYARAMUDU, J., GUDURI, B.R. and RAJULU, V.A. (2010) Characterization of new natural cellulosic fabric Grewia tilifolia, *Carbohydrate Polymers.* 79(4), pp. 847-851.
28. KIM, T.H., KIM, J.S., SUNWOO, C. and LEE, Y.Y. (2003) Pretreatment of corn stover by aqueous ammonia, *Bioresource Technology*. 90, pp. 39-47.
29. KUMAR, A., PRASAD, B. and MISHRA, I.M. (2008) Adsorptive removal of acrylonitrile by commercial grade activated carbon: Kinetics, equilibrium and thermodynamics, *Journal of Hazardous Materials*. 152(2), pp. 589-600.
30. LI, C., KNIERIM, B., MANISSERI, C., ARORA, R., SCHELLER, H.V., AUER, M., VOGEL, K.P., SIMMONS, B.A. and SINGH, S. (2010) Comparison of dilute acid and ionic liquid of switchgrass: Biomass recalcitrance, delignification and enzymatic saccharification, *Bioresource Technology*. 101(13), pp. 4900-4906.
31. NOBLE, K-L. (1997) Waterborne polyurethanes, *Progress in Organic Coatings*. 32(1-4), pp. 131-136.
32. OFOMAJA, A.E., NAIDOO, E.B. and MODISE, S.J. (2009) Removal of copper (II) from aqueous solution by pine and base modified pine cone powder as biosorbent, *Journal of Hazardous Materials*. 168(2-3), pp. 909-917.

33. OUAJAI, S. and SHANKS, R.A. (2005) Composition, structure and thermal degradation of hemp cellulose after chemical treatments, *Polymer degradation & Stability*. 89(2), pp. 327-335.
34. ÓRFÃO, J.J.M., ANTUNES, F.J.A. AND FIGUEIREDO J.L. (1999) Pyrolysis kinetics of lignocellulosic materials – three independent reaction models, *Fuel*. 78, pp. 349-358.
35. PHOLOSI, A., OFOMAJA, A.E. and NAIDOO, E.B. (2013) Effect of chemical extractants on the biosorptive properties of pine cone powder: Influence on Pb (II) removal mechanism, *Journal of Saudi Chemical Society*. 17(1), pp. 77-86.
36. QIU, X., TAO, S., REN, X. and HU, S. (2012) Modified cellulose films with controlled permeatability and biodegradability by crosslinking with toluene diisocyanate under homogenous conditions, *Carbohydrate Polymers.* 88(4), pp. 1272-1280.
37. RAVEENDRAN, K., GANESH, A. and KHILAR, K.C. (1996) Pyrolysis characteristics of biomass and biomass components, *Fuel*. 75(8), pp. 987-998.
38. SARKAR, S. and ADHIKARI, B. (2001) Synthesis and characterization of lignin-HTPB copolyurethane, *European Polymer Journal*. 37(7), pp. 1391-1401.
39. SAYGIDEGER, S., GULNAZ, O., ISTIFLI, E.S., and YUCEL, N. (2005) Adsorption of Cd(II), Cu(II) and Ni(II) ions by *Lemna minor* L.: Effect of physicochemical environment, *Journal of Hazardous Materials*. 126(1-3), pp. 96-104.
40. SGRICCIA, N., HAWLEY, M.C. and MISRA, M. (2008) Characterization of natural fibre surfaces and natural fibre composites, *Composites: Part A.* 39(10), pp. 1632-1637.
41. SHI, J. and LI, J. (2012) Metabolites and chemical group changes in the wood-forming tissue of *Pinus koraiensis* under inclined conditions, *BioResources.* 7(3), pp. 3463-3475.
42. SIM, S.F., MOHAMED, M., LU, N.A.L.M.I., SAFITRI, N., SARMAN, N.S.P. and SAMSUDIN, S.N.S. (2012) Computer-assisted analysis of Fourier Transform Infrared (FTIR) spectra for characterization of various treated and untreated agriculture biomass, *BioResources*. 7(4), pp. 5367-5380.
43. SINGH, S., WU, C. and WILLIAMS, P.T. (2012) Pyrolysis of waste materials using TGA-MS and TGA-FTIR as complementary characterization techniques, *Journal of Analytical and Applied Pyrolysis*. 94, pp. 99-107.

44. SIQUEIRA, G., BRAS, J. and DUFRESNE, A. (2010) New process of chemical grafting of cellulose nanoparticles with a long chain isocyanate, *Langmuir*. 26(1), pp. 402-411.
45. STANKOVICH, S., PINER, R.D., NGUYEN, S.T. and RUOFF, R.S. (2006) Synthesis and exfoliation of isocyanate-treated graphene oxide nanoplatelets, *Carbon*. 44(15), pp. 3342-3347.
46. STENSTAD, P., ANDRESEN, M., TANEM, B.S. and STENIUS, P. (2008) Chemical surface modifications of microfibrillated cellulose, *Cellulose*. 15(1), pp. 35-45.
47. SUBRAMANIAN, K., KUMAR, P.S., JEYAPAL, P. and VENKATESH, N. (2005) Characterization of lignocellulosic seed fibre from Wrightia tinctoria plant for textile applications-an explanatory investigation, *European Polymer Journal*. 41, pp. 853-861.
48. SUKSABYE, P. and THIRAVETYAN, P. (2012) Cr(VI) adsorption from electroplating plating wastewater by chemically modified coir pith, *Journal of Environmental Management*. 102, pp. 1-8.
49. VALODKAR, M. and THAKORE, S. (2010) Isocyanate crosslinked reactive starch nanoparticles for thermo-responsive conducting applications, *Carbohydrate Research*. 345(16), pp. 2354-2360.
50. Yang, H., Yan, R., Chen, H., Lee, D.H. and Zheng, C. (2007) Characteristics of hemicellulose, cellulose and lignin pyrolysis, *Fuel*. 86, pp. 1781-1788.
51. Yang, H., Yan, R., Chin, T., Liang, D.T., Chen, H. and Zheng, C. (2004) Thermogravimetric Analysis – Fourier Transform Infrared analysis of palm oil waste pyrolysis, *Energy & Fuels*. 18, pp. 1814-1821.
52. ZHA, F., LI, S. and CHANG, Y. (2008) Preparation and adsorption property of chitosan beads bearing β-cyclodextrin cross-linked by 1.6-hexamethylene diisocyanate, *Carbohydrate Polymers*. 72, pp. 456-461.

5 RESULTS AND DISCUSSION (PART 2): KINETIC STUDIES

5.1 INTRODUCTION

The chapter presents and discusses the adsorption kinetic results of the adsorption of 2-nitrophenol onto pine cone biomass. It reports on the following in detail: effect of solution pH, adsorbent dose, kinetic models and diffusion processes.

5.2 KINETIC STUDIES

5.2.1 Effect of solution pH

The effect of solution pH on the adsorption of 2-nitrophenol using Raw, Raw-HMDI, Fenton treated and Fenton treated-HMDI pine cone biomass was studied in the pH range 1-10 and the results are presented in Figure 5.1. Solution pH plays a very important role in the biosorption process as it influences both biosorbent and biosorbate properties (Ho and Ofomaja, 2007). The surface charge of the pine cone biosorbent is depended on solution pH and its pH_{pzc}. At pH > pH_{pzc}, the pine cone biomass surface is negatively charged and is positively charged at pH < pH_{pzc}. The pH_{pzc} values for Raw, Raw-HMDI, Fenton treated and Fenton treated-HMDI pine cone were found to be 7.49, 6.68, 5.4 and 6.12 respectively. The 2-nitrophenol biosorbate is predominantly in protonated form at pH < pK_a and in deprotonated form at pH > pK_a (Liu et al., 2010). The pK_a of 2-nitrophenol is 7.17 at 298 K (El-Sheikh et al., 2013). The adsorption capacity was calculated as follows:

$$q_e = \frac{(C_0 - C_e)V}{m} \tag{5.1}$$

Where, q_e is the equilibrium sorption capacity (mg/g), C_0 is the initial 2-nitrophenol concentration (mg/dm^3), C_e is the equilibrium 2-nitrophenol concentration (mg/dm^3), V is solution volume (dm^3) and m is mass of biosorbent (g).

The optimum pH was found to be around 6 as shown in Figure 5.1 for all the pine cone biosorbents and is close to their pH_{pzc} values presented in Table 4.5. Adsorption capacity values for the pine cone biosorbents at pH 6 were found to be 25.04 mg/g for Raw, 31.96 mg/g for Raw-HMDI, 33.72 mg/g for Fenton treated and 52.12 mg/g for Fenton treated-HMDI. The results show that pine cone biomass modification via Fenton treatment and cross-

linking using HMDI increased its affinity for 2-nitrophenol. At low pH, that is, at pH < pH_{pzc} of the biosorbents and pH < pK_a of 2-nitrophenol the adsorption capacity decreases and this might be due to: (1) adsorption of protons on the active sites, and/or (2) electrostatic repulsive force between biosorbate and biosorbent, and/or (3) repulsion between the sorbate molecules (Ofomaja, 2011). The adsorption capacity also decreases at higher pH values, that is, at pH > pH_{pzc} of the biosorbents and pH > pK_a of 2-nitrophenol. At these pH values the biosorbent surfaces are negatively charged and the 2-nitrophenol mainly exists in deprotonated form. Hence, electrostatic repulsion force exists between the 2-nitrophenol and the pine cone surfaces. The magnitude of the electrostatic repulsion force depends on the amount of charge on the biosorbent surface and extent of dissociation of 2-nitrophenol. Electrostatic repulsion force also exists between the adsorbed phenolic anions in the biosorbent pores. A higher degree of dissociation of the 2-nitrophenol also decreases its hydrophobic character causing a reduction in affinity between biosobate and biosorbent (Liu et al., 2010).

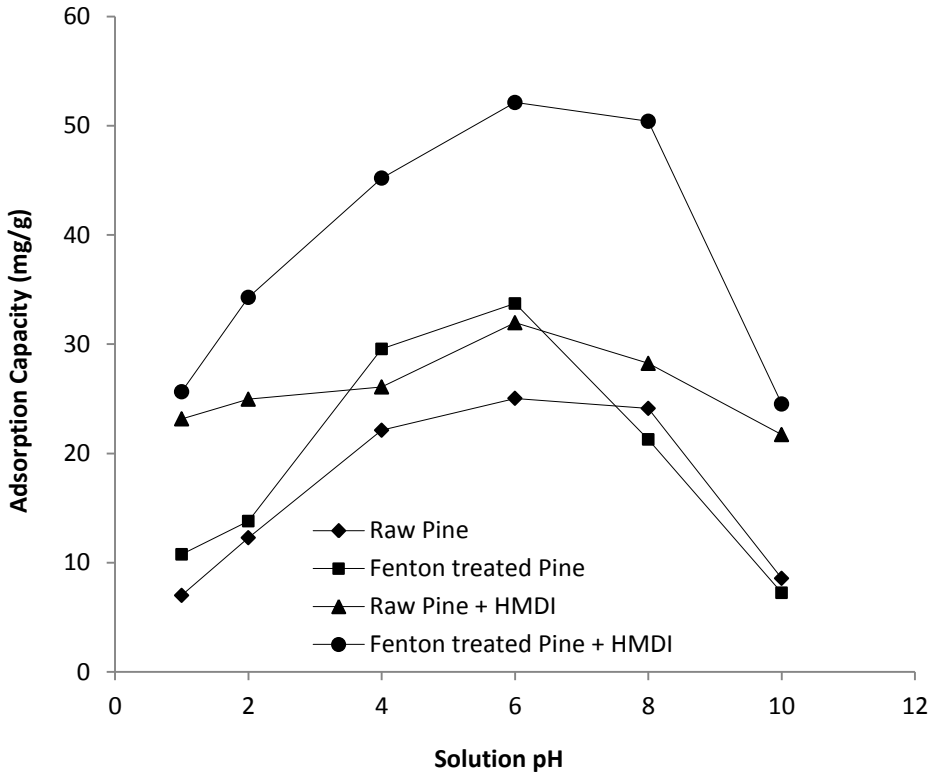

Figure 5.1 Effects of solution pH on the adsorption of 2-nitrophenol using pine cone biomass. Adsorbent dose: 0.5 g/dm^3, initial adsorbate concentration: 50 mg/dm^3, solution volume: 100 cm^3, agitation speed: 100 rpm, temperature: 299 K.

5.2.2 Adsorbent dose

The plots in Figures 5.2-5.5 show the effect of adsorbent dose on percentage uptake and adsorption capacity of 2-nitrophenol. The percentage 2-nitrophenol removal was calculated as follows:

$$\%R = \frac{(C_0 - C_e)}{C_0} \times 100 \qquad (5.2)$$

Where, *% R*, is percentage 2-nitrophenol removed from solution, C_0 and C_e are initial and equilibrium concentration (mg/dm^3) of 2-nitrophenol respectively.

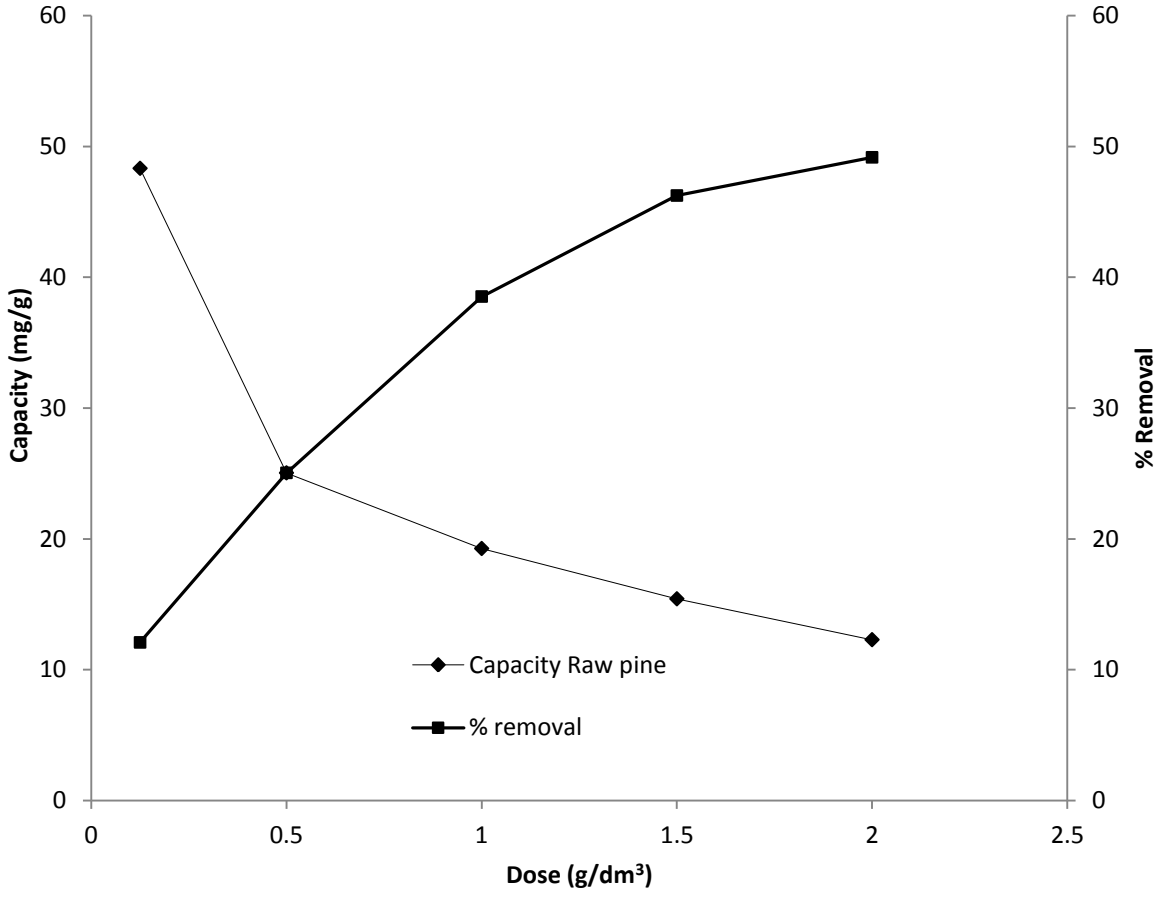

Figure 5.2 Effect of Raw pine dose on 2-nitrophenol adsorption. Initial pH: 6, initial adsorbate concentration: 50 mg/dm^3, solution volume: 100 cm^3, agitation speed: 100 rpm, temperature: 299 K.

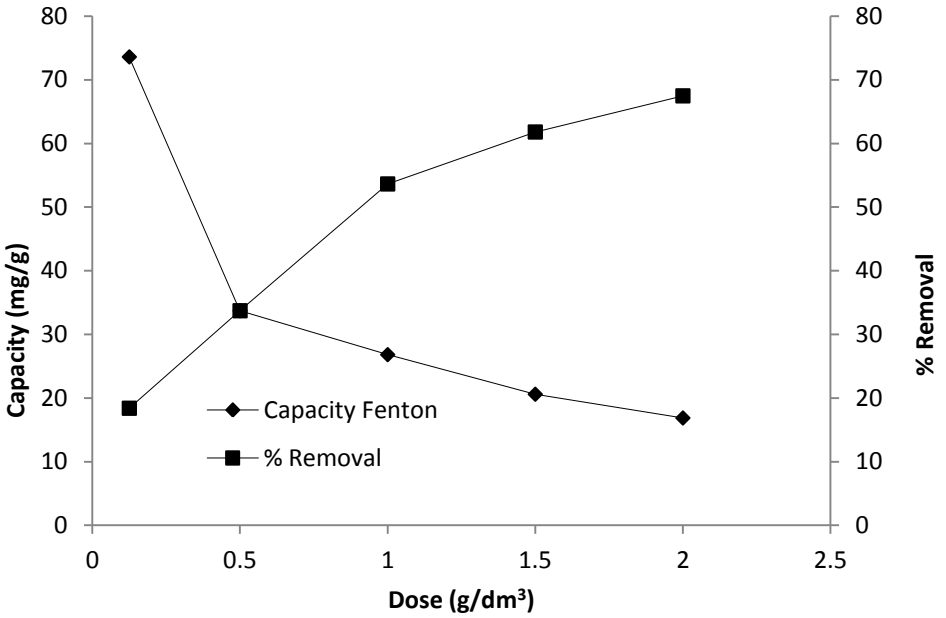

Figure 5.3 Effect of Fenton treated pine dose on 2-nitrophenol adsorption. Initial pH: 6, initial adsorbate concentration: 50 mg/dm^3, solution volume: 100 cm^3, agitation speed: 100 rpm, temperature: 299 K.

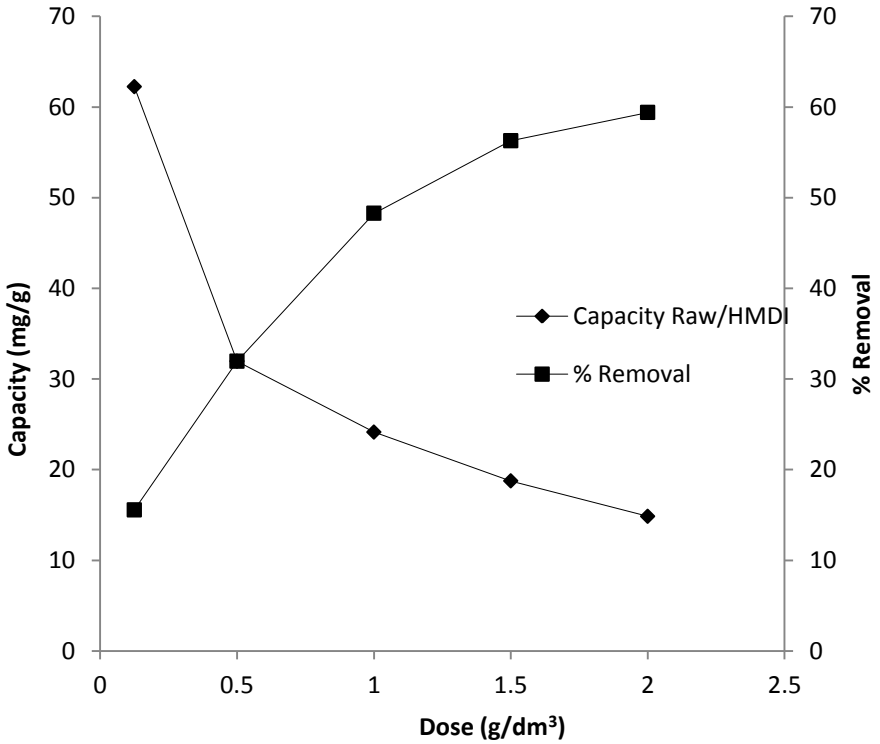

Figure 5.4 Effect of Raw-HMDI pine dose on 2-nitrophenol adsorption. Initial pH: 6, initial adsorbate concentration: 50 mg/dm^3, solution volume: 100 cm^3, agitation speed: 100 rpm, temperature: 299 K.

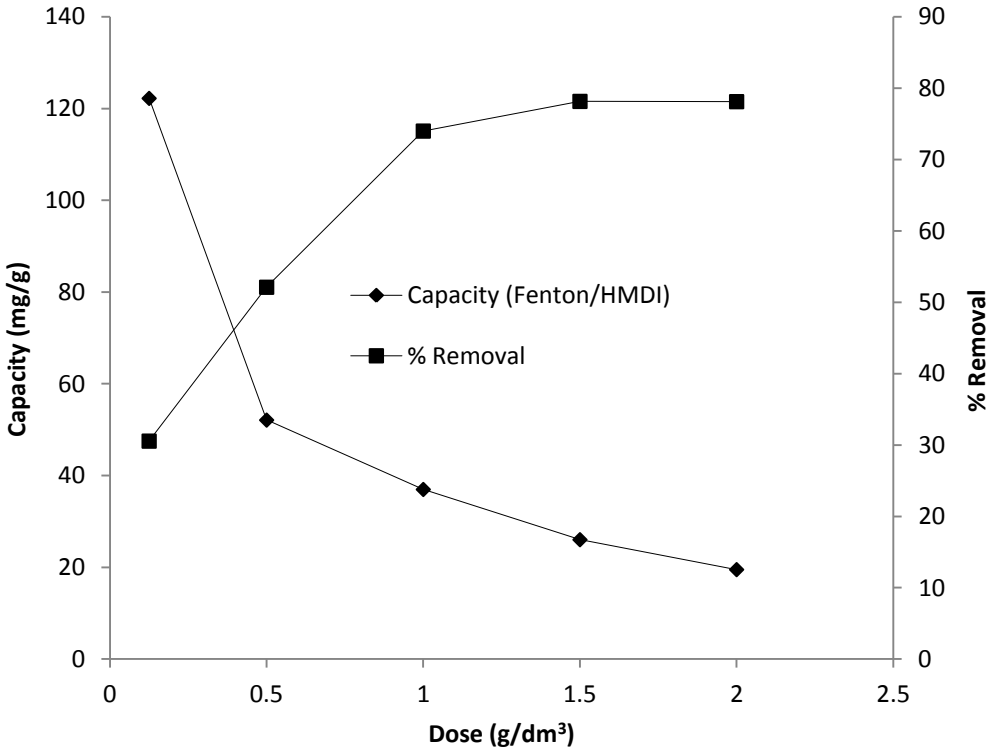

Figure 5.5 Effect of Fenton treated-HMDI pine dose on 2-nitrophenol adsorption. Initial pH: 6, initial adsorbate concentration: 50 mg/dm^3, solution volume: 100 cm^3, agitation speed: 100 rpm, temperature: 299 K.

For the Raw pine, adsorption capacity decreases from 48.32 mg/g to 15.41 mg/g as adsorbent dose increases from 0.125 g/dm^3 to 1.5 g/dm^3, but only decreases from 15.41 mg/g to 12.29 mg/g as the adsorbent dose increases from 1.5 g/dm^3 to 2 g/dm^3. The percentage 2-nitrophenol removal increases from 12.08 % to 46.29 % as adsorbent dose increases from 0.125 g/dm^3 to 1.5 g/dm^3, but only increases from 46.29 % to 49.16 % as adsorbent dose increases from 1.5 g/dm^3 to 2 g/dm^3.

For the Raw-HMDI pine, adsorption capacity decreases from 62.24 mg/g to 18.76 mg/g as adsorbent dose increases from 0.125 g/dm^3 to 1.5 g/dm^3, but only decreases from 18.76 mg/g to 14.85 mg/g as the adsorbent dose increases from 1.5 g/dm^3 to 2 g/dm^3. The percentage 2-nitrophenol removal increases from 15.56 % to 56.28 % as adsorbent dose increases from 0.125 g/dm^3 to 1.5 g/dm^3, but only increases from 56.28 % to 59.40 % as adsorbent dose increases from 1.5 g/dm^3 to 2 g/dm^3.

For the Fenton treated pine, adsorption capacity decreases from 73.60 mg/g to 20.60 mg/g as adsorbent dose increases from 0.125 g/dm^3 to 1.5 g/dm^3, but only decreases from 20.60 mg/g to 16.84 mg/g as the adsorbent dose increases from 1.5 g/dm^3 to 2 g/dm^3. The percentage 2-nitrophenol removal increases from 18.40 % to 61.80 % as adsorbent dose increases from 0.125 g/dm^3 to 1.5 g/dm^3, but only increases from 61.80 % to 67.48 % as adsorbent dose increases from 1.5 g/dm^3 to 2 g/dm^3.

For the Fenton treated-HMDI pine, adsorption capacity decreases from 122.24 mg/g to 26.05 mg/g as adsorbent dose increases from 0.125 g/dm^3 to 1.5 g/dm^3, but only decreases from 26.05 mg/g to 19.53 mg/g as the adsorbent dose increases from 1.5 g/dm^3 to 2 g/dm^3. The percentage 2-nitrophenol removal increases from 30.56 % to 78.16 % as adsorbent dose increases from 0.125 g/dm^3 to 1.5 g/dm^3, but decreases from 78.16 % to 78.12 % as adsorbent dose increases from 1.5 g/dm^3 to 2 g/dm^3.

The plots show a similar pattern. Analysis of the plots in Figures 5.2-5.5 reveals that as adsorbent dose increases from 0.125 g/dm^3 to 1.5 g/dm^3 there is a marked decrease in adsorption capacity, but a small decrease in adsorption capacity is observed when adsorbent dose increases from 1.5 g/dm^3 to 2 g/dm^3. An analogous trend is also observed with percentage 2-nitrophenol removal. As adsorbent dose increases from 0.125 g/dm^3 to 1.5 g/dm^3 there is a marked increase in percentage 2-nitrophenol removal, but only a small increase is noted as adsorbent dose increases from 1.5 g/dm^3 to 2 g/dm^3. All the plots show a decrease in adsorption capacity and consequent increase in percentage removal of 2-nitrophenol with increase in adsorbent dose. The decrease in adsorption capacity is due to increase in number of adsorbent particles with constant 2-nitrophenol concentration. The observed increase in percentage removal of adsorbate is attributed to an increase in number of biosorption sites. The observed result suggests that the optimum adsorbent dose for the pine cone biosorbents for the adsorption process is 1.5 g/dm^3. The results also show that pine modification enhanced its biosorptive capability towards 2-nitrophenol.

5.2.3 Kinetic models

Adsorption is an equilibrium separation process involving five main stages namely: (1) bulk diffusion, (2) film diffusion, (3) surface adsorption, (4) intraparticle diffusion and (5) pore diffusion. Amongst these processes mentioned, the slowest process is the rate-determining or

controlling step. The adsorption kinetic curves for 2-nitrophenol adsorption onto pine cone biomass at 299 K and concentrations ranging from 100 to 400 mg/dm^3 are presented in Figures 5.6-5.9.

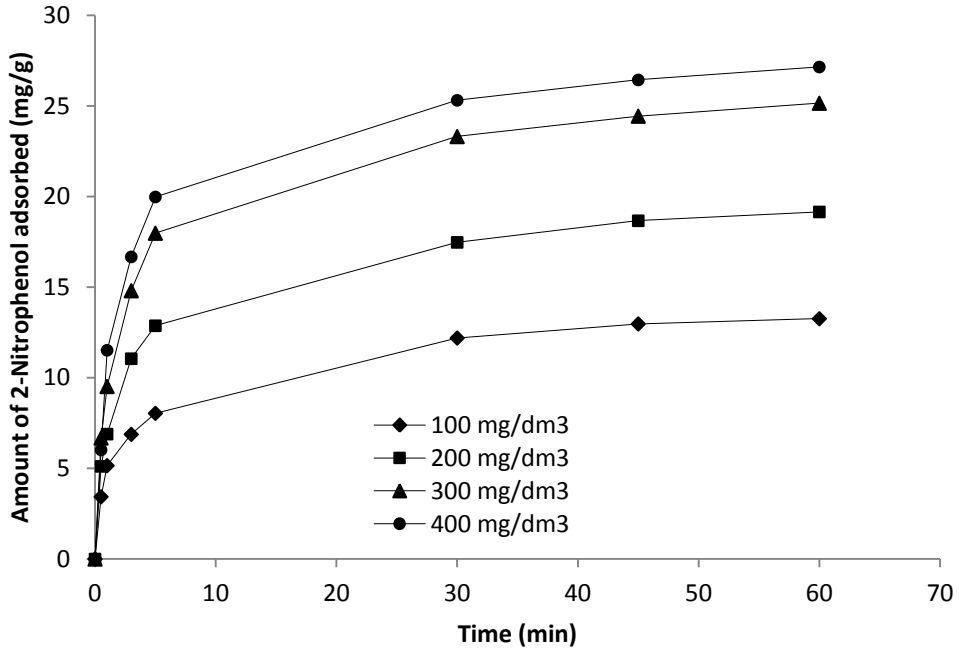

Figure 5.6 Adsorption kinetics of 2-nitrophenol on Raw pine. Initial pH: 6, adsorbate dose: 1.5 g/dm^3, solution volume: 10 cm^3, agitation speed: 100 rpm, temperature: 299 K.

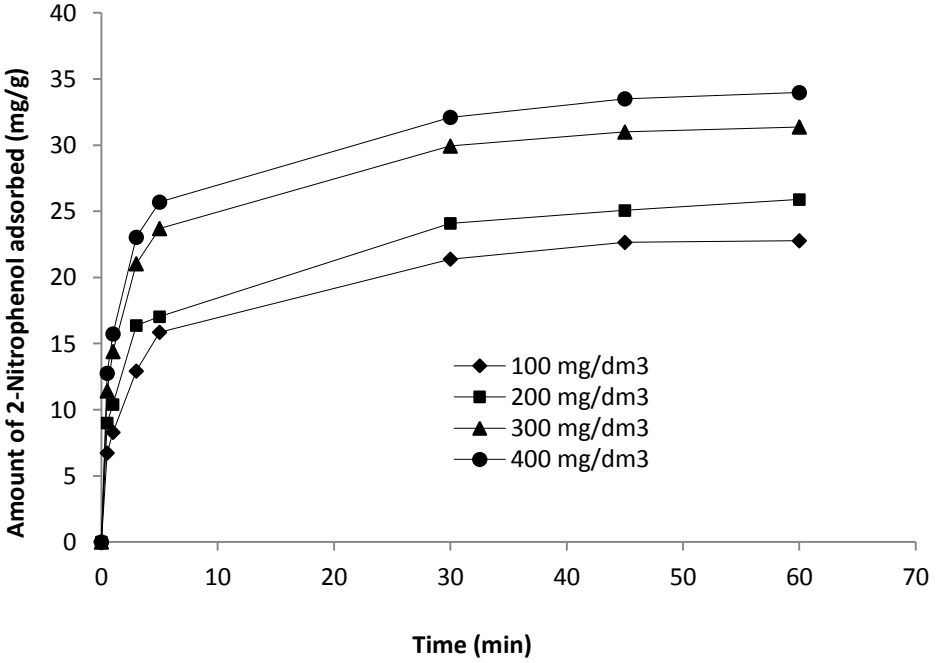

Figure 5.7 Adsorption kinetics of 2-nitrophenol on Raw-HMDI pine. Initial pH: 6, adsorbate dose: 1.5 g/dm^3, solution volume: 10 cm^3, agitation speed: 100 rpm, temperature: 299 K.

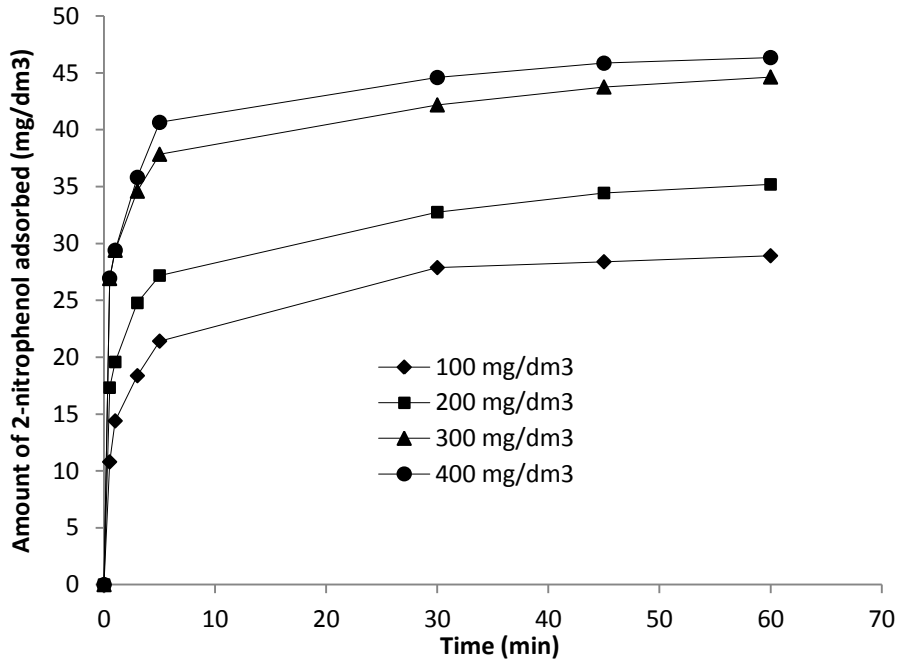

Figure 5.8 Adsorption kinetics of 2-nitrophenol on Fenton treated pine. Initial pH: 6, adsorbate dose: 1.5 g/dm^3, solution volume: 10 cm^3, agitation speed: 100 rpm, temperature: 299 K.

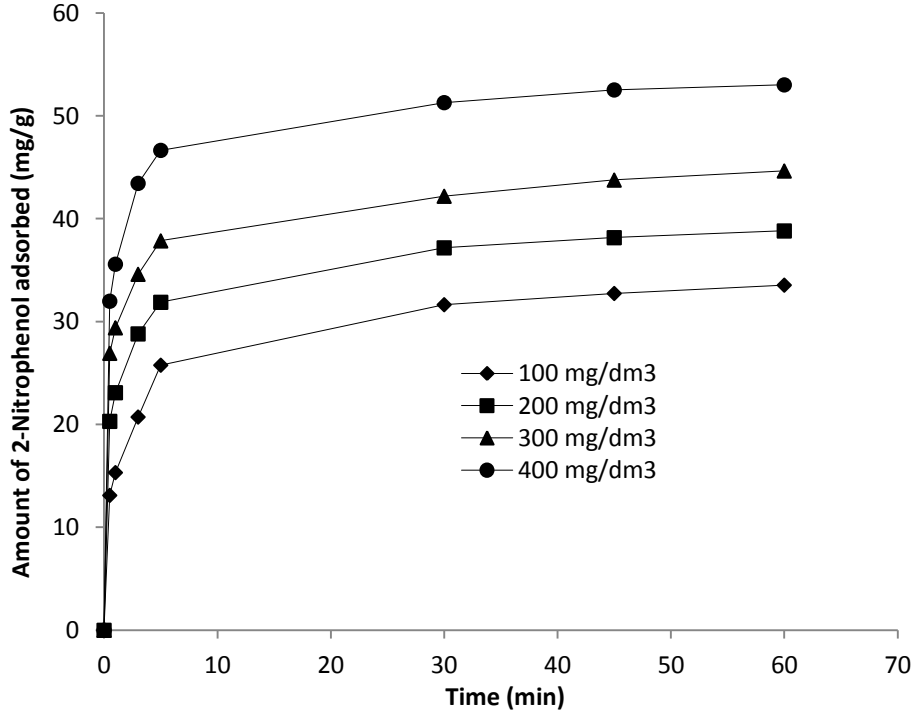

Figure 5.9 Adsorption kinetics of 2-nitrophenol on Fenton treated-HMDI pine. Initial pH: 6, adsorbate dose: 1.5 g/dm^3, solution volume: 10 cm^3, agitation speed: 100 rpm, temperature: 299 K.

The shapes of the adsorption kinetic curves of 2-nitrophenol on pine cone biomass in Figures 5.6-5.9 are all similar and are divided into two kinetic profiles. An initial rapid uptake between 0-5 minutes and a slower rate from 5 minutes till equilibrium is reached at 60 minutes.

The adsorption capacity of the pine sorbents increases with an increase in adsorbate concentration. An opposite pattern is observed with the % removal of 2-nitrophenol, which shows a decrease as 2-nitrophenol concentration increases. For example, Raw pine shows an adsorption capacity of 13.26 mg/g at 100 mg/dm^3 and 27.15 mg/g at 400 mg/dm^3, but % removals of 19.89 at 100 mg/dm^3 and 10.18 at 400 mg/dm^3. This is attributed to an increase in adsorbate molecules with no change in number of adsorption sites since adsorbent mass is not changing.

The adsorption capacities show an increase due to Fenton treatment and cross-linking using HMDI. At 400 mg/dm^3 2-nitrophenol concentration, the pine biomass had the following adsorption capacities: Raw, 27.15 mg/g; Raw-HMDI, 33.98 mg/g; Fenton treated, 46.35 mg/g; and Fenton treated-HMDI, 53.01 mg/g. The magnitude of the pine biomass adsorption capacities increased in the order: Fenton treated-HMDI > Fenton treated > Raw-HMDI > Raw.

The increase in oxygenated surface groups and the hydrophobic character imparted on the pine due to cross-linking using HMDI created conditions favouring uptake of 2-nitrophenol from aqueous solution.

It can be observed from Figures 5.6-5.9, that initial adsorption of 2-nitrophenol onto the pine cone biomass is rapid. The adsorption kinetics of the pine biomass is in the order: Fenton treated-HMDI > Fenton treated > Raw-HMDI > Raw. This suggests that the increase in porosity and hydrophobic character of the biomass due to Fenton treatment and HMDI cross-linking caused a reduction in diffusion resistance resulting in fast adsorption kinetics. The plots also show that the kinetics of the initial adsorption of 2-nitrophenol increase with an increase in initial adsorbate concentration. This is due to an increase in concentration gradient between the bulk solution and the adsorbent resulting in a decrease in external mass transfer resistance.

The experimental kinetic data for 2-nitrophenol adsorption onto the pine cone biomass was fitted to the pseudo-first-order and pseudo-second-order kinetic models. Non-linear regression was used to determine the rate constants and kinetic parameters.

5.2.3.1 Pseudo-first-order model

The non-linear form of the pseudo-first-order rate equation (Kumar, 2006) can be expressed as:

$$q_t = q_e\left(1 - \exp^{-k_1}\right) \tag{5.3}$$

Where, q_e (mg/g) and q_t (mg/g) are the adsorption capacity at equilibrium and time t respectively and k_1 (1/min) is the rate constant. A non-linear plot of q_t against t is used to calculate k_1. The pseudo-first-order constants and error functions for 2-nitrophenol adsorption onto pine cone biomass are presented in Table 5.1.

The pseudo-first-order constants at an initial 2-nitrophenol concentration of 100 mg/dm^3 at 299 K are: (1) Raw pine; q_e*(experimental)* = 13.26 mg/g, q_e*(calculated)* = 12.60 mg/g, k_1 = 0.2846 1/(min), (2) Raw-HMDI pine; q_e*(experimental)* = 22.78 mg/g, q_e*(calculated)* = 21.91 mg/g, k_1 = 0.3350 1/(min), (3) Fenton treated pine; q_e*(experimental)* = 28.92 mg/g, q_e*(calculated)* = 26.13 mg/g, k_1 = 0.5647 1/(min), and (4) Fenton treated-HMDI pine; q_e*(experimental)* = 33.55 mg/g, q_e*(calculated)* = 31.33 mg/g, k_1 = 0.5254 1/(min). The experimental and calculated adsorption capacity values increase as 2-nitrophenol concentration increases and exhibit small variations. The rate constant increases due to modification of pine biomass via Fenton treatment and cross-linking using HMDI. The rate constant also increases as 2-nitrophenol concentration increases due to an increase in collision frequency between adsorbate and adsorbent. This shows that the adsorption rate increased due to pine modification and increase in 2-nitrophenol concentration.

The coefficient of determination, r^2 and the percentage variable error, *% var* or % variance was used for error analysis. The pine sorbents had the following values: Raw, r^2= 0.9363 and % variance = 1.74; Raw-HMDI, r^2= 0.9662 and % variance = 3.60; Fenton treated, r^2= 0.9161 and % variance = 10.10; and Fenton treated-HMDI, r^2= 0.9214 and % variance = 12.63. The r^2 for Raw pine is lower than that for Raw-HMDI pine.

The plots in Figures 5.10-5.13 compare experimental and modelled equilibrium capacities for adsorption of 2-nitrophenol on pine cone biomass. The experimental data shows good correlation with the pseudo-first-order model in the first five minutes of the adsorption. After this initial period the experimental data shows a poor fit.

5.2.3.2 Pseudo-second-order model

The non-linear form of the pseudo-second-order rate equation (Kumar, 2006) can be expressed as:

$$q_t = \frac{k_2 q_e^2 t}{1 + k_2 q_e t} \tag{5.4}$$

Where, q_e and q_t (mg/g) are the adsorption capacities at equilibrium and time t respectively and k_2 (g/mg.min) is the rate constant. The values of q_e and k_2 are calculated from a non-linear plot of q_t against t. The initial adsorption rate (mg/g.min) is expressed as:

$$h = k_2 q_e^2 \tag{5.5}$$

The pseudo-second-order constants and error functions for 2-nitrophenol adsorption onto pine cone biomass are presented in Table 5.2. The pseudo-second-order constants at an initial 2-nitrophenol concentration of 100 mg/dm^3 at 299 K are: (1) Raw pine; q_e*(experimental)* = 13.26 mg/g, q_e*(calculated)* = 13.27 mg/g, k_2 = 0.0333 g/mg.min, h = 5.86 mg/g.min, , (2) Raw-HMDI pine; q_e*(experimental)* = 22.78 mg/g, q_e*(calculated)* = 23.04 mg/g, k_2 = 0.0223 g/mg.min, h = 12.05 mg/g.min, , (3) Fenton treated pine; q_e*(experimental)* = 28.44 mg/g, q_e*(calculated)* = 28.92 mg/g, k_2 = 0.0313 g/mg.min, h = 74.04 mg/g.min, , and (4) Fenton treated-HMDI pine; q_e*(experimental)* = 33.55 mg/g, q_e*(calculated)* = 32.89 mg/g, k_2 = 0.0262 g/mg.min, h = 28.34 mg/g.min. The experimental and predicted adsorption capacity values increase as initial 2-nitrophenol concentration increases and are in very good agreement. The rate constant increases due to modification of pine biomass with Fenton treatment and cross-linking using HMDI. The rate constant also decreases as initial 2-nitrophenol concentration increases. This shows that the adsorption rate increased due to biosorbent modification and decrease in adsorbate concentration. The initial adsorption rate increases with an increase in initial adsorbate concentration, with modified pine samples showing higher initial adsorption

rates than the Raw pine. This suggests initial rapid uptake due to an increase in adsorbate molecules and indicates higher affinity of modified pine surfaces for the adsorbate. The decrease in rate of adsorption as adsorbate concentration increases can be attributed to repulsion and/or steric effects between adsorbate molecules.

The results of the two error functions used for error analysis are: Raw, r^2= 0.9739 and % variance = 0.71; Raw-HMDI, r^2= 0.9870 and % variance = 1.07; Fenton treated, r^2= 0.9786 and % variance = 2.57; and Fenton treated-HMDI, r^2= 0.9796 and % variance = 3.70. The r^2 for Raw pine is lower than that for Raw-HMDI.

The plots in Figures 5.10-5.13 compare experimental and modelled equilibrium capacities for adsorption of 2-nitrophenol on pine cone biomass. The experimental data shows good correlation with the pseudo-second-order model throughout the entire adsorption process.

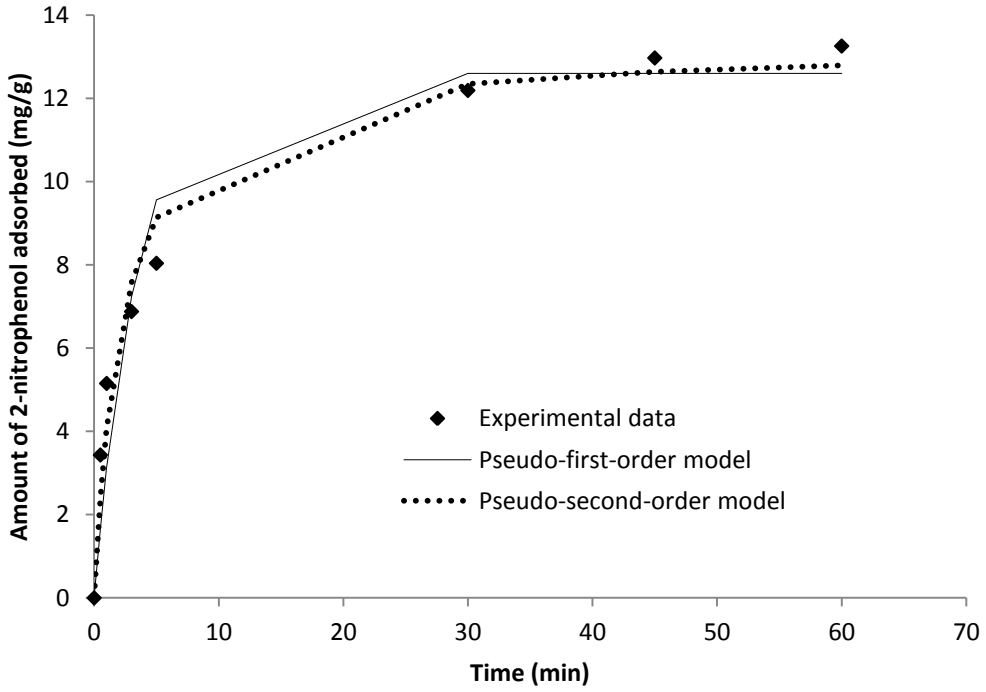

Figure 5.10 Comparison of predicted equilibrium capacities of kinetic models with experimental data for 2-nitrophenol adsorption on Raw pine.

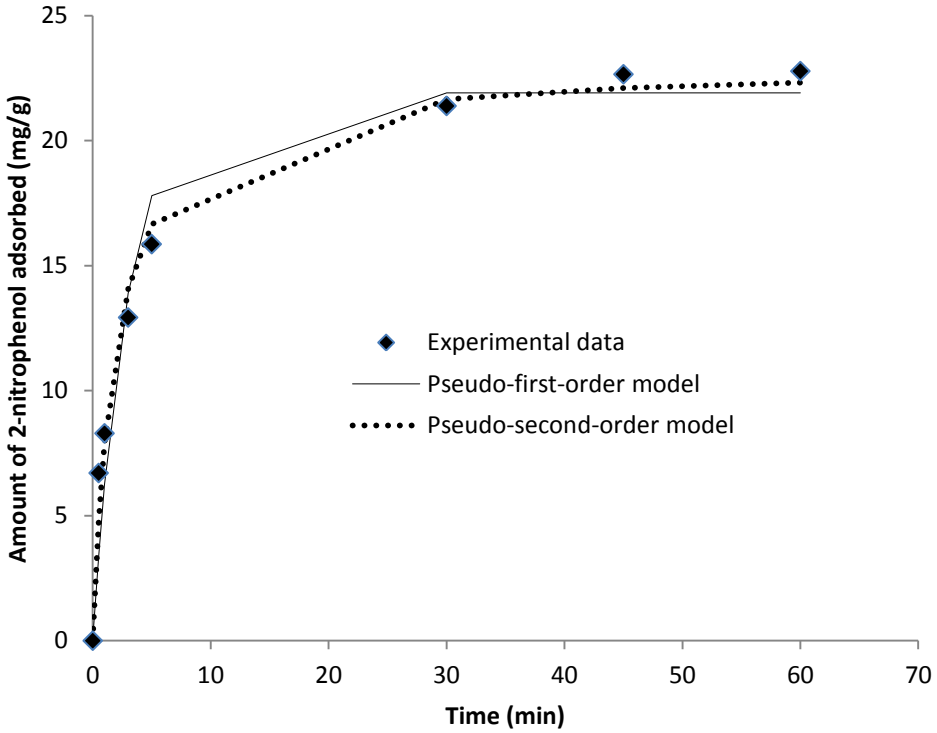

Figure 5.11 Comparison of predicted equilibrium capacities of kinetic models with experimental data for 2-nitrophenol adsorption on Raw-HMDI pine.

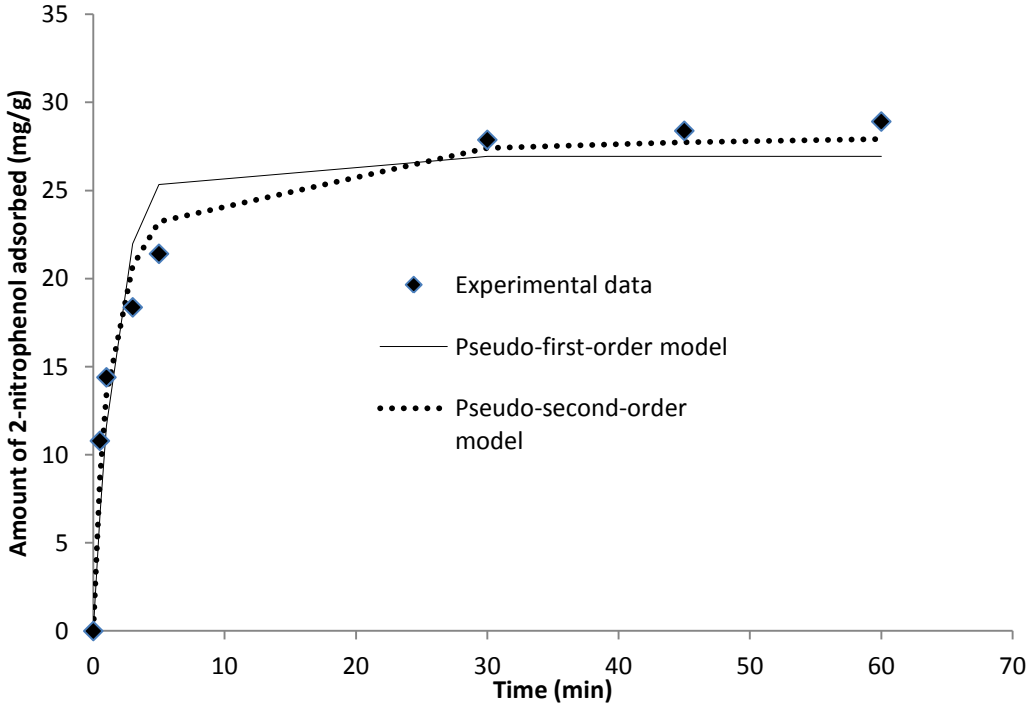

Figure 5.12 Comparison of predicted equilibrium capacities of kinetic models with experimental data for 2-nitrophenol adsorption on Fenton treated pine.

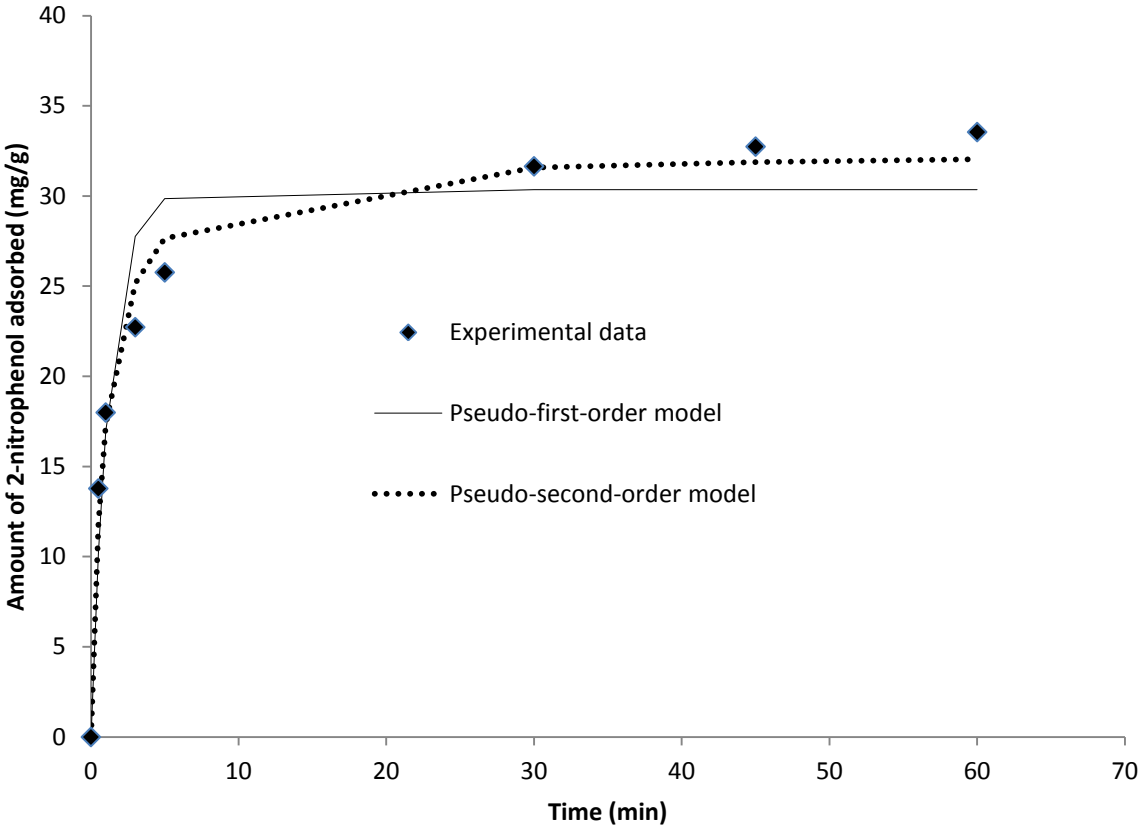

Figure 5.13 Comparison of predicted equilibrium capacities of kinetic models with experimental data for 2-nitrophenol adsorption on Fenton treated-HMDI pine.

Table 5.1 Pseudo-first-order kinetic modelling of different concentrations of 2-nitrophenol adsorption on pine cone biomass.

Sample	Parameters	100 mg/dm^3	200 mg/dm^3	300 mg/dm^3	400 mg/dm^3
Raw Pine	q_e(mg/g)(*exp*)	13.26	19.15	25.15	27.15
	q_e (mg/g)	12.60	18.12	23.74	25.84
	k_1 (1/min)	0.2846	0.3352	0.3905	0.4067
	r^2	0.9363	0.9597	0.9534	0.9754
	% Variable Error	1.74	2.30	4.51	2.92
Raw-HMDI pine	q_e(mg/g)(*exp*)	22.78	25.89	31.38	33.98
	q_e (mg/g)	21.91	24.32	29.67	30.68
	k_1 (1/min)	0.3350	0.3713	0.5095	0.8608
	r^2	0.9662	0.9162	0.9540	0.9188
	% Variable Error	3.60	8.15	6.85	13.05
Fenton treated pine	q_e(mg/g)(*exp*)	28.92	35.19	44.64	46.35
	q_e (mg/g)	26.93	31.01	40.71	42.31
	k_1 (1/min)	0.5647	1.1688	1.4887	1.6589
	r^2	0.9161	0.8906	0.9511	0.9392
	% Variable Error	10.08	17.43	12.56	16.68
Fenton-HMDI pine	q_e(mg/g)(*exp*)	33.55	38.81	48.79	53.01
	q_e (mg/g)	30.36	35.59	44.69	49.26
	k_1 (1/min)	0.5254	1.0398	1.5697	1.7651
	r^2	0.9206	0.9471	0.9453	0.9601
	% Variable Error	12.22	10.91	16.80	14.48

Table 5.2 Pseudo-second-order kinetic modelling of different concentrations of 2-nitrophenol adsorption on pine cone biomass.

Sample	Parameters	100 mg/dm^3	200 mg/dm^3	300 mg/dm^3	400 mg/dm^3
Raw pine	q_e(mg/g)(*exp*)	13.26	19.15	25.15	27.15
	q_e (mg/g)	13.27	19.10	24.15	27.27
	k_2 (g/mg min)	0.0333	0.0268	0.0222	0.0220
	h (mg/g min)	5.86	9.78	12.95	16.81
	r^2	0.9739	0.9899	0.9895	0.9959
	% Variable Error	0.71	0.57	1.01	0.48
Raw-HMDI pine	q_e(mg/g)(*exp*)	22.78	25.89	31.38	33.98
	q_e (mg/g)	23.04	25.33	31.11	33.50
	k_2 (g/mg min)	0.0223	0.0267	0.0274	0.0277
	h (mg/g min)	12.05	17.13	26.52	29.96
	r^2	0.9870	0.9740	0.9887	0.9876
	% Variable Error	1.07	2.52	1.63	2.06
Fenton treated pine	q_e(mg/g)(*exp*)	28.44	33.51	42.62	45.02
	q_e (mg/g)	28.92	35.19	44.64	46.35
	k_2 (g/mg min)	0.0313	0.0446	0.0612	0.0619
	h (mg/g min)	74.04	77.57	81.61	86.09
	r^2	0.9786	0.9709	0.9887	0.9825
	% Variable Error	2.57	4.66	2.90	4.88
Fenton-HMDI pine	q_e(mg/g)(*exp*)	33.55	38.81	48.79	53.01
	q_e (mg/g)	32.89	37.49	47.19	51.62
	k_2 (g/mg min)	0.0262	0.0470	0.0491	0.0546
	h (mg/g min)	28.34	66.06	109.34	145.49
	r^2	0.9796	0.9805	0.9861	0.9959
	% Variable Error	3.70	3.84	4.28	2.99

5.2.4 Diffusion processes

Adsorption is a multi-step process involving the migration of adsorbate molecules to external surface of adsorbent followed by diffusion into the pores. A film or boundary layer forms around a solid in an aqueous phase. During adsorption, the adsorbate molecules move from the bulk solution via the boundary layer onto the adsorbent surface and finally diffuse into the pores. The plots in Figures 5.14-5.17 show the external mass transfer diffusion plots for sorption of 2-nitrophenol onto pine cone biomass at 299 K. The external mass transfer diffusion rate constants were determined from plot of C_t/C_0 at different initial concentrations of 2-nitrophenol against time, where C_t and C_0 represent adsorbate concentration at time t and initial adsorbate concentration (mg/dm^3). The slope of the curve is taken as the external mass transfer diffusion rate constant, k_s on the assumption that the relationship is linear for the first initial rapid stage (due to external mass transfer) that is in the first 5 minutes of 2-nitrophenol sorption on pine biomass. The external mass transfer diffusion rate constants for adsorption of 2-nitrophenol on pine biomass are presented in Table 5.3. The k_s (1/min) values for 2-nitrophenol (200 mg/dm^3) adsorption onto pine biomass at 299 K are 0.0169 for Raw, 0.0480 for Raw-HMDI, 0.0480 for Fenton treated and 0.0556 for Fenton treated-HMDI. The external mass transfer diffusion rate constants increase in magnitude due to modification of the pine biomass, but decrease with an increase in initial adsorbate concentration. This shows that the Fenton treatment and cross-linking using HMDI improved the affinity between adsorbate and adsorbent, thus increasing the concentration gradient between the bulk solution and solid surface resulting in an increase in external diffusion rates. The external mass transfer diffusion rate constants decrease with an increase in initial adsorbate concentration due to an increase in resistance of the boundary layer. The number of adsorbent particles and total surface area for interaction become smaller as adsorbate concentration increases resulting in an increase in boundary layer resistance (Ofomaja, 2011) thereby reducing the external diffusion rates. This suggests that the initial rapid uptake in the adsorption of 2-nitrophenol by pine cone biomass is controlled by external mass transfer.

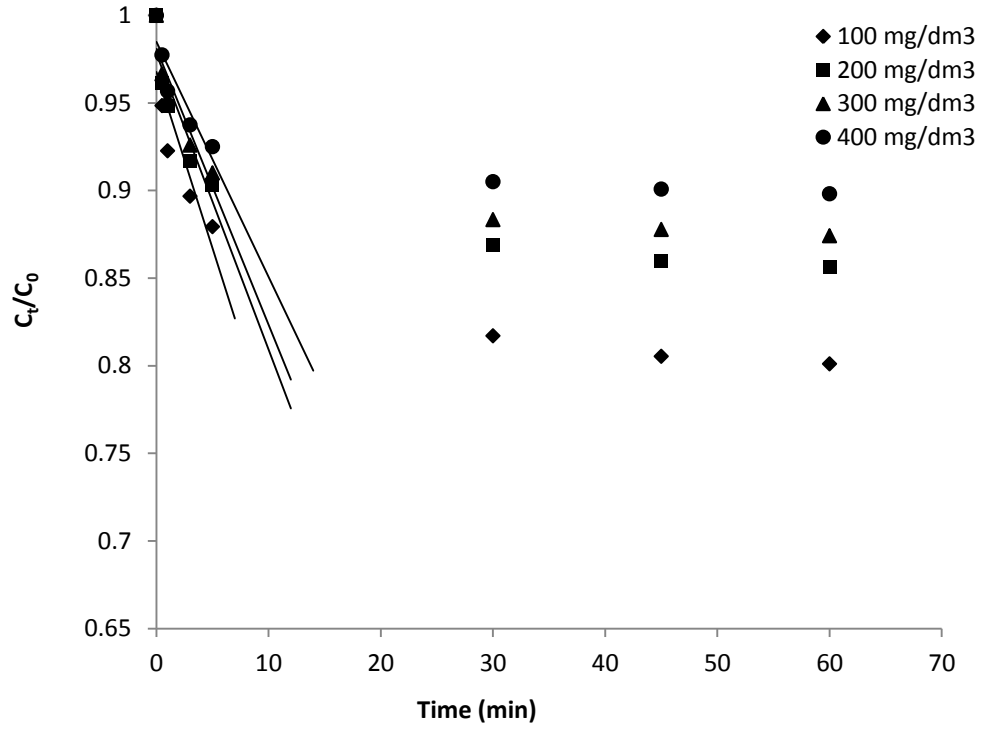

Figure 5.14 External mass transfer diffusion plot for 2-nitrophenol adsorption onto Raw pine.

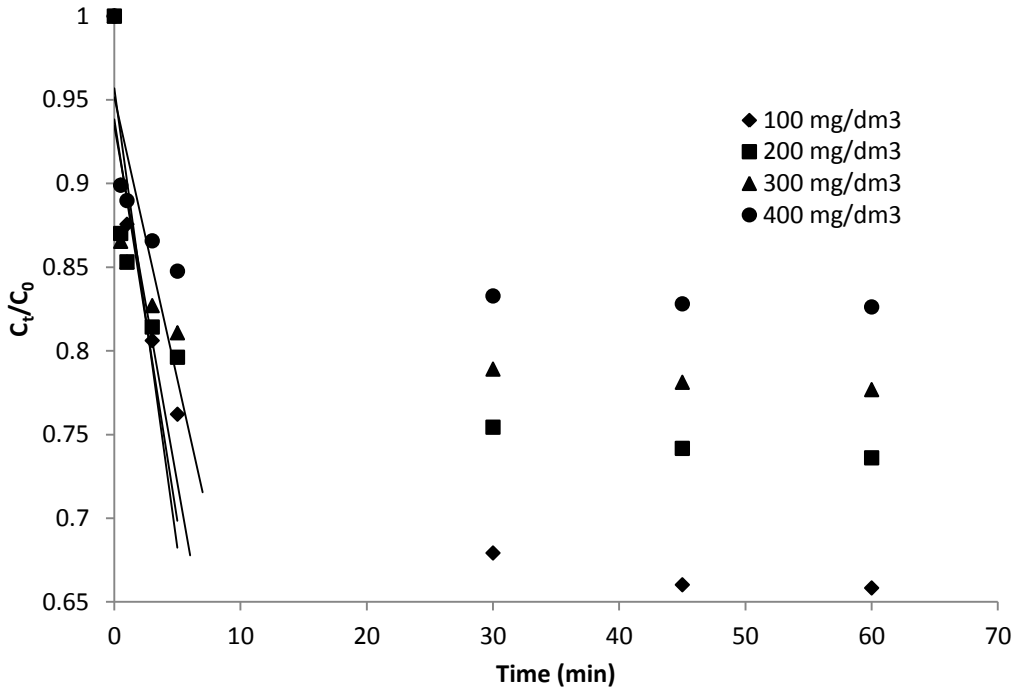

Figure 5.15 External mass transfer diffusion plot for 2-nitrophenol adsorption onto Raw-HMDI pine.

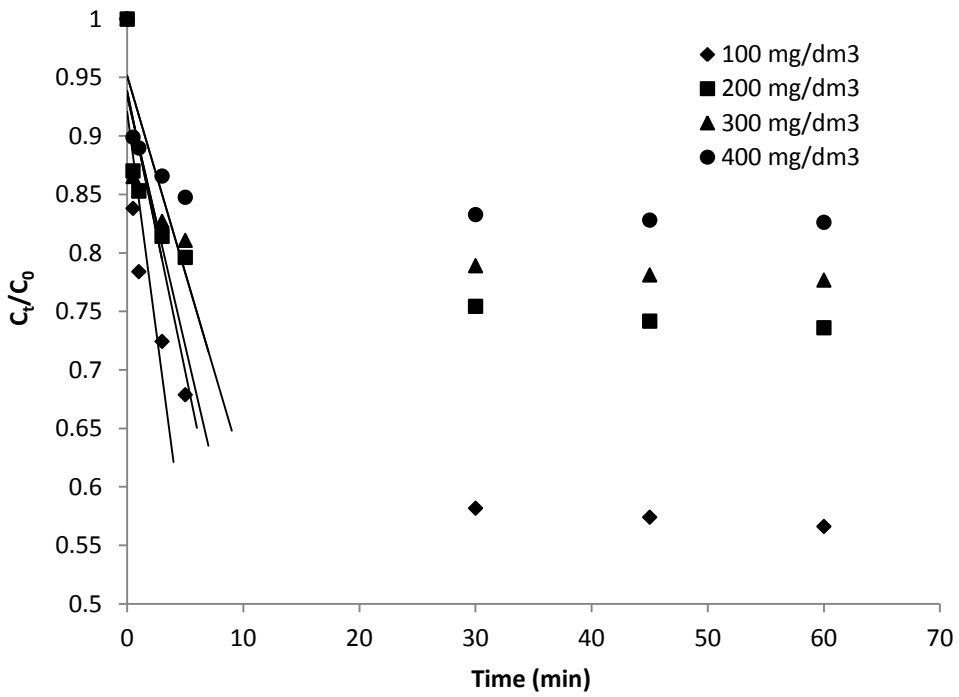

Figure 5.16 External mass transfer diffusion plot for 2-nitrophenol adsorption onto Fenton treated pine.

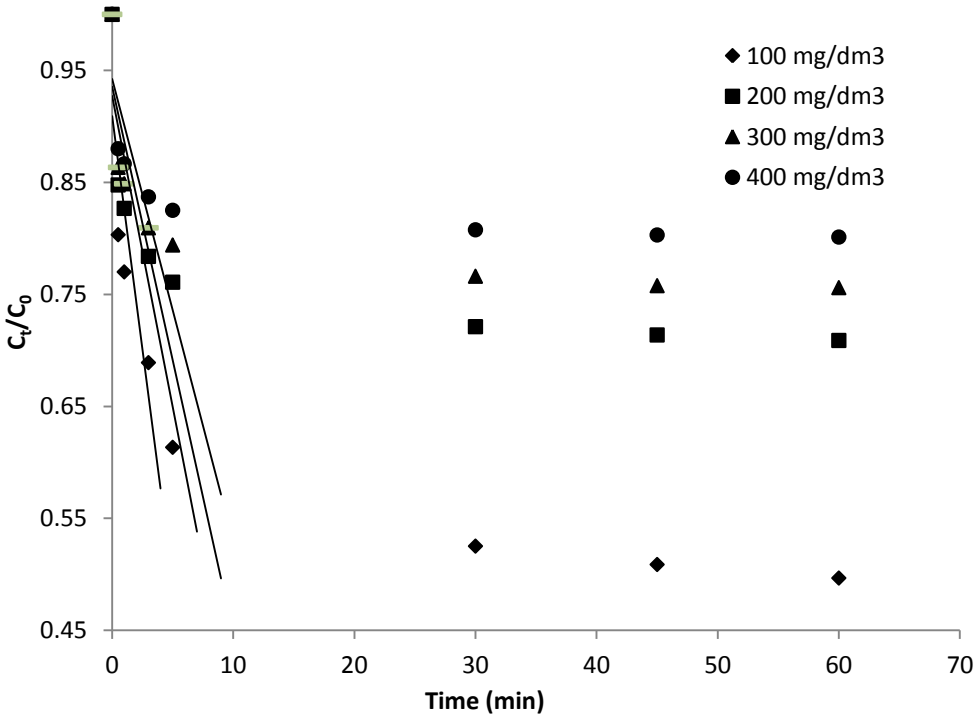

Figure 5.17 External mass transfer diffusion plot for 2-nitrophenol adsorption onto Fenton treated-HMDI pine.

Table 5.3 External mass transfer and diffusion coefficients at different adsorbate concentrations.

Sample	Parameters	100 mg/dm^3	200 mg/dm^3	300 mg/dm^3	400 mg/dm^3
Raw pine	External Mass transfers				
	k_s (1/min)	0.0201	0.0169	0.0157	0.0130
	Boyd Diffusion model				
	D_2 (cm^2/s)	3.03×10^{-10}	4.14×10^{-10}	4.30×10^{-10}	5.04×10^{-10}
	D_1 (cm^2/s)	2.75×10^{-9}	3.21×10^{-9}	3.50×10^{-9}	3.62×10^{-9}
Raw-HMDI pine	External Mass transfers				
	k_s (1/min)	0.0549	0.0480	0.0428	0.0337
	Boyd Diffusion model				
	D_2 (cm^2/s)	3.69×10^{-10}	4.47×10^{-10}	4.95×10^{-10}	5.02×10^{-10}
	D_1 (cm^2/s)	3.34×10^{-9}	3.56×10^{-9}	4.39×10^{-9}	4.45×10^{-9}
Fenton treated pine	External Mass transfers				
	k_s (1/min)	0.0749	0.0480	0.0428	0.0221
	Boyd Diffusion model				
	D_2 (cm^2/s)	3.84×10^{-10}	4.02×10^{-10}	4.24×10^{-10}	5.14×10^{-10}
	D_1 (cm^2/s)	4.27×10^{-9}	5.12×10^{-9}	6.45×10^{-9}	6.51×10^{-9}
Fenton-HMDI pine	External Mass transfers				
	k_s (1/min)	0.0615	0.0556	0.0488	0.0412
	Boyd Diffusion model				
	D_2 (cm^2/s)	4.14×10^{-10}	4.60×10^{-10}	5.32×10^{-10}	5.94×10^{-10}
	D_1 (cm^2/s)	5.75×10^{-9}	5.76×10^{-9}	6.25×10^{-9}	6.92×10^{-9}

The effect of film diffusion on the overall diffusion process needs to be examined as intraparticle diffusion has been ruled out due to the small pore size and pore volume determined by BET surface area on the pine cone biomass. Assuming that the pine biosorbent is spherical with a radius *a* (cm) and that the diffusion follows Fick's law, the mathematical relation between uptake times is (Crank, 1975):

$$\frac{q_t}{q_e} = 6\left(\frac{D_t}{a^2}\right)^{0.5}\left\{\pi^{-0.5} + 2\sum_{n=1}^{\infty} ierfc\,\frac{\pi a}{D_t^{0.5}}\right\} - 3\frac{D_t}{a^2} \qquad (5.6)$$

When *t* is small, *D* is replaced by D_1 and Equation 5.6 becomes:

$$\frac{q_t}{q_e} = 6\left(\frac{D_1}{\pi a^2}\right)^{0.5} t^{0.5} \qquad (5.7)$$

The plots of q_t/q_e against $t^{0.5}$ are presented in Figures 5.18-5.21 and show two sections in the curves represented by straight lines. There is an initial rapid stage followed by a slow uptake. The film diffusion coefficient (D_1) values for the pine biomass at the different initial concentrations of 2-nitrophenol are calculated from a gradient of the plots in Figures 5.18-5.21 and are presented in Table 5.3. As *t* becomes large, Equation (5.6) can be written as:

$$\left(1 - \frac{q_t}{q_e}\right) = \frac{6}{\pi^2}\exp\left(\frac{-D_2\pi^2}{a^2}t\right) \qquad (5.8)$$

If $B = \pi^2\frac{D_2}{a^2}$, Equation (5.8) simplifies to:

$$Bt = -0.4997 - \ln\left(1 - \frac{q_t}{q_e}\right) \qquad (5.9)$$

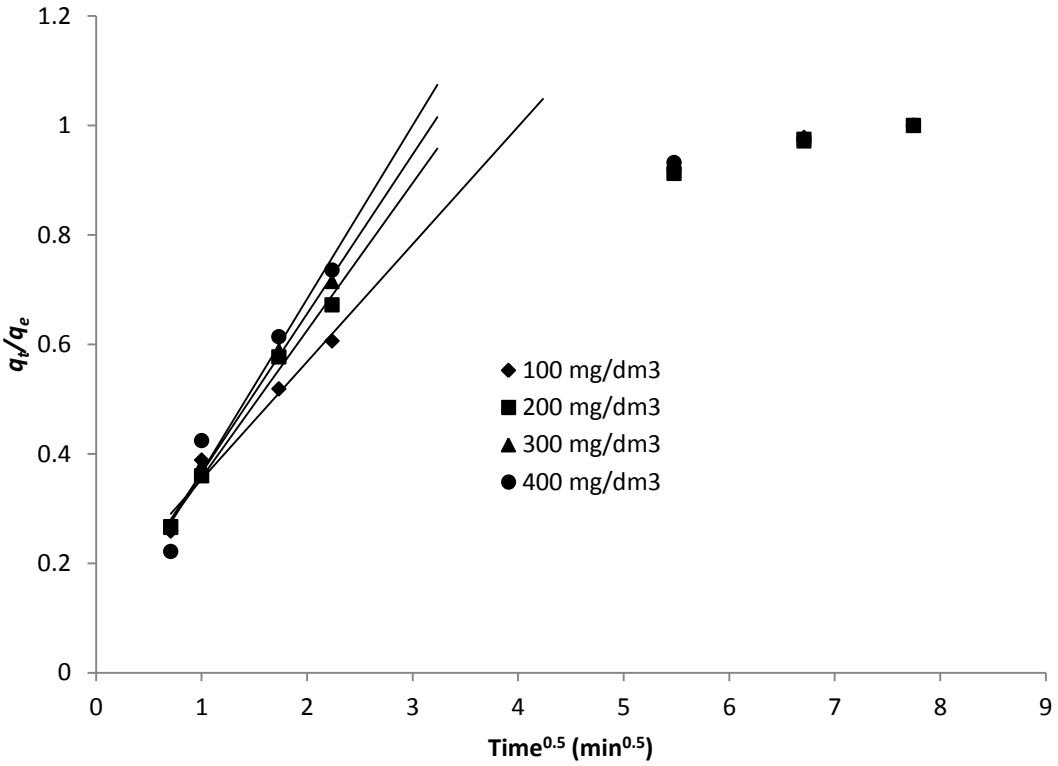

Figure 5.18 Plot of fractional uptake of 2-nitrophenol onto Raw pine against square root of time.

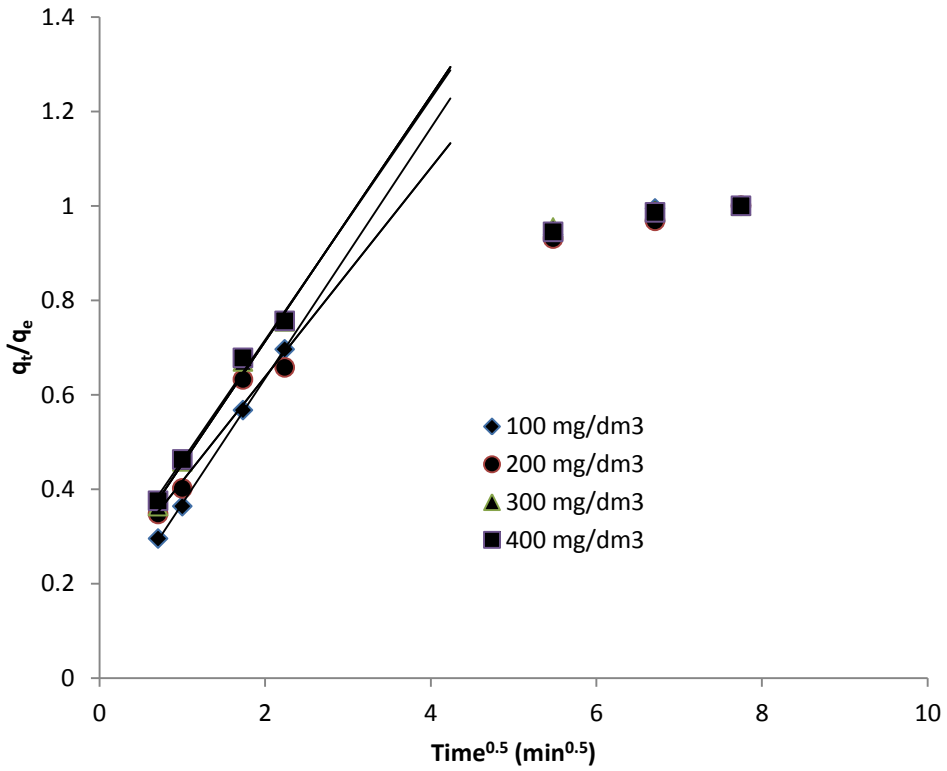

Figure 5.19 Plot of fractional uptake of 2-nitrophenol onto Raw-HMDI pine against square root of time.

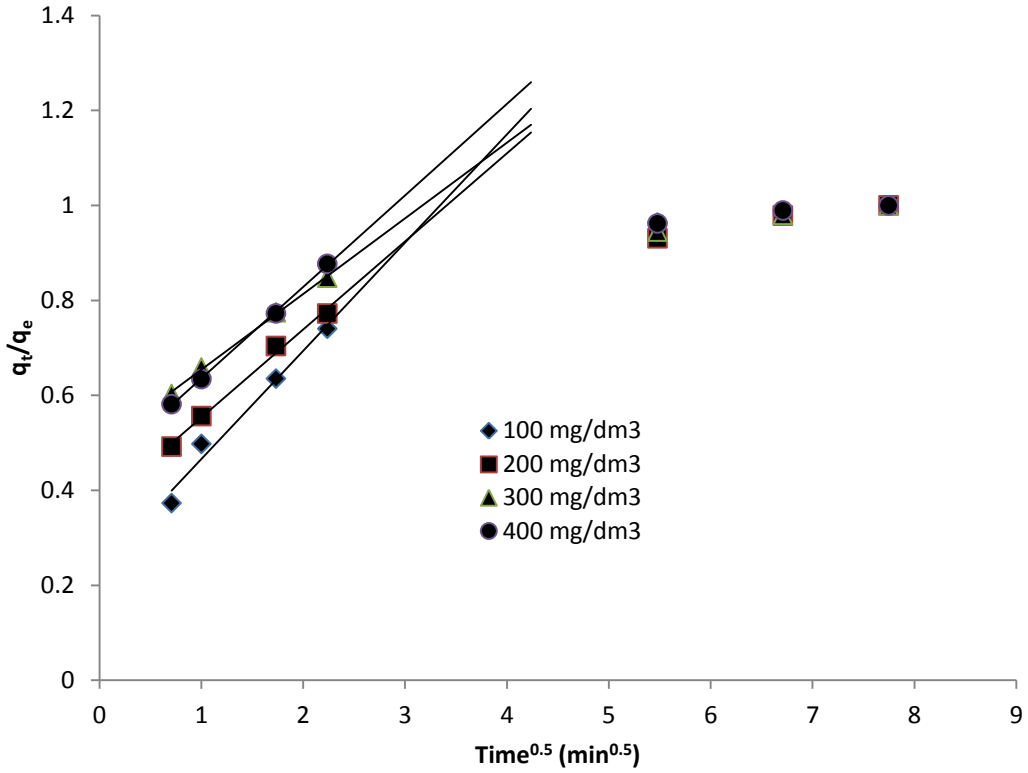

Figure 5.20 Plot of fractional uptake of 2-nitrophenol onto Fenton treated pine against square root of time.

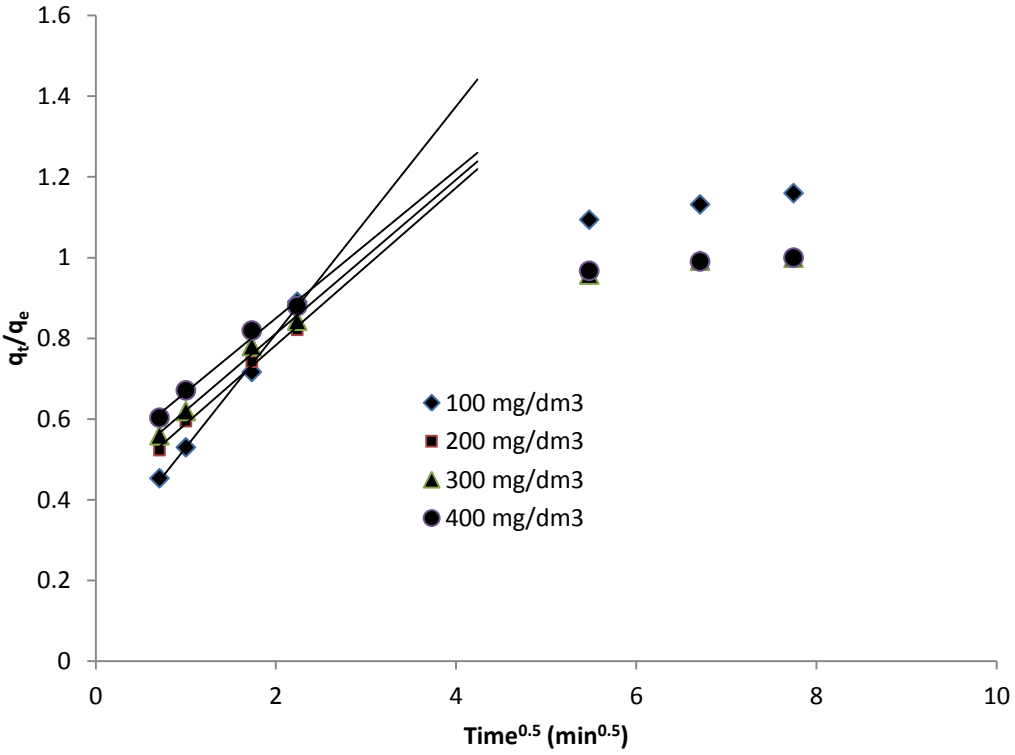

Figure 5.21 Plot of fractional uptake of 2-nitrophenol onto Fenton treated-HMDI pine against square root of time.

A plot of *Bt* against *t* at different initial concentrations of 2-nitrophenol gives slope *B*, which is then used to calculate the pore diffusion coefficient, D_2 (since $B = D_2\pi^2/a^2$) whose values are presented in Table 5.3. From a plot of *Bt* against *t*, it is possible to conclude whether external transport or intraparticle diffusion is the controlling step. The Boyd plots for adsorption of 2-nitrophenol onto pine biomass at different initial concentrations of 2-nitrophenol are presented in Figures 5.22-5.25. All the Boyd plots of the pine cone biomass show linear relationships which do not pass through the origin in the initial stage of 2-nitrophenol adsorption. The plots cut the y-axis between -0.25 and 0.50. This shows that external mass transfer is the controlling step in the initial stage of the adsorption. The intercept values become more positive due to surface modification of pine biomass and increase in initial concentration of 2-nitrophenol. This signifies an increase in external mass transfer processes due to modification of pine biomass and increase in initial adsorbate concentration. Modification of pine biomass created surface conditions conducive to external mass transfer processes. This can be a result of the increase in porosity and hydrophobic nature imparted upon the pine biomass by Fenton treatment and cross-linking using HMDI. The increase in external mass transfer due to an increase in initial adsorbate concentration can be attributed to increase in concentration gradient between the bulk solution and adsorbent surface.

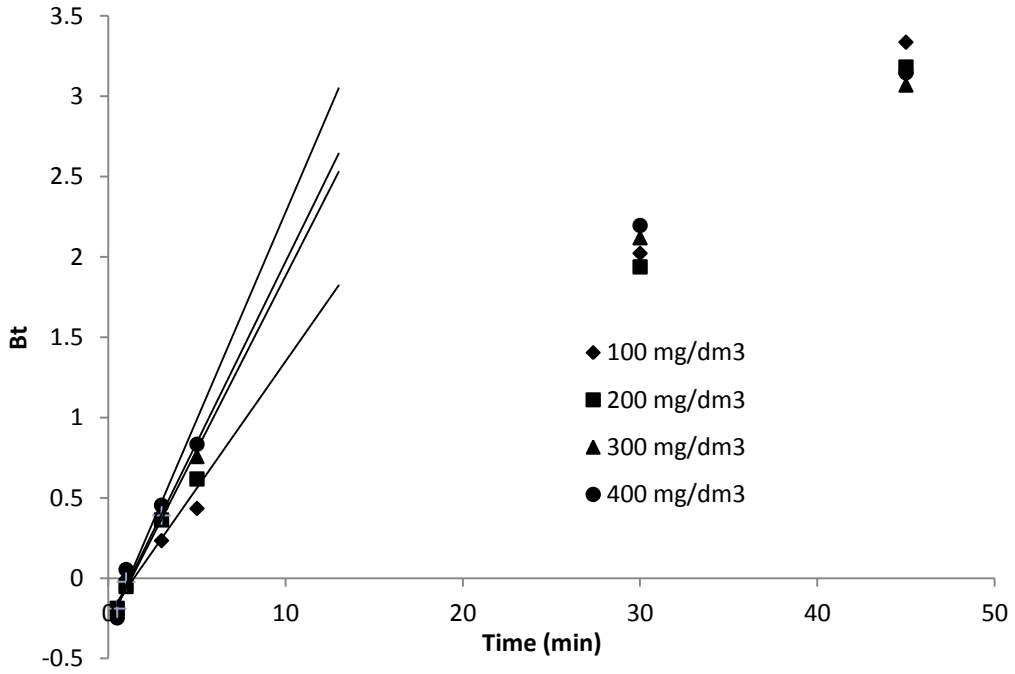

Figure 5.22 Boyd plots for 2-nitrophenol adsorption onto Raw pine.

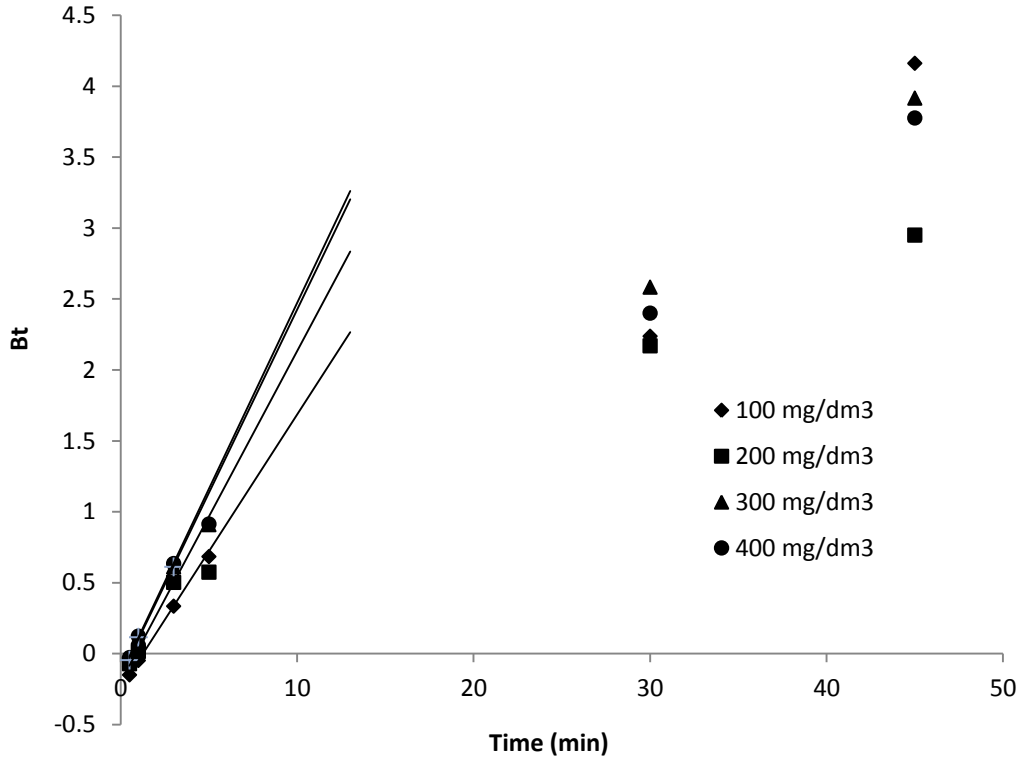

Figure 5.23 Boyd plots for 2-nitrophenol adsorption onto Raw-HMDI pine.

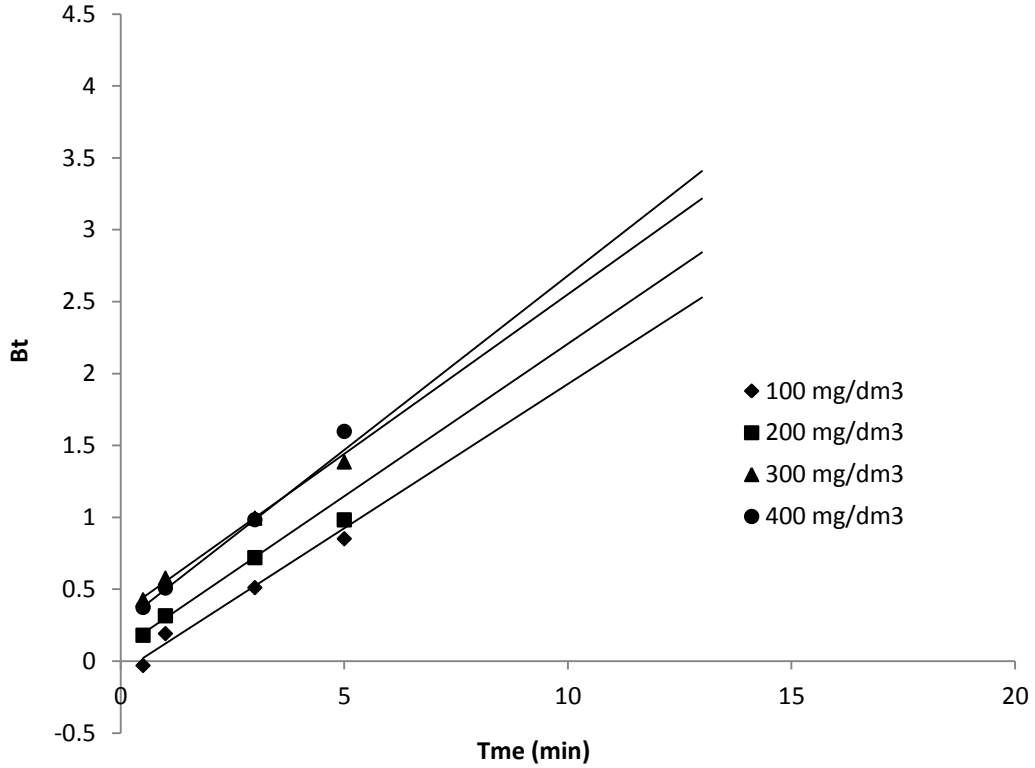

Figure 5.24 Boyd plots for 2-nitrophenol adsorption onto Fenton treated pine.

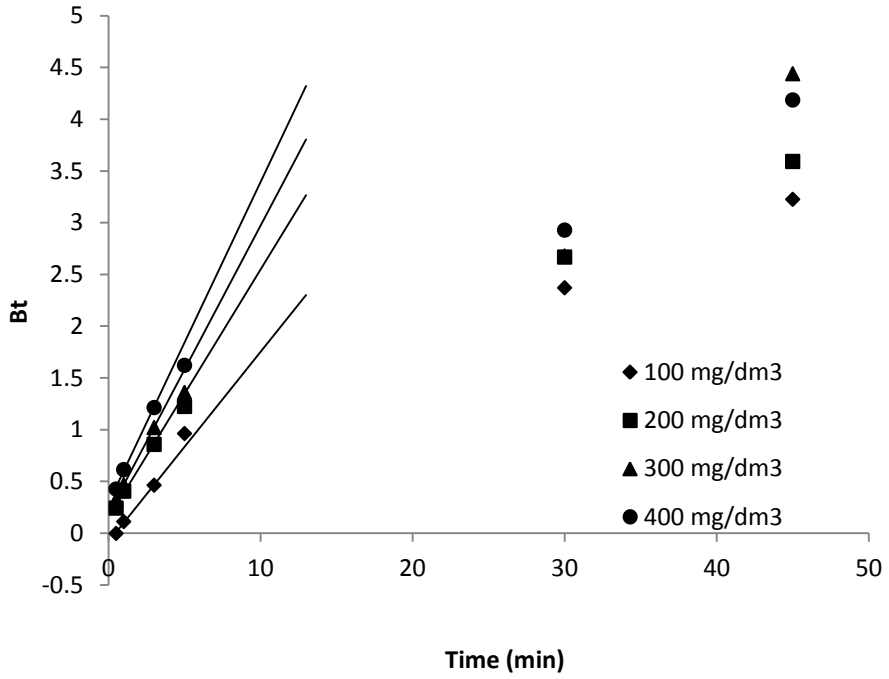

Figure 5.25 Boyd plots for 2-nitrophenol adsorption onto Fenton-HMDI pine.

The calculated values of film diffusion (D_1) coefficients increase with an increase in initial concentration of 2-nitrophenol. This is attributed to an increase in concentration gradient between the bulk solution and biosorbent surface resulting in an increase in film diffusion. The modified pine biomass also showed higher values for the diffusion coefficients than the raw pine. This shows that pine cone biomass modification via Fenton treatment and cross-linking using HMDI improved the sorbent surface resulting in faster diffusion across the boundary layer and into the pores. Fenton treatment made the surface more porous whilst cross-linking using HMDI increased its hydrophobic character. The hydrophobic nature of the modified pine biomass resulted in a decrease in boundary layer effect and an increase in film diffusion.

5.3 CONCLUSION

The optimum pH for the adsorption of 2-nitrophenol onto pine cone biomass was determined to be 6. This pH value is close to the pH_{pzc} for the pine cone biomass and the pK_a of the adsorbate. The optimum adsorbent dosage was determined as 1.5 g/dm^3. The adsorption kinetics show a good fit with the pseudo-second-order model. The r^2 values are close to one and the % variable errors are very small. The theoretical and experimental uptakes are also in

good agreement. This suggests that surface adsorption is the controlling step in the adsorption of 2-nitrophenol onto pine cone biomass. The analysis of diffusion processes showed that the initial rapid stage during the adsorption is due to external mass transfer processes. The experimental adsorption data was not fit to intraparticle model since BET surface area determination showed that the pine cone biomass has small pore sizes and pore volumes. The results show that modification of pine biomass improved its adsorption capabilities towards 2-nitrophenol. The modification also increased magnitude of kinetic and diffusion parameters.

5.4 REFERENCE

1. EL-SHEIKH, A.H., NEWMAN, A.P., SAID, A.J., ALZAWAHREH, A.M. and ABU-HELAL, M.M. (2013) Improving the adsorption efficiency of phenolic compounds into olive wood biosorbents by pre-washing with organic solvents: Equilibrium, kinetic and thermodynamic aspects, *Journal of Environmental Management*. 118, pp. 1-10.
2. CRANK, J. (1975) The Mathematics of Diffusion, 2nd edition, Claredon Press, Oxford.
3. HO, Y.S. and OFOMAJA, A.E. (2007) Effect of pH on cadmium biosorption by coconut copra meal, *Journal of Hazardous Materials*. 137, pp. 356-362.
4. KUMAR, K.V. (2006) Linear and non-linear regression analysis for the sorption kinetics of methylene blue onto activated carbon, *Journal of Hazardous Materials*. 137(3), pp. 1538-1544.
5. LIU, Q-S., ZHENG, T., WANG, P., JIANG, J-P. and LI N. (2010) Adsorption isotherm, kinetic and mechanism studies of some substituted phenols on activated carbon fibers, *Chemical Engineering Journal*. 157, pp. 348-356.
6. OFOMAJA, A.E. (2011) Kinetics and pseudo-isotherm studies of 4-nitrophenol adsorption onto mansonia wood sawdust, *Industrial Crops and Products*. 33, pp. 418-428.

6 RESULTS AND DISCUSSION (PART 3): EQUILIBRIUM STUDIES

6.1 INTRODUCTION

The chapter presents results and discussions on equilibrium studies for 2-nitrophenol adsorption using Raw, Raw-HMDI, Fenton treated and Fenton treated-HMDI pine cone biosorbents. It gives an in depth analysis of the adsorption isotherms and thermodynamics.

6.2 EQUILIBRIUM STUDIES

Equilibrium relationships also known as adsorption isotherms describe how pollutants interact with the adsorbent materials and are important in elucidation of adsorption mechanism pathways and design of adsorption systems (Argun et al., 2008; Rangabhashiyam et al., 2014). They provide information about the distribution of adsorbate between the liquid and solid phases at various equilibrium concentrations.

The shape of an adsorption isotherm is important as it indicates the type of the adsorption isotherm model that can describe the experimental adsorption data. Giles et al. (1974) proposed a general classification based on the initial slope of the adsorption isotherms with 4 main shapes being observed (C, L, H and S). This information was used in determination of equilibrium adsorption isotherm equations to fit the experimental data. The plots in Figure 6.1 show adsorption isotherms of 2-nitrophenol onto pine cone biomass. All the plots of the different pine biomass show the same shape. Using the classification proposed by Giles et al. (1974), the plots fall under the S-shape. The S-type is always a result of at least two opposite mechanisms (Mahmoud et al., 2012). The experimental data for 2-nitrophenol adsorption onto the pine cone biosorbents was then fitted to the following equilibrium adsorption models: Freundlich, Hill and Redlich-Peterson.

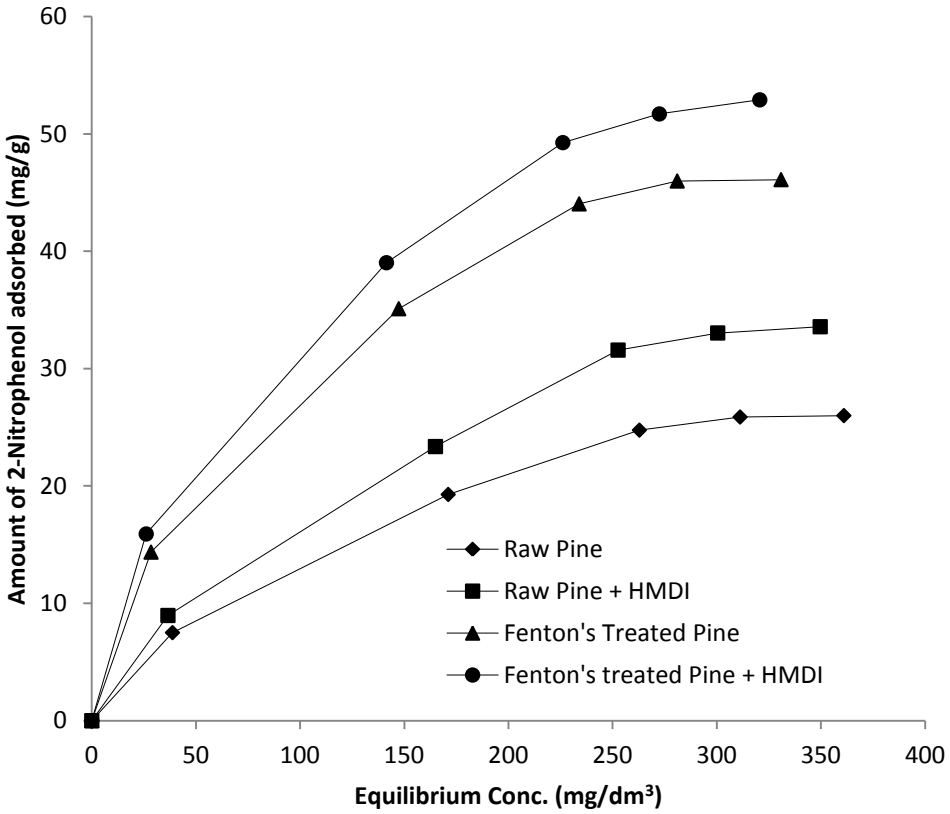

Figure 6.1 Adsorption isotherms of 2-nitrophenol on the various pine cone biosorbents

6.2.1 Error analysis

To circumvent bias due to linearization (Chin et al., 2012), the isotherm parameters were determined by non-linear regression. Non-linear regression involves mathematical calculation of isotherm parameters using the original form of the isotherm model. Two error functions were employed to verify and substantiate the equilibrium isotherm model showing the best-fit to the experimental data. They are the coefficient of determination and the percentage variance. Error functions are used as a guideline to measure the accuracy of a mathematical model. A comparison of the two error functions for the three equilibrium adsorption isotherm models used to fit the experimental data for the pine cone biomass at 299 K is shown in Table 6.1.

In order to establish correlation or goodness of fit between experimental data and the equilibrium isotherm models (Freundlich, Hill and Redlich-Peterson), graphs were plotted and are presented in Figures 6.2-6.5. The graphs are plotted in the form of 2-nitrophenol

adsorbed per unit mass of pine cone biomass (mg/g), against the concentration of 2-nitrophenol left in solution at equilibrium (mg/dm^3) at 299 K.

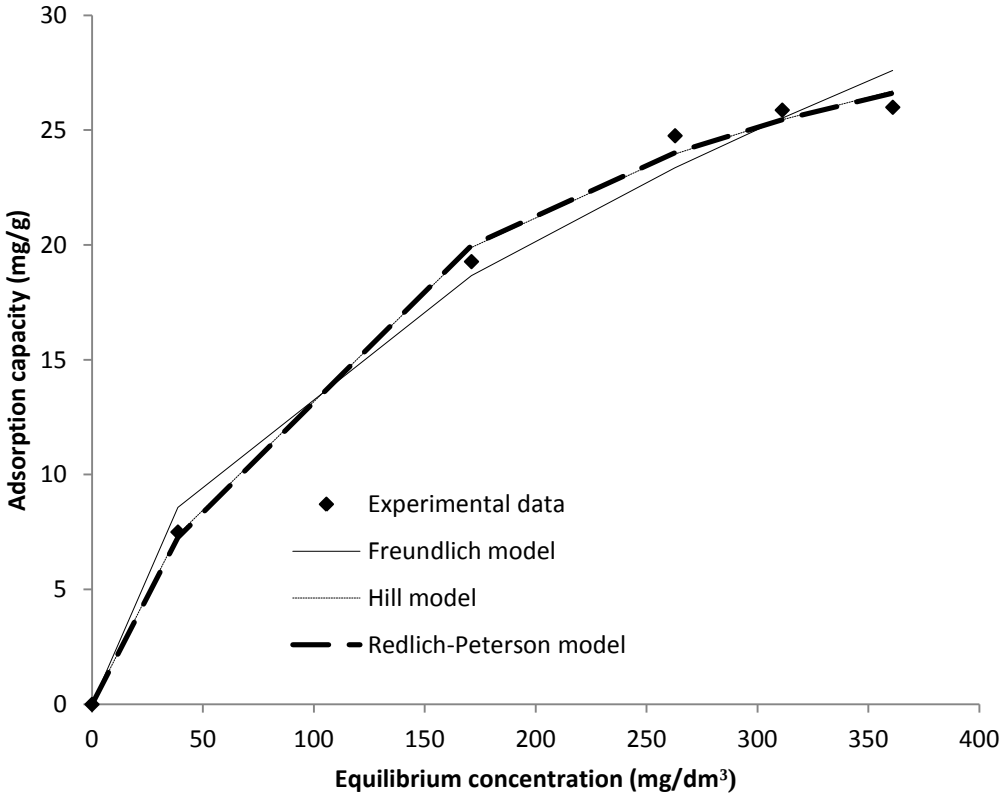

Figure 6.2 Comparison of modelled adsorption capacities with equilibrium experimental data for adsorption of 2-nitrophenol onto Raw pine.

As shown in Figure 6.2, experimental data of adsorption of 2-nitrophenol onto Raw pine cone shows a better fit with the Hill and Redlich-Peterson isotherm models than with the Freundlich isotherm model. This is also augmented by results in Table 6.1 about the two error functions. The Freundlich model has an r^2 value of 0.9899 and % variance of 1.5304, whilst the Hill model has an r^2 value of 0.9972 and % variance of 0.5689. The Redlich-Peterson model has an r^2 value of 0.9973 and % variance of 0.5513. This shows that the Freundlich isotherm parameters exhibit the least correlation with experimental data as the r^2 value is the least and the % variance is the largest amongst the three equilibrium isotherm parameters under scrutiny. The two error functions values for Hill and Redlich-Peterson models are very close with only small differences being observed. This also shows a correlation in the results from the two different error methods.

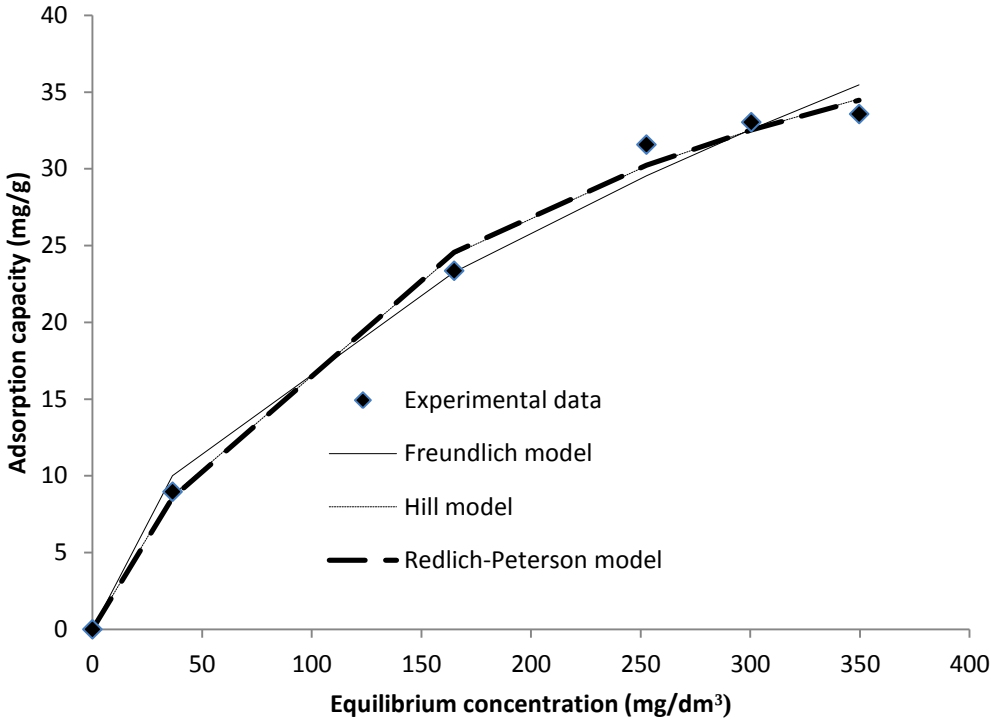

Figure 6.3 Comparison of modelled adsorption capacities with equilibrium experimental data for adsorption of 2-nitrophenol onto Raw-HMDI pine

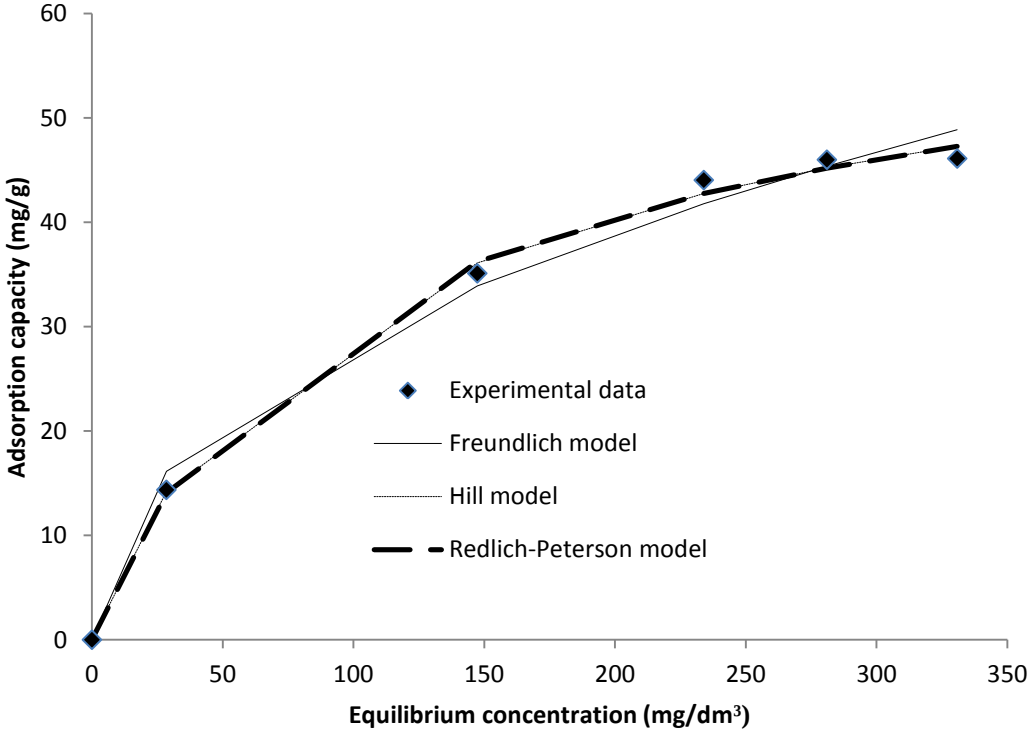

Figure 6.4 Comparison of modelled adsorption capacities with equilibrium experimental data for adsorption of 2-nitrophenol onto Fenton treated pine

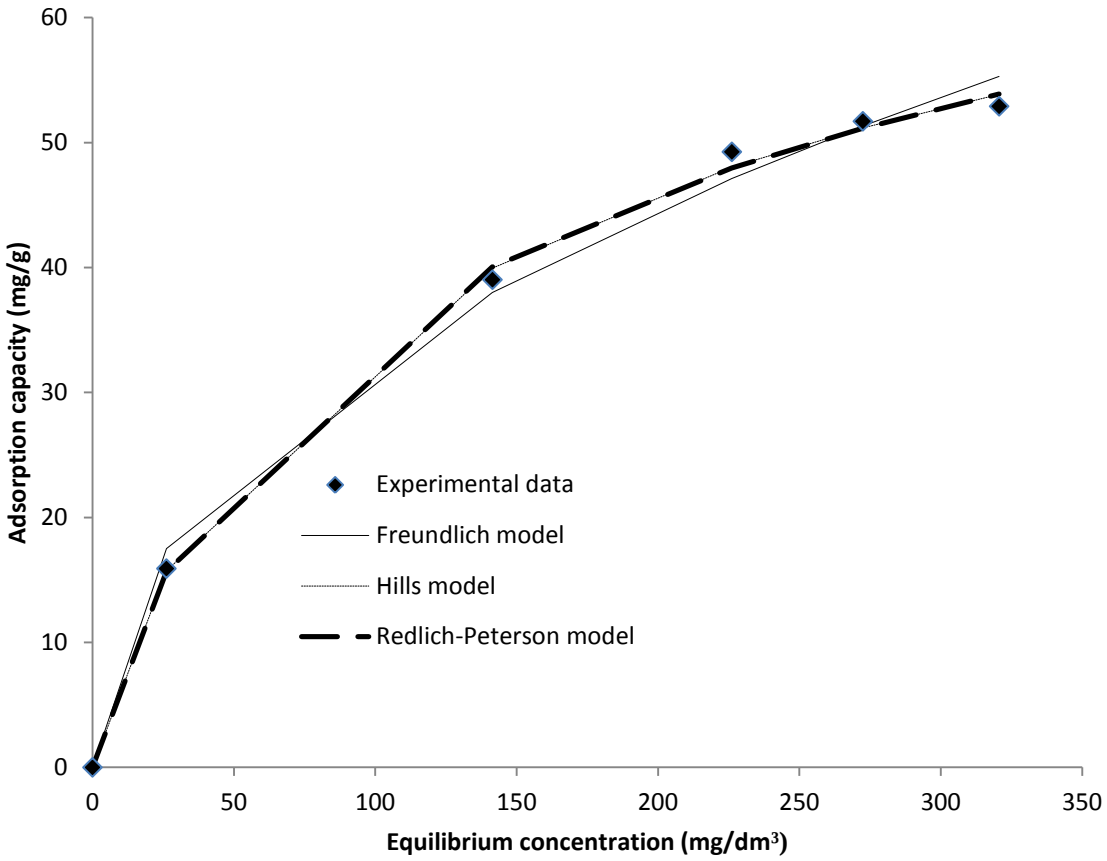

Figure 6.5 Comparison of modelled adsorption capacities with equilibrium experimental data for adsorption of 2-nitrophenol onto Fenton treated-HMDI pine.

The same trend with the error functions values in Table 6.1 for the Raw pine is observed with the other pine cone biomass samples (Raw-HMDI, Fenton treated and Fenton treated-HMDI). The Freundlich isotherm model had the least r^2 values and the highest % variances in comparison to the Hill and Redlich-Peterson isotherm models. The r^2 values and the % variances for Hill and Redlich-Peterson models are very close as shown in Table 6.1. The plots (Figures 6.3-6.5) also show better fit of the experimental data with Hill and Redlich-Peterson models than with the Freundlich isotherm model. This suggest that the experimental data for 2-nitrophenol adsorption onto Raw, Raw-HMDI, Fenton treated and Fenton treated-HMDI pine cone biosorbents shows to fit better to Hill and Redlich-Peterson isotherm models than to the Freundlich isotherm model.

Table 6.1 A comparison of coefficient of determination and % variance for three isotherm models in the biosorption of 2-nitrophenol by pine cone biomass at 299 K.

Pine cone biomass	Freundlich		Hill		Redlich-Peterson	
	r^2	% variance	r^2	% variance	r^2	% variance
Raw	0.9899	1.5304	0.9972	0.5689	0.9973	0.5513
Raw-HMDI	0.9911	2.2414	0.9957	1.4449	0.9956	1.4804
Fenton treated	0.9906	4.4057	0.9975	1.5551	0.9974	1.6526
Fenton-HMDI	0.9941	3.5291	0.9985	1.1961	0.9983	1.3639

6.2.2 Adsorption isotherms

The adsorption isotherms of 2-nitrophenol on Raw, Raw-HMDI, Fenton treated and Fenton treated-HMDI pine biomass were investigated at 299 K, 309 K, 319 K and 329 K and, the results are presented in Figures 6.6-6.9.

As can be seen from Figure 6.1, the biomass show the following order in terms of intense adsorption at low concentrations and higher adsorption capacities: Fenton treated-HMDI pine > Fenton treated pine > Raw-HMDI pine > Raw pine. This seems to suggest that the mechanism of 2-nitrophenol adsorption by the pine cone biosorbents is mainly via hydrophobic interactions and pore filling phenomenon. Fenton treatment and cross-linking with HMDI increased biomass porosity and hydrophobic character. This accounts for the increase in biosorbate affinity due to Fenton treatment and HMDI cross-linking. Nevertheless, adsorption isotherms will not conclusively provide information on adsorption reactions. Therefore, it is necessary to fit the experimental data to the most appropriate adsorption isotherm equations for reliable prediction of adsorption parameters (Rangabhashiyam et al., 2014).

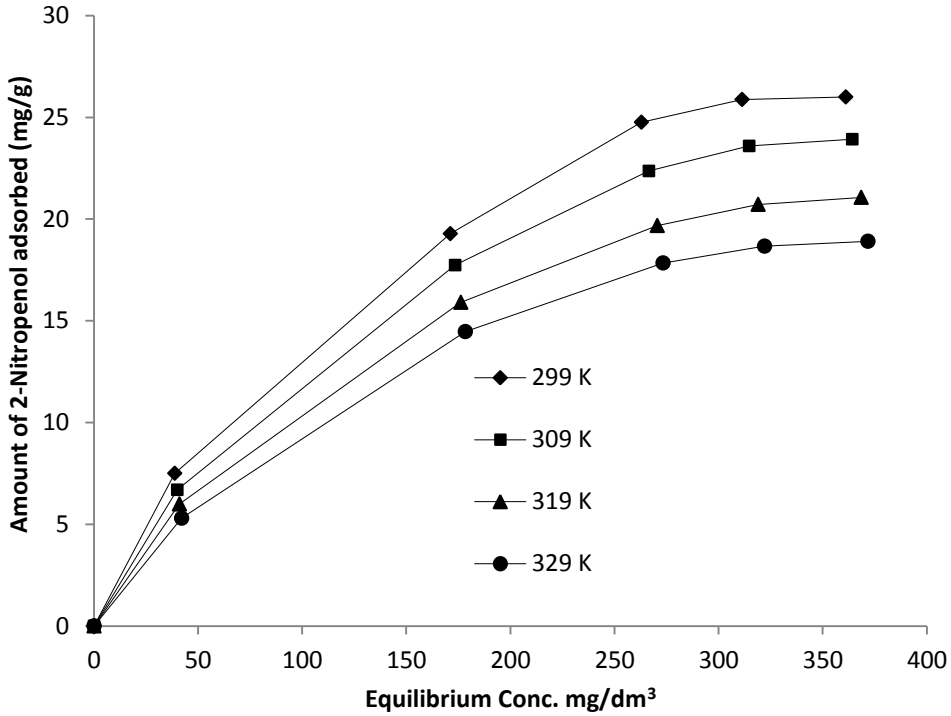

Figure 6.6 Adsorption isotherms of 2-nitrophenol on Raw pine biomass

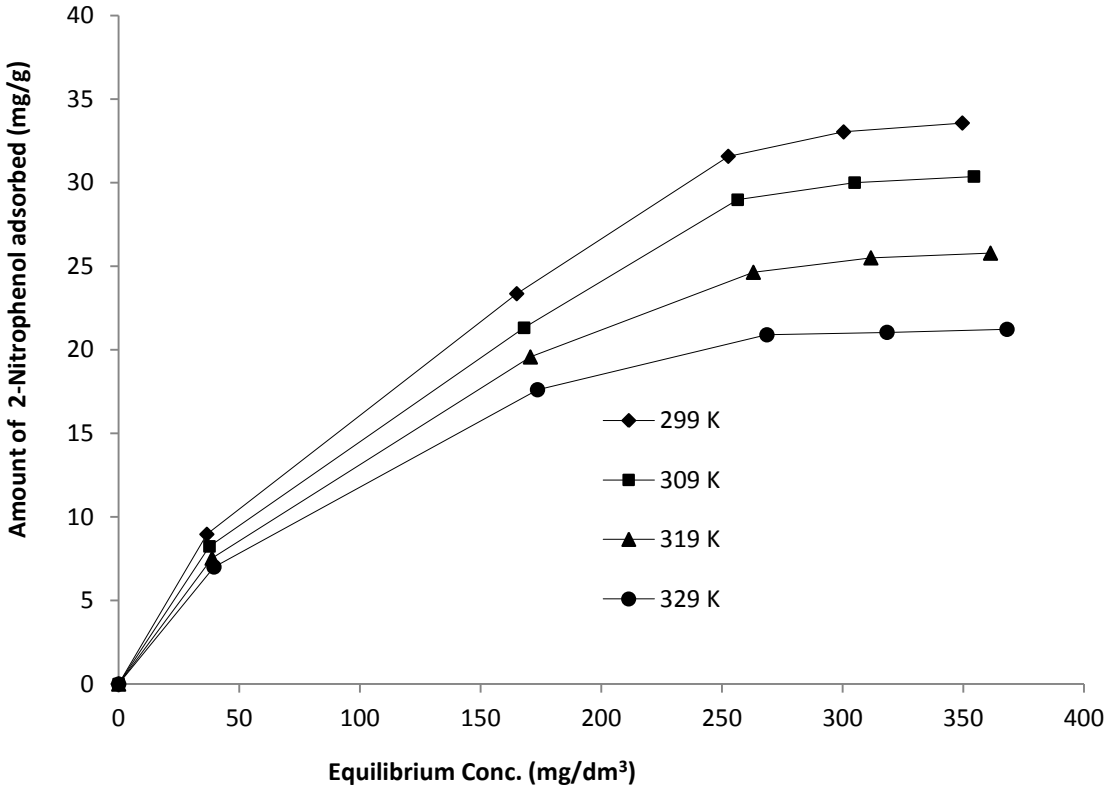

Figure 6.7 Adsorption isotherms of 2-nitrophenol on Raw-HMDI pine biomass

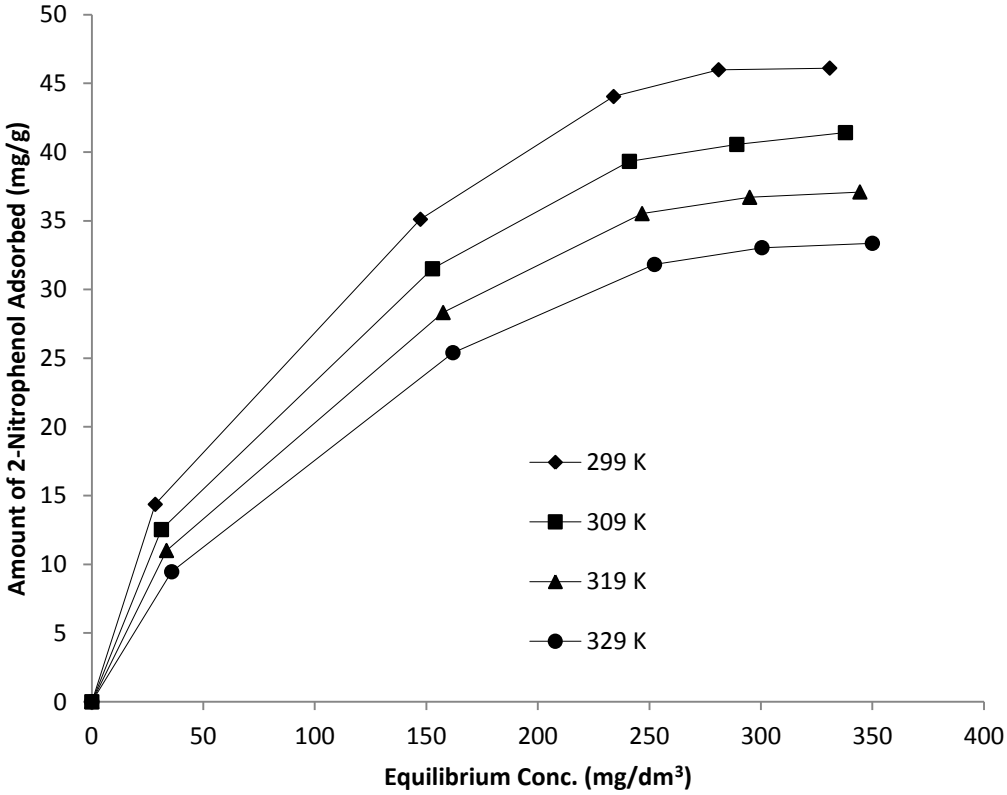

Figure 6.8 Adsorption isotherms for 2-nitrophenol on Fenton treated pine biomass

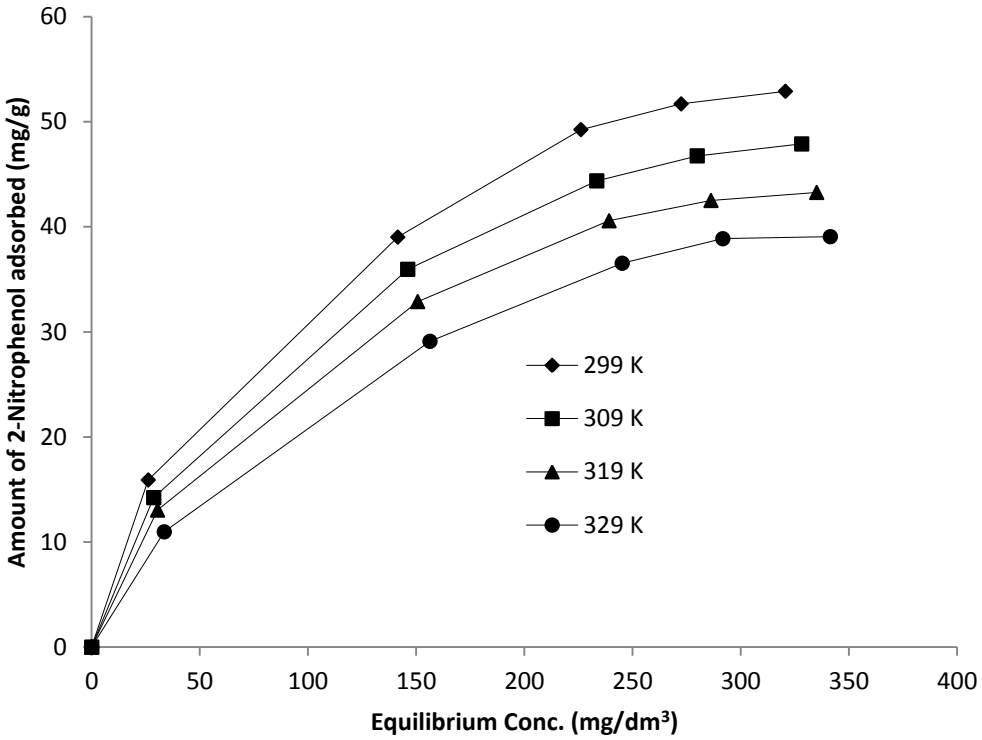

Figure 6.9 Adsorption isotherms for 2-nitrophenol on Fenton treated-HMDI pine biomass

The experimental data for 2-nitrophenol adsorption onto the pine cone biomass was fit to Freundlich, Hill and Redlich-Peterson equilibrium isotherm models. The equilibrium adsorption parameters of the three models on Raw, Raw-HMDI, Fenton treated and Fenton treated-HMDI pine cone biosorbents were calculated and are presented in Tables 6.2-6.5. The experimental data showed good fit with Redlich-Peterson and Hill models. A poor correlation was noted between experimental results and the Freundlich model.

6.2.2.1 Freundlich model

The Freundlich expression which describes multilayer adsorption on a heterogenous surface with interaction between adsorbed molecules is shown as:

$$q_e = K_F C_e^{1/n} \qquad (6.1)$$

Where, C_e is equilibrium adsorbate concentration (mg/dm^3) and q_e is amount of adsorbate adsorbed (mg/g). K_F ((mg/g)/(mg/dm^3)^n) and n are the Freundlich equation parameters. n is indicative of the intensity of the adsorption and suggests the favourability and capacity of the

adsorbent-adsorbate system. According to the model, $n > 1$ represents favourable adsorption conditions and K_F indicates adsorption capacity.

At 299 K, the Freundlich constants for: (1) Raw pine; K_F = 1.26 (mg/g)/(mg/dm^3)^n and n = 1.91, (2) Raw-HMDI pine; K_F = 1.33 (mg/g)/(mg/dm^3)^n and n = 1.78, (3) Fenton treated pine; K_F = 3.56 (mg/g)/(mg/dm^3)^n and n = 2.21, and (4) Fenton treated-HMDI pine; K_F = 3.92 (mg/g)/(mg/dm^3)^n and n = 2.18. The experimental data shows the least goodness of fit with the Freundlich isotherm model for 2-nitrophenol adsorption onto pine cone biomass. This suggest that adsorption of 2-nitrophenol onto the pine cone biomass does not completely follow multilayer adsorption and shows uniformity of biosorbent surface. All the n values are greater than one suggesting favourable adsorption. The K_F values for the pine cone biomass increase in the order: Fenton treated-HMDI > Fenton treated >Raw-HMDI > Raw. This shows that the Fenton's treatment and HMDI modification did increase the biosorptive capabilities of the pine cone biomass towards 2-nitrophenol.

6.2.2.2 Redlich-Peterson model

The three parameter isotherm equation which incorporates the features of both the Langmuir and Freundlich isotherms is represented as:

$$q_e = \frac{K_R C_e}{1 + a_R C_e^{\beta}} \tag{6.2}$$

Where $0 < \beta \leq 1$. When $\beta = 1$, the equation gives the Langmuir form:

$$q_e = \frac{K_R C_e}{1 + a_R C_e} \tag{6.3}$$

When $\beta = 0$, the equation follows Henry's Law:

$$q_e = \frac{K_R C_e}{1 + a_R} \tag{6.4}$$

Where, a_R ($dm^3/mg)^{\beta}$ and K_R (dm^3/mg) are isotherm constants and β is an exponent. It approaches the Freundlich model at high concentrations and is in concurrence with the low concentration limit of the Langmuir equation.

At 299 K, the Redlich-Peterson constants were: (1) Raw pine; K_R = 0.2212 dm^3/mg, a_R = 0.0035 $(dm^3/mg)^{\beta}$ and β = 1.08, (2) Raw-HMDI pine; K_R = 0.2839 dm^3/mg, a_R = 0.0064 $(dm^3/mg)^{\beta}$ and β = 0.97, (3) Fenton treated pine; K_R = 0.6880 dm^3/mg, a_R = 0.0173 $(dm^3/mg)^{\beta}$ and β = 0.93, and Fenton treated-HMDI pine; K_R = 0.9426 dm^3/mg, a_R = 0.0375 $(dm^3/mg)^{\beta}$ and β = 0.83. The Redlich-Peterson model suggests that the adsorption of 2-nitrophenol onto pine cone biomass is a hybrid mechanism of the Freundlich and Langmuir equations which does not follow ideal monolayer adsorption (Chin et al., 2012). The β values are all close to unity suggesting that the adsorption is more of Langmuir than Freundlich form.

6.2.2.3 Hill model

This three-parameter model views adsorption as a cooperative phenomenon, with adsorbed molecules influencing affinity of adsorbent at other binding sites (Ringot et al., 2007). The Hill equation is represented as:

$$q_e = \frac{q_{\max} C_e^{n_H}}{K_D + C_e^{n_H}} \qquad (6.5)$$

Where, q_{max} is the Hill isotherm maximum uptake saturation (mg/g), K_D is the Hill constant (mg/dm^3), n_H is the Hill cooperativity coefficient, q_e is the adsorption capacity (mg/g) and C_e is the equilibrium adsorbate concentration (mg/dm^3). According to the model three possibilities in binding are possible:

(1) $n_H > 1$, positive cooperativity;

(2) $n_H = 1$, non-cooperative and;

(3) $n_H < 1$, negative cooperativity.

At 299K, the Hill isotherm constants are: (1) Raw pine; q_{max} = 38.18 mg/g, n_H = 1.02 and K_D = 172.41 mg/dm^3, (2) Raw-HMDI pine; q_{max} = 58.02 mg/g, n_H = 0.94 and K_D = 164.87 mg/dm^3, (3) Fenton treated pine; q_{max} = 66.80 mg/g, n_H = 0.89 and K_D = 74.19 mg/dm^3, and (4) Fenton treated-HMDI pine; q_{max} = 86.36 mg/g, n_H = 0.80 and K_D = 61.07 mg/dm^3. The

Hill model explains the adsorption as a positive cooperation between adsorbate molecules and raw pine (since $n_H > 1$), but a negative cooperativity between adsorbate molecules and raw-HMDI, Fenton treated and Fenton treated-HMDI pine cone (their n_H values are all < 1). The q_{max} values for the pine cone biomass are in the order: Fenton treated-HMDI > Fenton treated > Raw-HMDI > Raw. As q_{max} implies maximum specific uptake corresponding to site saturation (mg/g), an increase in this value suggest an increase in number of adsorption sites and capacity due to Fenton treatment and HMDI modification of the cone biomass.

Table 6.2 Isotherm parameters for the adsorption of 2-nitrophenol onto Raw pine

ISOTHERM MODEL	**299 K**	**309 K**	**319 K**	**329 K**
Freundlich				
K_F (mg/g)/(mg/dm^3)^n	1.26	1.07	0.98	0.87
N	1.91	1.86	1.90	1.88
Hills				
q_{max} (mg/g)	38.18	34.63	29.10	24.85
n_H	1.02	1.05	1.09	1.17
K_D (mg/dm^3)	172.41	200.75	219.07	294.44
Redlich-Peterson				
K_R (dm^3/mg)	0.2212	0.1895	0.1654	0.1362
a_R (dm^3/mg)$^\beta$	0.0035	0.0027	0.0022	0.0009
B	1.08	1.11	1.14	1.26

Table 6.3 Isotherm parameters for the adsorption of 2-nitrophenol onto Raw-HMDI pine

ISOTHERM MODEL	**299 K**	**309 K**	**319 K**	**329 K**
Freundlich				
K_F (mg/g)/(mg/dm^3)^n	1.33	1.23	1.35	1.60
N	1.78	1.80	1.96	2.23
Hills				
q_{max} (mg/g)	58.02	50.42	35.17	24.67
n_H	0.94	0.96	1.08	1.28
K_D (mg/dm^3)	164.87	174.66	192.05	288.32
Redlich-Peterson				
K_R (dm^3/mg)	0.2839	0.2448	0.2190	0.1992
a_R (dm^3/mg)$^\beta$	0.0064	0.0042	0.0027	0.0012
B	0.97	1.03	1.14	1.23

Table 6.4 Isotherm parameters for the adsorption of 2-nitrophenol onto Fenton treated pine

ISOTHERM MODEL	**299 K**	**309 K**	**319 K**	**329 K**
Freundlich				
K_F (mg/g)/(mg/dm^3)^n	3.56	2.86	2.34	1.83
N	2.21	2.14	2.07	1.98
Hills				
q_{max} (mg/g)	66.80	57.39	50.16	44.28
n_H	0.89	0.97	1.04	1.11
K_D (mg/dm^3)	74.19	100.76	136.85	196.14
Redlich-Peterson				
K_R (dm^3/mg)	0.6880	0.5092	0.3867	0.2920
a_R (dm^3/mg)$^\beta$	0.0173	0.0096	0.0048	0.0021
B	0.93	0.99	1.07	1.17

Table 6.5 Isotherm parameters for the adsorption of 2-nitrophenol onto Fenton treated-HMDI pine

ISOTHERM MODEL	**299 K**	**309 K**	**319 K**	**329 K**
Freundlich				
K_F (mg/g)/(mg/dm^3)^n	3.92	3.35	3.01	2.12
N	2.18	2.14	2.13	2.12
Hills				
q_{max} (mg/g)	86.36	70.49	61.05	56.13
n_H	0.80	0.89	0.94	1.09
K_D (mg/dm^3)	61.07	79.73	92.68	143.14
Redlich-Peterson				
K_R (dm^3/mg)	0.9426	0.6823	0.5598	0.3848
a_R (dm^3/mg)$^\beta$	0.0375	0.0181	0.0121	0.0052
B	0.83	0.91	0.96	1.04

6.2.3 Adsorption thermodynamics

The thermodynamic parameters for 2-nitrophenol adsorption onto the pine cone biomass are presented in Table 6.6 and were determined using the following equations:

$$\Delta G° = -RT \ln K \quad (6.6)$$

$$\Delta G° = \Delta H° - T\Delta S° \quad (6.7)$$

Where, $\Delta G°$ is the Gibbs free energy (kJ/mol), R is the ideal gas constant (kJ/K/mol), T is the temperature (K), K is the equilibrium constant (dm^3/mol) and is derived from Redlich-Peterson equation, $\Delta H°$ is the enthalpy change of reaction (kJ/mol) and $\Delta S°$ is the entropy change (kJ/mol/K).

Table 6.6 Thermodynamic parameters for 2-nitrophenol adsorption onto Raw, Raw-HMDI, Fenton treated and Fenton treated-HMDI pine cone

	ΔG° (kJ/mol)				**ΔH° (kJ/mol)**	**ΔS° (kJ/mol/K)**
Samples	**299 K**	**309 K**	**319 K**	**329 K**		
Raw pine	-1.15	-0.80	-0.46	-0.06	-11.95	-0.036
Raw-HMDI	-1.78	-1.45	-1.21	-0.98	-9.64	-0.026
Fenton treated	-3.98	-3.34	-2.71	-2.03	-23.36	-0.065
Fenton-HMDI	-4.56	-4.08	-3.69	-2.79	-21.68	-0.057

As shown in Table 6.6, all the thermodynamic parameters (ΔG, ΔH and ΔS) have negative values for all the pine cone biosorbents under investigation. Magnitude of the negative values of Gibbs free energy is in the order: Fenton treated-HMDI pine > Fenton treated pine > Raw-HMDI pine > Raw pine. This indicates reinforced adsorption due to the Fenton treatment and HMDI modification of pine cone biomass. The negative values of the Gibbs free energy show that the adsorption of 2-nitrophenol onto the pine cone biosorbents was spontaneous and suggest that it was due to physisorption (Argun et al., 2008). Values for Gibbs free energy between 0 and -20 kJ/mol indicate physisorption, whilst those between -80 and -

100 kJ/mol indicate chemisorption (Yu et al., 2004). The spontaneous nature of the adsorption decreases with an increase in temperature. Negative values of enthalpy change show that the adsorption is exothermic, which is in agreement with experimental observations. The adsorption isotherm plots showing the uptake of 2-nitrophenol with the various pine cone biosorbents in Figures 6.6-6.9, show that adsorption capacity decreases with an increase in temperature. The exothermic nature of the adsorption process further corroborates that it is due to physisorption rather than chemisorption (Liu et al., 2010). The negative entropy values indicate a decrease in degree of randomness at the solid/liquid interface due to the adsorption process.

6.3 CONCLUSION

Experimental results for 2-nitrophenol adsorption onto pine cone biomass showed better correlation with Redlich-Peterson and Hill models. This suggests that the mechanism does not show complete multilayer coverage with cooperative phenomena between adsorbate molecules. Thermodynamic parameters showed that the adsorption is feasible, spontaneous, and exothermic and results in a decrease in degree of disorder at the solid/liquid interface. An increase in temperature resulted in a decrease in adsorption capacity. This suggests that the adsorption is physical rather than chemical. The equilibrium results presented herein show that adsorption of 2-nitrophenol onto pine cone biomass follows the order: Fenton treated-HMDI > Fenton treated > Raw-HMDI > Raw. Hence, it can be concluded that Fenton treatment and HMDI cross-linking modification did increase the adsorptive capabilities of the pine cone biomass.

6.4 REFERENCE

1. ARGUN, M.E., DURSUN, S., KARATAS, M. and GÜRÜ, M. (2008) Activation of pine cone using Fenton oxidation for Cd (II) and Pb (II) removal, *Bioresource Technology*. 99(18), pp. 8691-8698.
2. CHIN, L.S., CHEUNG, W.H., ALLEN, S.J. and McKAY, G. (2012) Error analysis of adsorption isotherm models for acid dyes onto bamboo derived activated carbon, *Chinese Journal of Chemical Engineering*. 20(3), pp. 535-542.
3. GILES, C.H., SMITH, D. and HUITSON, A. (1974) A general treatment and classification of the solute adsorption isotherm. I. Theoretical, *Journal of Colloid Interface Science*. 47(3), pp. 755-765.
4. LIU, Q-S., ZHENG, T., WANG, P., JIANG, J-P. and LI N. (2010) Adsorption isotherm, kinetic and mechanism studies of some substituted phenols on activated carbon fibers, *Chemical Engineering Journal*. 157(2-3), pp. 348-356.
5. MAHMOUD, D.K., SALLEH, M.A.M. and KARIM, W.A.W.A.K. (2012) Langmuir-model application on solid-liquid adsorption using agricultural wastes: Environmental application review, *Journal of Purity, Utility Reaction and Environment*. 1(4), pp. 170-199.
6. OFOMAJA, A.E., UNUABONAH, E.I. and OLADOJA, N.A. (2010) Competitive modelling for the biosorptive removal of copper and lead ions from aqueous solution by Mansonia wood sawdust, *Bioresource Technology*. 101, pp. 3844-3852.
7. RANGABHASHIYAM, S., ANU, N., NANDAGOPAL, M.S.G. and SELVARAJU, N. (2014) Relevance of isotherm models in biosorption of pollutants by agricultural byproducts, *Journal of Environmental Chemical Engineering*. 2(1), pp. 398-414.
8. RINGOT, D., LERZY, B., CHAPLAIN, K., BONHOURE, J-P., AUCLAIR and LARONDELLE, Y. (2007) In vitro biosorption of ochratoxin A on the yeast industry by-products: Comparison of isotherm models, *Bioresource Technology*. 98, pp. 1812-1821.

9. YU, Y., ZHUANG, Y.Y., WANG, Z.H. and QIU, M.Q. (2004) Adsorption of water-soluble dyes onto modified resin, *Chemosphere*. 54(3), pp. 425-430.

7 CONCLUSION AND RECOMMENDATIONS

7.1 CONCLUSION

A number of researchers have investigated the ability of agricultural waste materials to remove pollutants from aqueous solution in both their natural and modified forms. The main achievement of this study was the synthesis of a novel hydrophobic biomaterial composite from pine cone and HMDI which acted as an efficient adsorbent for the removal of 2-nitrophenol from simulated industrial wastewater and to compare the effect of Fenton treatment of pine cone on cross-linking with HMDI.

Fenton treatment of pine cone effectively removed plant extractives, pigments and resin acids among other soluble organic compounds. The treatment also resulted in an increase in oxygenated functional groups on the pine surface thereby reducing the pH_{pzc} and increasing the BET surface area by creating small pores on the pine surface. The Raw and Fenton treated pine was successfully cross-linked using HMDI, a bi-functional cross-linker. The reaction took place in hexane solvent under a N_2 gas atmosphere with dibutyltin dilaurate as catalyst. This modification resulted in a less hydrophilic composite with increased affinity of the composite for hydrophobic pollutants. The final composites produced from the Raw and Fenton treated pine on optimization of reaction variables were characterized using FTIR, TGA, XRD, SEM, EDX and BET. The optimum reaction conditions were found to be: 0.2 g of pine, 3.5 cm^3 HMDI and 1.5 cm^3 catalysts at 50 °C for 4 hours under inert conditions. The results obtained from analytical techniques and WPG calculations confirmed that the pine cone biomass was successfully cross-linked using HMDI.

Four samples which includes the Raw pine cone, HMDI modified raw pine cone, Fenton's reagent treated pine cone and the Fenton's treated and HMDI modified pine cone were then applied for the removal of 2-nitrophenol from aqueous solution. The Fenton treated-HMDI pine biomass gave the highest adsorption capacity amongst the pine and treated pine biomass which were also under scrutiny. The pine and treated biomass adsorption capacity were in the following

order: Fenton treated-HMDI > Fenton treated > Raw-HMDI > Raw. This showed that pine biomass modification with Fenton's reagent and HMDI did enhance its affinity for the adsorbate.

Adsorption kinetic data were fitted to the pseudo-first-order and pseudo-second-order kinetic models. The coefficient of determination and percent variable error methods were used to determine which kinetic model gave a better fit to the experimental data. The pine and modified pine biomass had r^2 values between 0.8906 and 0.9754, and % variable error between 1.74 and 17.43 when the adsorption kinetic data was fitted to the pseudo-first-order model. When the same data was fitted to the pseudo-second-order kinetic model, the r^2 values were between 0.9709 and 0.9959, with % variable error between 0.48 and 4.88. This shows that the experimental adsorption kinetic data of 2-nitrophenol onto pine and modified pine cone biomass showed better correlation with the pseudo-second-order kinetic model. This suggests that surface adsorption is the controlling step in the adsorption of 2-nitrophenol onto pine and modified pine cone biomass. Diffusion process analysis showed that the initial rapid stage during the adsorption is due to external mass transfer processes of adsorbate from the bulk solution onto the biosorbent surface. The results also show that modification of pine biomass improved its adsorption capabilities towards 2-nitrophenol and also increased magnitude of kinetic and diffusion parameters. The modified pine biosorbents had the highest rate constants and diffusion coefficients.

Equilibrium adsorption studies were conducted and the data was fit to Freundlich, Redlich-Peterson and Hill equilibrium isotherm models. The shape of the isotherms obtained from adsorption of 2-nitrophenol onto the pine and modified pine biomass are similar and fall under the S-type isotherm. The experimental data was not fit to the Langmuir isotherm model (which is the most commonly used isotherm model) because the shape of the adsorption isotherms for 2-nitrophenol adsorption onto pine and modified pine biomass did not fall under the L-type isotherm. The coefficient of determination and percent variable error were used for error analysis. The r^2 values and % variable error for fitting of the adsorption experimental data to the Freundlich isotherm model were between 0.9899-0.9941

and 1.5304–4.4057, respectively. For the Hill model, the r^2 values were between 0.9957 and 0.9985, while the % variable error values were between 0.5689 and 1.5551. The r^2 values for fitting of the data to the Redlich-Peterson isotherm model were between 0.9956 and 0.9983, while the % variable errors had values between 0.5513 and 1.6526. The experimental equilibrium adsorption data for 2-nitrophenol adsorption onto pine and modified pine cone biomass showed a better fitting with Redlich-Peterson and Hill equilibrium isotherm models, but a poor fit with the Freundlich isotherm model. This suggests that the mechanism does not follow complete multilayer coverage and that the adsorption shows cooperative phenomena between adsorbate molecules. Thermodynamic parameters showed that the adsorption is feasible, spontaneous, and exothermic. The negative entropy results show a decrease in degree of disorder at the solid/liquid interface. The decrease in adsorption capacity due to an increase in temperature suggests that the adsorption is physical rather than chemical. The equilibrium results showed that adsorption of 2-nitrophenol onto pine cone biomass follows the order: Fenton treated-HMDI > Fenton treated > Raw-HMDI > Raw. This shows an increase in affinity by the adsorbent for the adsorbate. Hence, it was concluded that Fenton treatment and HMDI cross-linking modification did increase the adsorptive capabilities of the pine cone biomass. The treatments also influenced the equilibrium isotherm parameters.

7.2 RECOMMENDATIONS

The adsorption capacity of the hydrophobic biomaterial composite (Fenton treated-HMDI pine) towards phenol and other phenolic derivatives (mono-, di-, tri-, chloro- and nitro-substituted) needs to be explored as this will show: (1) the effect of pollutant molecular size, (2) the effect of different and number of substituent groups on the pollutant on the overall biosorption process and (3) determine selectivity of the biosorbent towards the phenols in a multi-component pollutant systems.